Mathematical modeling of plant-herbivore interactions: Stability analysis and period-doubling bifurcation in a modified Nicholson-Bailey model

by

Maram Ibrahim Albayyadhi

M.S., University of Regina, 2013

AN ABSTRACT OF A DISSERTATION

submitted in partial fulfillment of the
requirements for the degree

DOCTOR OF PHILOSOPHY

Department of Mathematics
College of Arts and Sciences

KANSAS STATE UNIVERSITY
Manhattan, Kansas

2024

Abstract

A Nicholson-Bailey model was initially created with the purpose of examining the dynamics of the population between a parasite and its host. In 1935, Nicholson and Bailey proposed a model for predicting the interactions between *Encarsia Formosa* parasites and *Trialeurodes Vaporariorum* hosts that focused on the interaction between parasites and hosts[1]. In the study of biological systems, these types of models, such as discrete-time equations, can be considered invaluable tools for studying the interactions between two species. This dissertation presents a refined iteration of the Nicholson-Bailey discrete host-parasite model in the first Chapter 1. The research unfolds in several chapters. The initial chapter provides a comprehensive background and reviews pertinent literature. Subsequently, fundamental definitions of ordinary differential equations are expounded upon, elucidating key concepts in dynamical systems such as stability analysis, manifold theory and bifurcations. Moreover, essential results and theorems pertinent to the study are delineated. In the second chapter, an investigation scrutinizes the dynamics of the newly formulated host-parasite model, featuring three essential parameters confined to the first quadrant. A rescaling technique is employed to condense the model into a two-parameter format, capturing its dynamics. Notably, the model consistently manifests two boundary steady states, with the potential emergence of a third interior steady state under specific parameter conditions. Utilizing linearized stability analysis, thresholds for system stability are identified, distinguishing between stable and unstable regimes. Further exploration delves into the long-term stability of steady states and center manifold theory, particularly focusing on non-hyperbolic steady states and transitions from stable to unstable regions. The analysis explores bifurcation scenarios, including two-parameter bifurcations, by varying parameter ranges. It highlights period-doubling bifurcations that lead to chaotic behavior as eigenvalues cross critical thresholds. Numerical simulations support the theoretical results, confirming the conclusions.

Mathematical modeling of plant-herbivore interactions: Stability analysis and period-doubling bifurcation in a modified Nicholson-Bailey model

by

Maram Ibrahim Albayyadhi

M.S., University of Regina, Canada, 2013

A DISSERTATION

submitted in partial fulfillment of the
requirements for the degree

DOCTOR OF PHILOSOPHY

Department of Mathematics
College of Art and Sciences

KANSAS STATE UNIVERSITY
Manhattan, Kansas

2024

Approved by:

Major Professor
Majid Jaberi-Douraki

Copyright

Abstract

A Nicholson-Bailey model was initially created with the purpose of examining the dynamics of the population between a parasite and its host. In 1935, Nicholson and Bailey proposed a model for predicting the interactions between *Encarsia Formosa* parasites and *Trialeurodes Vaporariorum* hosts that focused on the interaction between parasites and hosts[1]. In the study of biological systems, these types of models, such as discrete-time equations, can be considered invaluable tools for studying the interactions between two species. This dissertation presents a refined iteration of the Nicholson-Bailey discrete host-parasite model in the first Chapter 1. The research unfolds in several chapters. The initial chapter provides a comprehensive background and reviews pertinent literature. Subsequently, fundamental definitions of ordinary differential equations are expounded upon, elucidating key concepts in dynamical systems such as stability analysis, manifold theory and bifurcations. Moreover, essential results and theorems pertinent to the study are delineated. In the second chapter, an investigation scrutinizes the dynamics of the newly formulated host-parasite model, featuring three essential parameters confined to the first quadrant. A rescaling technique is employed to condense the model into a two-parameter format, capturing its dynamics. Notably, the model consistently manifests two boundary steady states, with the potential emergence of a third interior steady state under specific parameter conditions. Utilizing linearized stability analysis, thresholds for system stability are identified, distinguishing between stable and unstable regimes. Further exploration delves into the long-term stability of steady states and center manifold theory, particularly focusing on non-hyperbolic steady states and transitions from stable to unstable regions. The analysis explores bifurcation scenarios, including two-parameter bifurcations, by varying parameter ranges. It highlights period-doubling bifurcations that lead to chaotic behavior as eigenvalues cross critical thresholds. Numerical simulations support the theoretical results, confirming the conclusions.

Table of Contents

List of Figures

List of Tables

Acknowledgments

I am profoundly grateful to the Almighty, Allah, for His boundless grace and guidance. These grace and guidance have empowered me with the resilience and fortitude to successfully complete this dissertation. His blessings have been a constant source of inspiration and strength throughout this challenging journey, leading me to this significant achievement. With heartfelt gratitude, I acknowledge His divine intervention, shaping my path and fostering growth. This is as I embark on the next chapter of my academic and personal endeavors.

I extend my profound gratitude to my supervisor, Dr. Majid Jaberi-Douraki, whose unwavering dedication and support have been indispensable throughout this journey. I also extend my heartfelt thanks to the esteemed members of my committee, with special mention to Dr. Bacim Alali and Dr. Dinh-Liem Nguyen, whose insights and feedback have been invaluable. Additionally, I am deeply thankful to the faculty of the K-State Mathematics Department, particularly Dr. Andrew Bennett, Dr. Pietro Poggi-Corradini, Dr. Sarah Reznikoff, Dr. David Yetter, Dr. Nathan Albin and Dr. Victor Turchin for their unwavering support and contributions, which have greatly enriched my academic journey.

Furthermore, I am indebted to Dr. Reza Ghamarshoushtari, Dr. Lydia de Wolf and Ilyas Mustapha for their invaluable guidance throughout my doctoral program. Their mentorship, expertise, and encouragement have been instrumental in shaping my academic pursuits and personal growth.

My heartfelt gratitude extends to my family members, whose unwavering support has been the cornerstone of my success. To my beloved parents, Ibrahim Albayyadhi and Souad Bakkari, I owe an immeasurable debt of gratitude for their boundless love, encouragement, and patience.

I am deeply and foremost thankful to my husband, Dr. Hadi Mufti, whose unwavering encouragement and motivation have been my guiding light throughout this journey. Firstly

and lastly, without his unwavering support, both emotionally and financially, I would not have been able to overcome the challenges and achieve this milestone. His sacrifices, care, and patience have been a constant source of strength. I am equally appreciative of my siblings, Mohammad, Ahmad, Manar, Moayad, and Musab, whose support, prayers, and belief in me have been a source of inspiration.

Lastly, I am immensely grateful to my friends Azam Moradi and Malak Alsaati, Julee Youssef and my children, Dr. Yazan Mufti and Maysaa Mufti, whose unwavering love and support have been my driving force. Their understanding and devotion during this demanding period have been truly remarkable.

Dedication

To my beloved husband, Dr. Hadi Mufti,

To my children, Yazan and Maysaa,

With deepest love and gratitude

I dedicate this dissertation to you. Thank you for all the love, support, and encouragement you have given me. I cherish and love you more than anything.

Chapter 1

Introduction

Mathematical modeling entails the formulation of a system of equations, which extends to various types of equations such as differential, integral, or functional, collectively termed as models. Mathematical models are designed to encapsulate and portray phenomena such as biological or physiological events, whether observable directly or not. Leveraging mathematical principles, modeling enables researchers to delve into complex systems, predict outcomes, and examine scenarios that might prove arduous or impractical to investigate experimentally. Through rigorous scrutiny and validation, mathematical models serve as indispensable instruments for comprehending and unraveling the underlying mechanisms of natural phenomena[2]. This endeavor aids researchers in grasping real life challenges and is particularly pivotal in ecological research, facilitating the exploration of myriad variables such as plant defenses and the complexities of herbivore interactions impacting plant communities[3;4].

Furthermore, mathematical models in particular in terms of discrete-time dynamics, find widespread applications in physics, engineering, and mathematical biology. Continuous-time models exhibit distinct dynamical behaviors compared to discrete-time models with the latter often showcasing numerous complex dynamics[5–7].

Researchers and agricultural ecologists are keenly interested in discrete models describing interacting populations governed by differential equations. Discrete-time models are suitable for organisms with non-overlapping generations, such as annual plants and insect populations

with an annual life cycle. In contrast, continuous-time models are useful for organisms with overlapping generations dwelling in non-seasonal environments or seasonal environments with overlapping generations, such as perennial plants. Discrete-time models, in contrast to their continuous counterparts, can exhibit more complex or chaotic dynamical behavior. For instance, tropical insects with discrete generation periods, like Sugar-cane hoppers, exhibit rapid population growth, whereas those with overlapping generations, such as stylopids, affect host population dynamics through castration, thereby inducing discrete generations[8;9].

The fundamental interaction between plants and herbivores, steeped in predator-prey dynamics, has been a focal point in ecological discourse since antiquity. However, mathematical modeling of this interaction gained traction only in recent decades. Pioneering efforts by Lotka and Volterra laid the groundwork for modeling predator-prey relations, subsequently shaping modern approaches to modeling plant-herbivore interactions. These models, expanding upon the Lotka-Volterra framework, incorporate continuous and discrete-time dynamics, accounting for a spectrum of dynamics within plant-herbivore systems. This intricate relationship fosters a complex negative feedback loop critical for understanding ecosystem dynamics[10–13].

Caughley's delineation of plant-herbivore dynamics into non-interactive and interactive models underscores the complexity of these interactions. In non-interactive models, herbivores do not impede plant growth, implying minimal impact on vegetation growth rates or size. Consequently, biologists and agricultural ecologists favor difference equations, especially for species with non-overlapping generations, as they offer robust applications in discrete form[12;14].

For instance, the populations with short life cycles portray mostly non-overlapping generations; hence, the models are of the discrete nature. These include the recent past new mathematical approaches in the dynamical system, ranging from continuous to partial to discrete, all focusing on interactive systems[15]. According to McKendrick-von Foerster equation, Gutierrez et al. use a model based on partial differential equations for the effects of herbivores on different segments of plants[16;17]. In another strand of development, Leah Edelstein-Keshet proposed a model for a plant-herbivore system where the main variables are

plant quality and herbivore density[18]. Her study was based on the following mathematical model

$$\frac{dq}{dt} = f(q,h),$$
$$\frac{dh}{dt} = g(q,h)$$

where plant quality and herbivore population can be represented by the functional responses f and g, respectively. In accordance with the form of q and h, both functions were determined or conjectured using biological information for a particular system of plants and herbivores. Since q can be understood as the rate of change in plant quality and h can be understood as the rate of change in herbivore population density, both these changes are significant; considered to be in a time-dependent fashion to understand a change associated with plant quality and herbivore population density. The specific forms of these functions, denoted as q and etc. are determined or hypothesized, respectively, based on biological information that is quite system-specific to the plant and herbivore under study[19]. Biological information may pertain to plants' nutritive value, herbivore reproduction rates, and the efficiency of the plant being fed. It may also pertain to other ecological interactions. Such functional responses are incorporated into the mathematical model to be used in simulating and assessing plant-herbivore dynamics under a plethora of conditions and scenarios. This would provide in-depth knowledge of plant quality and herbivore population size, and how the two may be intertwined to impact dynamics overall within an ecosystem[20].

An interesting difference equation model was presented by Allen et al. in their paper that described the plant-herbivore system in order to uncover the dynamics and strategies of control in such ecological systems[21]. This model was developed considering two different control strategies, which remained independent: cane removal and pesticide application. The analysis pointed out the two steady-states within the system: one characterized by the fact of pest presence (disease state) and another one where the pest was absent (disease-free state)[22;23]. They have outlined, in the parameter space, different regions of global stability

of these steady-states. In addition, they showed that periodic solutions are present where global stability is absent. The periodic solutions bear the dynamics with chaotic areas. In the following system, you will find an overview of their analysis[24]:

$$F_{n+1} = \frac{F_n f(G_n)}{\alpha_1 + \alpha_2 F_n f(G_n)},$$
$$G_{n+1} = \alpha_3 (F_n + 1) G_n$$

here, F_0 and G_0 represent positive initial conditions, and the function f can take two forms f_1 or f_2 as follows:

$$f_1(G) = \frac{1}{1 + G^2},$$
$$f_2(G) = exp(-G).$$

Powell et al. undertook comprehensive research that extended mechanistic models from strategic population models of beetle outbreaks to those detailing the tactical behavior of beetles in selecting their host trees. Their analysis included both heuristic methods and empirical observations conducted in the field[25].

For instance, their qualitative heuristic comparison aligned Powell et al.'s representation of mountain pine beetle nesting population behavior more closely with observations made in 1980 by Geiszler et al. While Geiszler et al. focused on the cumulative number of successful mountain pine beetle attacks on a single focal tree, Powell et al. provided insights into the relative number of mountain pine beetles nesting in a focal tree per hour of flight[26]. Remarkably, the numbers depicted in Powell et al.'s diagram closely resembled those observed by Geiszler et al[27].

This represented an initial attempt to synthesize three distinct mathematical methodologies into a spatial framework for evaluating the risk of mountain pine beetle attack on individ-

ual hosts. Preliminary results from their study illustrate that stand microclimate—climatic factors measured at specific locations near Earth's surface—plays a central role in influencing attack risk, surpassing even host immunity and stand age[28].

Powell et al. also investigated deeply into the quantitative modeling and analysis of direct temperature control, exploring how these models exhibited dynamic seasonality in oviposition dates for succeeding generations. According to this analysis, the developmental circle map shows a stable steady state. It is related to univoltinism, which can result in high reproductive success in temperate climates by producing a single offspring throughout the season. Univoltine steady-states remained stable over wide temperature bands, but their edges were less stable due to disrupted maladaptive cycles, underscoring the intricate interplay between temperature and reproductive strategies.

Efforts to model the effects of periodic forcing on discrete-time have led to mathematical ecosystem models. These models are characterized by their dynamics defined through mathematical equations. It is worth noting that the specific equations employed may differ across ecosystems. As a result, a general form of such equation can be outlined[29]:

$$X_{n+1} = f(X_n) + F(t).$$

Here, X_n denotes the state of the ecosystem at time n, $f(X_n)$ describes the intrinsic dynamics of the ecosystem without external forcing, and $F(t)$ represents the periodic forcing function applied at time t.

For instance, in a basic Lotka-Volterra predator-prey model, the equations could be expressed as[30]:

$$P_{n+1} = P_n + rP_n(1 - P_n) - aP_nH_n + F(t),$$
$$H_{n+1} = H_n + bP_nH_n - dH_n + F(t),$$

where, P_n and H_n denote the number of prey (e.g., herbivores) and predators (e.g., car-

nivores) at time n, respectively. Parameters r, a, b, and d represent growth rates and interaction strengths, while $F(t)$ is the periodically applied forcing function over time t.

Summers et al. analyzed the effects of periodic forcing on four discrete-time ecosystem models[31]. Through their investigation, they demonstrated that such external stimuli could induce a property known as sensitive dependence on initial conditions, distinct from those identified in chaos theory. This property has the potential to alter the stability and dynamics of ecosystems, potentially leading to chaotic behavior. A periodic force is one that repeats itself at regular intervals and can be applied as a feedback stimulus. Their findings suggested that periodic forcing might indeed induce chaotic behavior. In a study by Summers, Danny, Justin G. Cranford, and Brian P. Healey, they examined four typical discrete-time ecosystem models under the effects of periodic forcing. They observed that periodic forcing can lead to dynamic chaos[31]. Moreover, Agiza et al[32] found chaotic dynamics in a discrete prey-predator model with Holling's Type II response function. In this study, natural death rates for predators were not taken into account. This discrete model exhibits a greater degree of dynamics than the continuous model, indicating that it is chaotic and complex. The model they presented was as follows:

$$x_{n+1} = ax_n(1 - x_n) - \frac{bx_n y_n}{1 + \alpha x_n},$$
$$y_{n+1} = \frac{cx_n y_n}{1 + \alpha x_n}$$

where a, b and c are positive parameters. The parameter a represents a prey's natural growth rate, similar to the growth rate found in the logistic equation. This models limited growth as the population approaches carrying capacity. parameters b and c govern the interactions between prey and predators: b illustrates the impact of predation on prey populations, while c illustrates the benefit predators gain from consuming pry. The variables x_n, and y_n represent prey and predator population densities respectively and vary as time changes based on the rules defined by model equations. The parameter α modified the inter-

action terms, restricting the growth rate of the predator population as the prey population increases.

Kartal analyzed the dynamics of a plant-herbivore model using both differential and difference equations[33]. This model can be represented by the following equations:

$$x_{n+1} = x_n\big(r - \alpha y_n\big)e^{-(r-\alpha y_n - rkx_n)},$$
$$y_{n+1} = y_n e^{\beta x_n - s}.$$

In Kartal's model, all parameters are positive, and he focuses on the behavior of the system within a specific sub-interval, which leads to difference equations that describe the system. As a result of his study, he discovered that the system was bounded, periodic, and had local and global stability conditions. Moreover, in certain regions of the parameter space, he identified Neimark-Sacker bifurcation.

In another study, Din et al. introduced a model of plant-herbivore interactions[34]. He performed bifurcation analysis and investigated chaos control in a plant-herbivore model with weak predator functional responses. In their study, they primarily examined topological classifications of steady-states. They demonstrated that the boundary steady state underwent transcritical bifurcation. In contrast, the positive steady state in the discrete-time plant-herbivore model experienced a Neimark–Sacker bifurcation. Based on the following equations, the model is defined as follows:

$$x_{n+1} = \frac{x_n}{a(1+y_n^2) + bx_n},$$
$$y_{n+1} = cy_n(1+x_n),$$

where x_n and y_n refer to the population densities of the plant (Grapevine) and the herbivore (Apple Twig Borer) respectively. The population dynamics in the model are influenced by

the parameters a, b and c, which all have positive values.

Predator and prey, parasite and host, mutualism, and competition between two species in nature can be classically modeled as follows:

$$P_{n+1} = f(P_n, H_n), \tag{1.1}$$
$$H_{n+1} = g(P_n, H_n).$$

By modeling both species' growth in the absence of the other, and by knowing the affect of their interaction on each other, the system in (1.1) is capable of describing the simultaneous population change. In its most basic form, such modelling can be described as follows:

$$P_{n+1} = aP_n + bP_nH_n,$$
$$H_{n+1} = cH_n + dP_nH_n.$$

Note that:

(i) If we choose $a > 1,\ b < 0,\ 0 < c < 1,$ and $d > 0$, then this will produce a predator-prey model in which growth and decline are exponential in the absence of the other species, where P_n represent the prey population.

(ii) If $a, c > 1$ and $b, d > 0$, then this will results in mutualism, where both species benefit from living together.

(iii) The terms P_nH_n refer to mass-actions in which species encounter randomly with significant outcomes, infecting or eating each other, for example.

In plant-herbivore interactions, Kang, Yun, Dieter Armbruster, and Yang Kuang[16] found quasiperiodicity, period-doubling, and chaos using a host-parasite model. According to observation, such a continuous model exhibits global stability at an interior steady state point.

Here is the typical methodology for discrete-generation host-parasite models

$$P_{n+1} = \lambda P_n f(P_n, H_n), \tag{1.2}$$

$$H_{n+1} = c\lambda P_n (1 - f(P_n, H_n)). \tag{1.3}$$

These models simulate the interaction between a host (a plant) and a parasite (a herbivore). In such models, P_n and H_n represent the biomass of the hosts (plants) and parasites (herbivores) in successive generations n and $n+1$ respectively. Here $\lambda = e^r$ represent the host's inherent rate of increase in the absence of the parasites where r indicate the intrinsic rate of increase, c is the biomass conversion constant and the function f indicates the fraction of hosts that survive parasitism each generation. As an alternative, f can indicate the probability of each host escaping parasites. Therefore, the complementary expression $1 - f$ indicates the probability of being parasitized in the second equation. As will be shown in the rest of this paper, n takes positive integer values. Among the simplest versions of this model are those of Nicholson[35] and Nicholson and Bailey[1] which investigated in depth a model in which the zero-term of one's Poisson distribution determines the proportion of hosts that escape parasitism, in particular,

$$f(P_n, H_n) = e^{-aH_n}. \tag{1.4}$$

In this case, a represents the mean number of encounters per host. As a result, $1 - e^{-aH_n}$ represents the probability of an attack on a host where $f = e^{-aH_n}$ represent Poisson distribution that describes the proportion of hosts escaping parasitism. In Equations (1.2) and (1.3), Equation (1.4) gives:

$$P_{n+1} = \lambda P_n e^{-aH_n}, \tag{1.5}$$

$$H_{n+1} = c\lambda P_n (1 - e^{-aH_n}). \tag{1.6}$$

Beddington et al.[36] propose the following modified Nicholson-Bailey model:

$$P_{n+1} = \lambda P_n e^{r(\frac{1-P_n}{P_{max}}) - aH_n}, \tag{1.7}$$

$$H_{n+1} = c\lambda P_n (1 - e^{-aH_n}). \tag{1.8}$$

Essentially, P_{max} is the so-called environment-imposed 'carrying capacity' for the host for carrying parasites without parasites in its environment. A host density dependence can be expressed as follows:

$$e^{r\left(\frac{1-P_n}{P_{max}}\right)}.$$

For a wide range of parameter values, what was an unstable positive steady state becomes locally stable, when no density-dependent relationship exists for host population growth[36]. In the case of other parameter values, there is a possibility that the model will generate attractors of different levels of complexity. These attractors can range from a set of regular limit cycles to weird and chaotic patterns.The structure of equations (1.7) and (1.8) illustrates that host density-dependence occurs at a particular stage of their life cycle according to the stage at which the parasites attack. The H_n herbivores hunt for P_n hosts before density-dependent growth regulation takes place. As a result, new herbivore generations are dependent on P_n, the original host population antecedent to parasitism.

A more realistic model could be created by using the following system

$$P_{n+1} = P_n e^{r\left(1-\frac{P_n}{k}\right)-bH_n}, \tag{1.9}$$

$$H_{n+1} = P_n(1 - e^{-aH_n}). \tag{1.10}$$

Additionally, when $b = a$, this model becomes Beddington's density-dependent predator-prey model[36]. Selecting an appropriate family chart (a set of coordinate changes dependent on a parameter), where $b = r$, the behavior of two populations is determined by a, r, and k. This system has the advantage that the Ricker difference equation $P_{n+1} = P_n e^{r\left(1-\frac{P_n}{k}\right)}$ confines the dynamics to $H = 0$ and limits the growth of the prey and prevents it from growing unrestrained.

In general, density-dependent models are represented by the following models according to[37]

$$P_{n+1} = P_n g(P_n) f(H_n), \tag{1.11}$$

$$H_{n+1} = P_n(1 - f(H_n)) \tag{1.12}$$

where f represents the fraction of prey that survives predation each generation. Conversely, when $a \neq b$, the previous result cannot be applied to system (1.9) and (1.10). In this case, we adopt a different approach in which this system can include both characteristics exhibited by the Neimark-Sacker bifurcation based on the following system

$$P_{n+1} = rP_n e^{-bH_n}, \tag{1.13}$$

$$H_{n+1} = P_n(1 - e^{-aH_n}) \tag{1.14}$$

as well as period-doubling bifurcations descended from Ricker map.

Based on the Neimark–Sacker bifurcation in the model, host and parasite populations

fluctuate around a mean value. These fluctuations would be stable and continue indefinitely under ideal conditions. This has been proven in[38] that the system (1.13) and (1.14) has a steady-state solution that is not trivial, whose value is stable within a given range of parameter values. In addition, there is a Neimark–Sacker bifurcation that produces attracting and repelling invariant curves in different areas of the parameter space.

Generally, a model of plant-herbivore interactions that was taken into account in[16] has the following form

$$P_{n+1} = P_n e^{r(1-\frac{P_n}{P_{max}})-aH_n}, \tag{1.15}$$

$$H_{n+1} = P_n e^{r(1-\frac{P_n}{P_{max}})}(1 - e^{-aH_n}). \tag{1.16}$$

Based on this, some of the following statements have been made by Asheghi[39]:

i. The P_n represents the biomass of a plant population after its defoliation but before it is attacked by the herbivore. Herbivore biomass, H_n, represents the biomass of herbivores in season n before they die.

ii. Plant biomass follows the dynamics of the Ricker model[40] in the absence of herbivores, particularly:

$$P_{n+1} = P_n e^{\left(1-\frac{p_n}{P_{max}}\right)},$$

assuming that r is a constant growth rate and that P_{max} is the maximum plant carrying capacity. The dynamics of rickers influence how much freshly-grown foliage is available for herbivores to consume.

iii. In prairie life it goes without saying that herbivores forage for foliage indiscriminately. In that case, the parameter a is designed to measure the amount of foliage that is consumed by herbivores. Since an herbivore's life cycle is one year, the larger the a, the faster it feeds.

iv. The biomass of a plant population decreases after herbivore attacks to a fraction e^{aH_n} of what it was in the absence of herbivores. As a result,

$$P_{n+1} = P_n e^{r(1-\frac{P-n}{P-max})-aH_n}.$$

v. Plant biomass is converted into herbivore biomass as a result of decreased biomass. It is assumed that c is a constant of one for biomass conversion. Accordingly, at the end of the season n, there will be

$$H_{n+1} = P_n e^{r\left(1-\frac{P_n}{P_{max}}\right)}(1 - e^{-aH_n}).$$

Kang et al.[16] investigated the interactions between specific plants and herbivores, developing a compelling host-parasite model. In their two-dimensional discrete-time model, they used leaf biomass and herbivore biomass as state variables. The model's parameter space included two key parameters: the growth rate of the host population and the damage inflicted by herbivores. The bifurcation diagrams presented within this parameter space were particularly insightful. The findings on bistability and the crisis of a strange attractor highlighted two potential strategies for managing herbivore populations: reducing the population below a certain threshold or enhancing the growth rate of the plant leaves. The model is described by the following equations:

$$x_{n+1} = x_n e^{r(1-x_n)-ay_n},$$
$$y_{n+1} = x_n e^{r(1-x_n)}(1 - e^{-ay_n}).$$

Armbruster et al.[16], presented the bifurcation diagram in the parameter space of equations (1.15) and (1.16) in their paper. Armbruster et al. suggests two ways to control the herbivore: by reducing the population below some threshold and by increasing the plant's growth rate.

Asheghi[39] examined the dynamic behavior of a discrete-time model represented by a two-dimensional map with four parameters. The analysis focused on local stability of steady-

states, period-doubling, and Neimark–Sacker bifurcations. Asheghi discovered that the standard forms of period-doubling and Neimark–Sacker bifurcations may exhibit either stability or instability. The plant–herbivore model is given by:

$$f(x, y) = xe^{r(1-\frac{x}{k})-by},$$
$$g(x, y) = x(1 - e^{-ay}),$$

where $x \geq 0$, $y \geq 0$, and all real parameters a, b, r, and k are positive with $a \neq b$.

Inspiration for our model arose from the significant impact of forest pests, which defoliate millions of acres of forest each year. This serves as just one example of the broader spectrum of plant-herbivore interactions, which pose significant challenges to both natural ecosystems and agricultural stability. Among these interactions, the European Gypsy Moth (Lymantria dispar or EGM) stands out as a particularly menacing threat to North America's forests. Originally introduced to Massachusetts in 1869, the European Gypsy Moth has wreaked havoc by devouring over 300 species of trees and shrubs in the northeastern United States alone. The insatiable appetite of gypsy moth caterpillars for foliage has earned them the notorious reputation of tree killers. Their feeding behavior not only damages trees but also renders them more susceptible to diseases and other pests.

Gypsy moths undergo a series of developmental stages, beginning as eggs and progressing through larval (caterpillar), pupal, and finally adult phases. Typically, female gypsy moths deposit between 500 to 1,000 eggs beneath tree bark. These eggs typically remain dormant until the spring season, with hatching occurring around April. Upon hatching, the caterpillars emerge and begin their feeding phase. By early summer, usually between June and early July, the caterpillars enter the pupal stage, where they undergo metamorphosis. Emerging from their pupae after approximately 10 to 14 days, adult Gypsy moths become active from July to August. During this time, they mate and lay eggs, continuing their lifecycle. It's noteworthy that the Gypsy moth population follows cyclic patterns, with fluctuations occurring in cycles that rise and fall over time. These fluctuations can result in large outbreaks of Gypsy moths, which can cause severe damage to trees and vegetation. Control measures

must be implemented to keep the Gypsy moth population in check[41–43].

Motivated by our understanding of ecological systems, we aim to develop a novel model depicted below. Our objective is to delve into the intricate dynamics of the system and unravel the annual occurrences driving its behavior.

In this study, we propose to explore a variation of the Nicholson-Bailey discrete host-parasite model. We present our modified Nicholson-Bailey model in the following manner:

$$\begin{aligned} x_{n+1} &= x_n f(x_n) g(y_n), \\ y_{n+1} &= x_n\big(1 - g(y_n)\big), \end{aligned} \tag{1.17}$$

where $f(x_n)$ and $g(y_n)$ are defined as following:

$$\begin{aligned} f(x_n) &= e^{r(1-x_n)}, \\ g(y_n) &= \frac{1}{1+\ln(by_n+1)}. \end{aligned}$$

Therefore equation (1.17) becomes:

$$\begin{aligned} x_{n+1} &= x_n e^{r(1-x_n)} \frac{1}{1+\ln(by_n+1)}, \\ y_{n+1} &= x_n\left(1 - \frac{1}{1+\ln(by_n+1)}\right), \end{aligned} \tag{1.18}$$

The discrete dynamical system induced by map (1.18) is given by

$$\begin{aligned} x_{n+1} =& \frac{x_n e^{r(1-x_n)}}{1+\ln(by_n+1)}, \\ y_{n+1} =& x_n\left(1 - \frac{1}{1+\ln(by_n+1)}\right), \end{aligned}$$

where the parameters r and b are positive, and $r \neq b$. We aim to conduct comprehensive

analyses on both local and global stability aspects of this model. Additionally, we will investigate the stability characteristics of period-doubling bifurcation phenomena within the system dynamics.

In conclusion, by taking into account the host population's growth and introducing a more comprehensive functional response to parasitism, our modified Nicholson-Bailey model gives more realism to the host-parasitoid interaction. It is anticipated that these changes will lead to a system that shows a wider range of behaviors. Furthermore, this will make our model more relevant to real-life applications where simple exponential decay and reproduction may not adequately capture actual dynamics in real-life situations like in Nicholson-Bailey's original model.

Following is a breakdown of this dissertation. In Chapter 2, we provide a comprehensive overview of discrete systems, examining concepts such as stability, center manifold, and bifurcation theory as applied to our models. Chapter 3 presents a scientific paper that investigates stability in the modified Nicholson-Bailey model, tracing the path to period-doubling bifurcation .

Chapter 2

Preliminaries

In this dissertation we examine steady-states stability in a modified Nicholson-Bailey discrete-time host-parasite model. We investigate whether these steady-states exhibit stability or instability and how the system's eigenvalues affect the model behavior. We also explore the possibility that parameter variations cause chaotic phenomena. Through several numerical simulations and analytical methods, this study unravels these dynamics under different conditions. This includes both boundary and interior steady-states in Chapter 3. Using the historical lineage of stability analysis and bifurcation theory for discrete-time dynamic systems, this dissertation places its contributions within the broader scientific discourse. It elucidates fundamental definitions and theorems crucial for understanding stability analysis. It integrates together insights from established principles such as the Stability Theorem and Center Manifold Theory. This dissertation provides a deeper understanding of the stability of the modified Nicholson-Bailey discrete-time model in complex systems by integrating historical context, theoretical foundations and novel empirical results. It sheds light on the relationship between the discrete-time model's parameters and stability, opening up the way for further advancements in this field.

2.1 Stability of a Steady State

Consider the function $F : \mathbb{R}^m \to \mathbb{R}^m$ and the sequence of generations at discrete time steps n, denoted by $X_n \in \mathbb{R}^m$. We define the discrete-time dynamical system as follows:

$$X_{n+1} = F(X_n), \quad n = 0, 1, \ldots \tag{2.1}$$

Let the initial population be represented by X_0. We define the steady state X^* as the value where $F(X^*) = X^*$ for some N. This means that once the system reaches X^* at time N, it remains at X^* for all subsequent time steps $n \geq N$. This condition characterizes the steady state of F. If the initial population X_{N_0} is close to X^*, and X_n remains close to or within a neighborhood of X^* for all $n \geq N_0$, we then describe X^* as a stable steady state.

To formally define stability, a steady-state point X^* is called stable if for all $\epsilon > 0$, there exists a neighborhood around X^* with a radius $\delta > 0$ such that for all initial states in the neighborhood, X_0 (i.e., $\|X_0 - X^*\| < \delta$), the future states will be within the ϵ-radius neighborhood of X^*. In other words:

$$\text{if} \quad \|X_0 - X^*\| < \delta, \quad \text{then} \quad \|X_n - X^*\| < \epsilon, \quad \forall n \geq 0 \quad .$$

Definition 2.1. *A steady state is called* ***(locally) Stable*** *if for any small $\epsilon > 0$, there exists a positive number $\delta = \delta(\epsilon)$. If the initial state X_0 is within this δ-neighborhood (i.e., $\|X_0 - X^*\| < \delta$), the solution X_n remains close to the steady state for all future steps n, specifically within a distance $\|X_n - X^*\| < \epsilon, \forall n \in \mathbb{N}$*[44].

Definition 2.2. *A steady state X^* is called* ***Asymptotically (locally) stable*** *if it is stable and there exists a positive constant c such that, when the initial state X_0 is close to the steady state (i.e., $\|X_0 - X^*\| < c$), the solution will converge to the steady state over time, that is, as n approaches infinity:*

$$\lim_{n\to\infty} \|X_n - X^*\| = 0.$$[44]

Definition 2.3. *The steady state X^* is called* ***unstable*** *if it is not stable*[44].

Theorem 2.1.1. *The stability of the steady state X^* can be calculated from the Jacobian matrix $J = DF(X^*)$, where D represents the derivative of F at X^*. If all eigenvalues of J have magnitudes less than 1, the steady state X^* is called stable. Conversely, if some eigenvalues of J have magnitudes greater than 1, the steady state X^* is considered unstable*[44].

Below we provide some more basic information regarding the Jacobian matrix and eigenvalues of J:

- **Jacobian Matrix:** The Jacobian matrix provides crucial insights into how small variations in the input variables influence the output behavior and dynamics of the function F. In the context of steady-state analysis, the Jacobian evaluated at the steady state X^* serves as a pivotal tool for evaluating the system's response to perturbations.

- **Eigenvalues and Stability:** The eigenvalues of the Jacobian matrix offer valuable information regarding the system's stability at the steady state:

  - **Stable Steady State:** If all eigenvalues possess magnitudes strictly less than one, though not necessarily on the unit circle, the steady state X^* is called locally stable. In such cases, perturbations around the steady state will gradually diminish over time.

  - **Unstable Steady State:** Conversely, if at least one eigenvalue exhibits a magnitude greater than one, the steady state X^* is considered unstable. Under these circumstances, perturbations will amplify, and the system will not revert to the steady state.

  - **Indeterminate Stability:** If at least one eigenvalue has a magnitude equal to 1, the linear analysis provided by the Jacobian matrix alone is not enough by itself in order to determine the stability of the steady state. In these cases, advanced techniques, such as center manifold theory, are needed to determine stability. These methods help to analyze the behavior of the system in the vicinity of the steady state and provide a more accurate determination of stability.

In this study, we outline two types of steady-states: hyperbolic steady-states and non-hyperbolic steady-states. The following is the formal definition of the term.

2.2 Characterization of Steady-States: Hyperbolic and Non-Hyperbolic Variants

The steady state X^* of the system $X_{n+1} = F(X_n)$, with $X \in \mathbb{R}^m$, is said to be **hyperbolic** if all eigenvalues of the Jacobian derivative $DF(X^*)$ have moduli different from 1. This means that the behavior of the system near the steady state is clearly either stable or unstable, but not marginally stable. Alternatively, X^* is **non-hyperbolic** if at least one of the eigenvalues of $DF(X^*)$ has a modulus of 1. This indicates a fine balance at the steady state, potentially leading to sustained oscillations or other complex dynamics due to the criticality in eigenvalues.

In our analysis, the application of transformations from the trace and determinant plane (tr det-plane) to other relevant planes emerges as a crucial concept. For this purpose, let us define the 2×2 matrix J as follows:

$$J = \begin{bmatrix} a & b \\ c & d \end{bmatrix}$$

This matrix J is derived from the Jacobian matrix $J = DF(X^*)$, which encapsulates locally essential information regarding the dynamics of the system at the steady state X^*. Within this framework, we introduce two fundamental quantities associated with J:

- **Trace** (tr): The trace of J, denoted as $tr = tr(J)$, represents the sum of its diagonal elements. It serves as a measure of the sum of the eigenvalues of J and provides insights into the overall behavior of the system.

- **Determinant** (det): The determinant of J, denoted as $det = det(J)$, is a scalar value computed as the product of its eigenvalues. This determinant captures crucial

information about the volume scaling factor induced by the transformation represented by J.

Both the trace and determinant are real numbers, offering valuable quantitative measures that underpin our analytical framework.

The following linearization theorem delineates the stability criteria governing the behavior of the system defined by the equations (2.1), wherein $X_0 = (x_0, y_0)$ represents the initial condition. The theorem provides a framework of the stability analysis for the system's trajectories for every possible initial condition in the two-dimensional space. Specifically, it examines the evolution of the state variables x and y governed by the iterative equations

$$x_{n+1} = f(x_n, y_n), \tag{2.2}$$
$$y_{n+1} = g(x_n, y_n).$$

2.3 Stability Properties of the Steady State

The following theorem known as the Linearized Stability Theorem, provides comprehensive conditions for analyzing the stability properties of the steady state X^* for each initial condition X_0 of (2.1) for the two-dimensional discrete-time system (2.2).

Theorem 2.3.1. *(Linearized Stability Theorem)*[45]

(i) If both roots of the quadratic equation

$$\lambda^2 - tr\ \lambda + det = 0 \tag{2.3}$$

*lie within the open unit disk $|\lambda| < 1$, then the steady state X^* of the discrete dynamic system (2.1) is called **locally asymptotically stable**.*

*(ii) Conversely, if at least one root of the equation (2.3) has an absolute value exceeding one, the steady state X^* of the discrete dynamic system (2.1) becomes **unstable**.*

(iii) *A necessary and sufficient condition for both roots to lie within the open unit disk* $|\lambda| < 1$ *is precisely defined by*

$$|tr| < 1 + det < 2, \tag{2.4}$$

in this scenario, the steady state X^* *of the discrete dynamic system* (2.1) *is referred to as a* ***sink****, indicating* ***local asymptotic stability****.*

(iv) *On the contrary, the steady state* X^* *transforms into a* ***repeller*** *if and only if both roots of the equation* (2.3) *have absolute values exceeding one, characterized by*

$$|det| > 1 \quad and \quad |tr| < |1 + det|. \tag{2.5}$$

(v) *A* ***saddle point*** *emerges if and only if one root of equation* (2.3) *has an absolute value less than one and the other exceeds one, satisfying the conditions*

$$tr^2 - 4det > 0 \quad and \quad |tr| > |1 + det|, \tag{2.6}$$

in this scenario, this ***saddle point*** *represents an* ***unstable steady state*** X^* *of the discrete dynamic system* (2.1)*.*

(vi) *Finally, a* ***non-hyperbolic point*** *occurs when one root has an absolute value equal to one, specified by*

$$|tr| = |1 + det|,$$

or when

$$det = 1 \quad and \quad |tr| \leq 2.$$

The following diagram in Figure 2.1 provides a graphical summary of the regions delineated by the Linearized Stability Theorem in the tr − det plane.

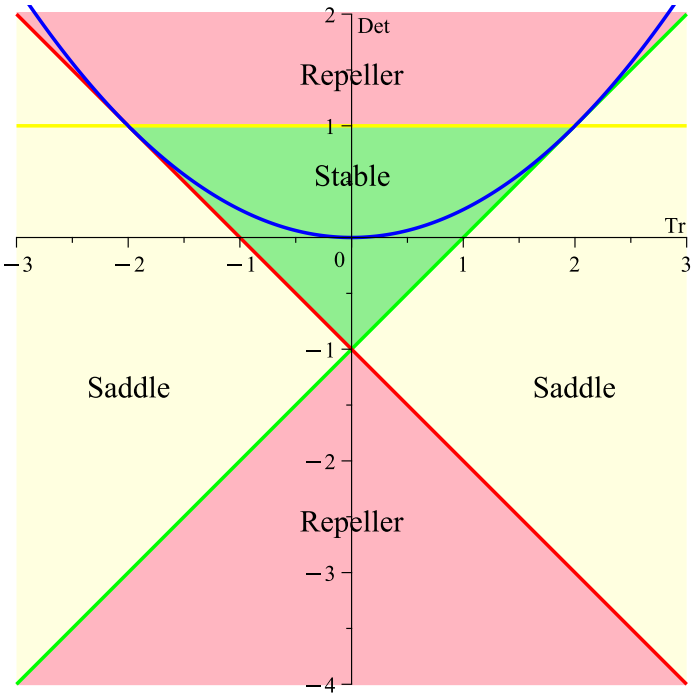

Figure 2.1: *Stability regions (stable, repelling, and saddle) in the trace-determinant plane.*

2.4 Stability Conditions

Using Linearized Stability Theorem (2.3.1), we derived the stability conditions as follows:

2.4.1 Stability Conditions

Based on inequality (2.4), we determine the stability conditions as:

$$\begin{cases} \det < 1 \\ \det > \mathrm{tr} - 1 \\ \det > -\mathrm{tr} - 1 \end{cases} \tag{2.7}$$

the first condition, $\det < 1$, follows from the right-hand side of inequality (2.4), while the condition $|\mathrm{tr}| < 1 + \det$ translates to $-1 - \det < \mathrm{tr} < 1 + \det$. Therefore, we derive the additional conditions $\det > \mathrm{tr} - 1$ and $\det > -\mathrm{tr} - 1$.

2.4.2 Repelling Condition

Based on inequality (2.5), we derive the repelling conditions as follows:

$$\begin{cases} \det < \mathrm{tr} - 1 \\ \det < -\mathrm{tr} - 1 \end{cases}$$

Or,

$$\begin{cases} \det > 1 \\ \det > \mathrm{tr} - 1 \\ \det > -\mathrm{tr} - 1 \end{cases} \tag{2.8}$$

2.4.3 Saddle Conditions

Based on inequality (2.6), we determine the saddle conditions as follows:

$$\begin{cases} \mathrm{tr} > 0 \\ \det < \mathrm{tr} - 1 \\ \det > -\mathrm{tr} - 1 \end{cases}$$

Or,

$$\begin{cases} \mathrm{tr} < 0 \\ \det > \mathrm{tr} - 1 \\ \det < -\mathrm{tr} - 1 \end{cases} \tag{2.9}$$

Understanding the dynamics of discrete-time systems based on nonlinear maps often relies on identifying key structures known as invariant manifolds. These manifolds play a crucial role in characterizing the behavior of the system by providing insights into its stability and evolution. Specifically, invariant manifolds allow for the computation of essential planes

such as the center manifold, stable manifold, and unstable manifold. These computations are fundamental in predicting the long-term behavior of dynamical systems, making invariant manifolds a central concept in the study of nonlinear dynamics and chaos theory.

2.5 Invariant Manifolds

Invariant manifolds predicting the long-term evolution of trajectories combines these trajectories that are asymptotically departing from or approaching an orbit, exhibiting key properties that remain unchanged under the system's dynamics. Of particular interest are stable and unstable manifolds, which respectively represent trajectories that converge toward or diverge away from a steady state point or periodic orbit. These manifolds are instrumental in analyzing its qualitative behavior. Additionally, center manifolds represent trajectories that evolve tangentially to the stable and unstable manifolds near steady states. Understanding invariant manifolds, including stable, unstable, and center manifolds, is essential for comprehending the complex dynamics of nonlinear systems and their behavior over time.

2.5.1 Stable and Unstable Manifolds

Let $\mathcal{X} \subset \mathbb{R}^m$ and defined the following function $F : \mathcal{X} \to \mathcal{X}$. Consider the sequence of generations at discrete-time steps n, denoted by $X_n \in \mathcal{X}$. This gives us the discrete-time dynamical system as follows:

$$X_{n+1} = F(X_n), \quad n = 0, 1, \ldots$$

The initial population represented by X_0, and the steady state of the function $F : \mathcal{X} \to \mathcal{X}$ represented by X^*, such that $F(X^*) = X^*$ for some N. This means that once the system reaches X^* at time N, it remains at X^* for all subsequent time steps $n \geq N$.

We define **stable** and **unstable** manifolds at X^* as follows:

$$W^s(X^*) = \{X \in \mathcal{X} : F^n(X) \to X^*,\ n \to \infty\},$$
$$W^u(X^*) = \{X \in \mathcal{X} : F^{-n}(X) \to X^*,\ n \to \infty\},$$

where X represents the state of the system at given discrete-time step, that is a point in the state space $\mathcal{X} \subset \mathbb{R}^m$. While, W^s represents the set of initial states whose trajectories eventually approach the stable steady state X^* as $n \to \infty$, and W^u represents the set of initial states whose trajectories move away from the stable steady state X^* as $n \to -\infty$[44].

The stable eigenspace E^s consists of the span of eigenvectors corresponding to eigenvalues with a modulus less than 1 indicating stability. Conversely, the unstable eigenspace E^u consists of the span of eigenvectors corresponding to eigenvalues with a modulus greater than 1. The following graph in Figure 2.2 illustrates the local stable and unstable manifolds that pass through origin $(0, 0)$.

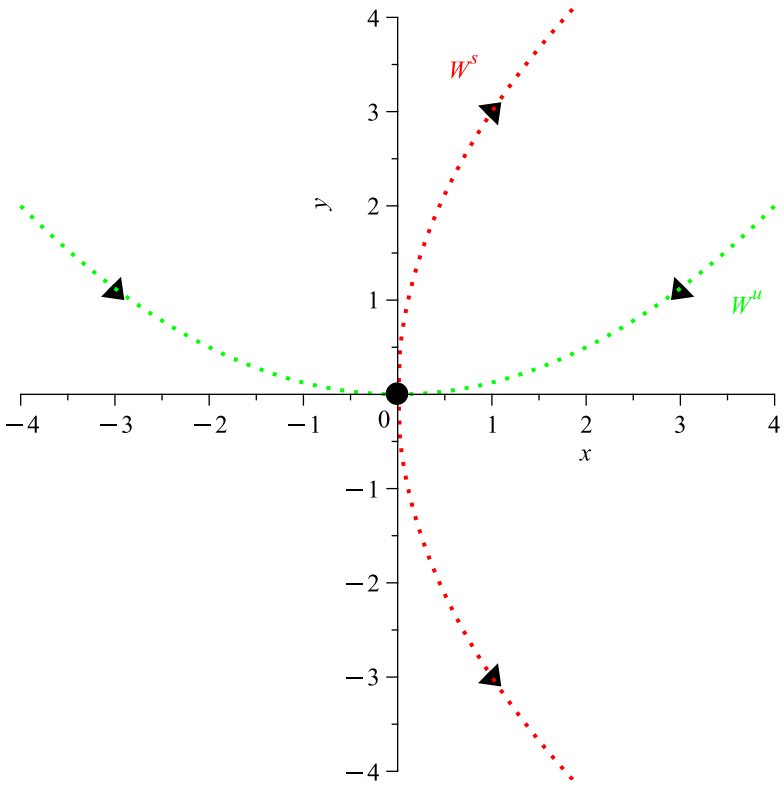

Figure 2.2: *The local stable and unstable manifolds pass through* $(0, 0)$.

Theorem 2.5.1. *(Invariant Manifold Theorem)*[46–48] *Assume that $F \in C^2$. Then there exist C^2 stable and unstable manifolds, W^s and W^u, which are tangent to E^s and E^u at $X = 0$, respectively. Additionally, there exists a C^1 center manifold, W^c, that is tangent to E^c at $X = 0$. Furthermore, the manifolds W^c, W^s, and W^u are all invariant under F.*

Now we will define the center manifold and provide a brief explanation of the center manifold theory.

2.5.2 Center Manifolds

In this section, we present the essential definitions and theorems required to analytically determine the center manifold, as well as the stable and unstable manifolds for any nonlinear system. To introduce the center manifold theory for maps, we begin with the following definition.

Definition 2.4. *(Center Manifold, Wiggins*[49]*) Suppose we have the map*

$$\begin{bmatrix} X \\ Y \end{bmatrix} \mapsto \begin{bmatrix} AX + F(X,Y) \\ BY + G(X,Y) \end{bmatrix}, \tag{2.10}$$

where X is the center variable, and Y is the stable variable and $(X,Y) \in \mathbb{R}^c \times \mathbb{R}^s$. Moreover, F and G are $\mathcal{C}^t$ $(t \geq 2)$ nonlinear, second order or higher, map in some neighborhood of the origin, A is a $c \times c$ matrix having eigenvalues with modulus one, and B is an $s \times s$ matrix having eigenvalues with modulus less than one.

We can present the map as a system of difference equation such that

$$\begin{aligned} X_{n+1} &= AX_n + F(X_n, Y_n), \\ Y_{n+1} &= BY_n + G(X_n, Y_n), \end{aligned} \tag{2.11}$$

where

$$F(0_c, 0_s) = 0_c, \quad \text{and} \quad DF(0,0) = 0_{c\times(c+s)},$$
$$G(0_c, 0_s) = 0_s, \quad \text{and} \quad DG(0,0) = 0_{s\times(c+s)}.$$

The study of the dynamics of the system at origin $(0,0)$ is of the utmost importance since we can always shift the steady state to origin by translation. As a result, the **center manifold** is defined locally as follows:

$$W^c(0) = \{(X,Y) \in \mathbb{R}^c \times \mathbb{R}^s | Y = h(X), |X| < \delta, h(0) = 0, Dh(0) = 0\}.$$

Here, δ is a sufficiently small positive constant that defines the neighborhood around the origin where the center manifold is valid. The function h represents the graph of the center manifold and satisfies the conditions $h(0) = 0$ and $Dh(0) = 0$, meaning that h passes through the origin and has a zero derivative at the origin, respectively. This ensures that the center manifold is tangent to the center eigenspace at the origin. Note that $(0,0)$ is a steady state of (2.10), and the linear approximation alone cannot determine its stability because at least one of the eigenvalues has a modulus of 1. Consequently, we have the following theorem.

Theorem 2.5.2. *(Wiggins[49]) There exists a $\mathcal{C}^t$ center manifold for solutions of map (2.10). The dynamics of map (2.10) restricted to the center manifold, for U sufficiently small, is given by the following the c- dimensional map*

$$U \longmapsto AU + F(U, h(U)), \quad U \in \mathbb{R}^c. \tag{2.12}$$

Theorem 2.5.3. *(Stability)[50]*

(i) Suppose the steady state of (2.12) is stable, asymptotically stable or unstable; then the steady state of (2.10) is also stable, asymptotically stable, or unstable respectively.

(ii) Suppose the steady state of (2.12) is stable. Then if (X_n, Y_n) is a steady state of (2.10)

with (X_0, Y_0) *sufficiently small, there is a solution* U_n *of* (2.10) *such that as* $n \to \infty$,

$$X_n = U_n + \mathcal{O}(e^{-\gamma n}),$$
$$Y_n = h(U_n) + \mathcal{O}(e^{-\gamma n}),$$

where $\gamma > 0$ *is a constant.*

In simpler words, this theorem states that for initial conditions of the entire system that are sufficiently close to the origin, the trajectories through them asymptotically approach a trajectory on the center manifold. Specifically, steady states near the origin, orbits with small amplitudes, and small homo-clinic and hetero-clinic orbits are all contained within the center manifold.

2.5.3 Center Manifold Theory

In order to compute the center manifold h, we consider it in the following form

$$Y = h^c(X) = a_2X^2 + a_3X^3 + \cdots + a_nX^n + \mathcal{O}(X^{n+1}) \equiv 0,$$

where $a_n \neq 0$, and $a_2, \cdots, a_n$ to be determined.

Every point (X, Y) of $W^c(0)$ satisfies the equation

$$Y_{n+1} = h(X_{n+1}). \tag{2.13}$$

By Substituting

$$X_{n+1} = AX_n + F\big(X_n, h(X_n)\big),$$
$$Y_{n+1} = h(X_{n+1}) = Bh(X_n) + G\big(X_n, h(X_n)\big),$$

into equation (2.13), it yields

$$h\Big(AX + F\big(X, h(X)\big)\Big) = Bh(X) + G\big(X, h(X)\big).$$

As a final step, we define $\mathcal{N}\big(h(X)\big)$ in order to find the center manifold as follows:

$$\mathcal{N}\big(h(X)\big) = h\Big(AX + F\big(X, h(X)\big)\Big) - Bh(X) - G\big(X, h(X)\big) = 0$$

An excellent graphical technique for assessing steady state stability is the cobweb diagram. When we calculate the center manifold, we use the cobweb diagram to ensure the stability of the steady state using the center manifold theory. On the $XY-$ plane, we plot a diagonal line $Y = X$ and the center manifold $Y = h(X)$ and by iteration of a point close enough to the origin. In Figure 2.3 as iteration goes forward the red endpoint gets closer and closer to the origin, so at this case origin is an attractor which means the steady state is stable. However, in Figure 2.4 as iteration goes foreword, the red endpoint goes away from origin, so at this case origin is repeller which means it is unstable steady state.

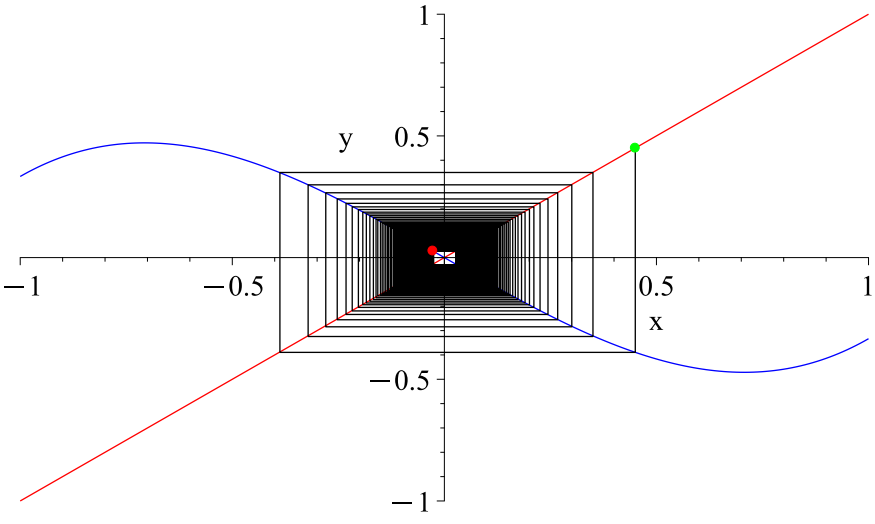

Figure 2.3: *Cobweb diagram of the center manifold* $h(x) = \frac{2}{3}x^3 - x$*, which shows the origin is stable a steady state point.*

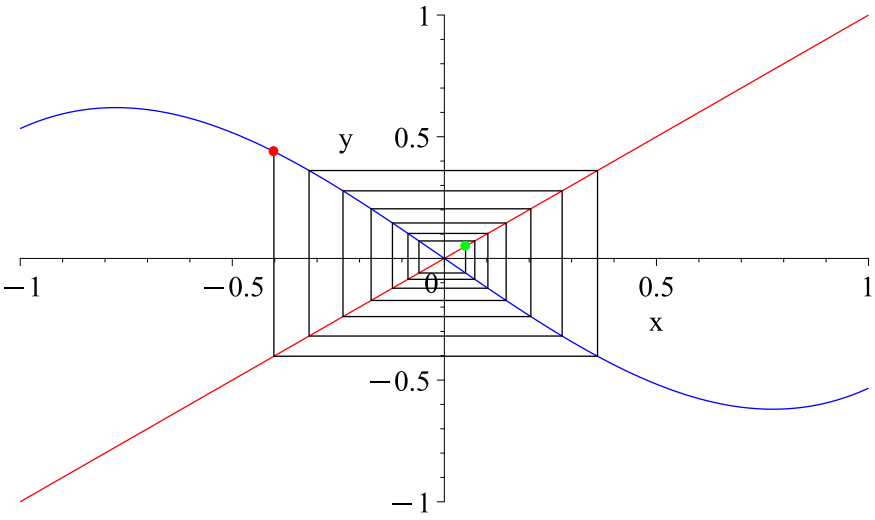

Figure 2.4: *Cobweb diagram of the center manifold* $h(x) = \frac{2}{3}x^3 - 1.2x$*, which shows the origin is unstable a steady state point.*

2.6 Global Stability

In dynamical systems theory, the global stability of a steady state is a fundamental property. This indicates that trajectories near the steady state converge to it over time, regardless of initial conditions. In other words, if a system exhibits global stability at a steady state, any trajectory starting sufficiently close to the steady state will eventually approach and remain near it indefinitely. This property is crucial in understanding the long-term behavior of dynamical systems, particularly in ecological and epidemiological models, where steady states represent stable states such as extinction or endemic steady state. Global stability analysis helps determine whether a system will persist in a particular state or eventually reach a different state over time.

2.6.1 Persistence of the Host

To study the global stability of a steady state in a discrete-time dynamical system, it is essential to understand the persistence of the host. This can be achieved by examining the eigenvalues of the Jacobian matrix at the steady state.[51]

Definition 2.5. *Suppose T is a topological space and $F : T \to T$ is a map. Let $N \subset T$ such that*

$$Inv(N, F) = \{x \in N \mid F^{\,n}(x) \in N \text{ for all } n \in \mathbb{Z}\}$$

then,

*(i) A compact set N is called an **isolating neighborhood** if $Inv(N, F) \subseteq int(N)$.*

*(ii) A set $S \subset T$ is called an **isolated invariant set** if there exist an isolating neighborhood N such that $S = Inv(N, F)$.*

Definition 2.6. *A **semi-flow** is a map $\omega : J \times T \longrightarrow T$, where $J \subseteq \mathbb{Z}$ that satisfies:*

(i) Discrete evolution property: The map $\omega(n, \cdot) : T \longrightarrow T$, defined by $\omega(n, x) = \omega_n(x)$ is continuous for all $n \in J$.

(ii) Semi group property:

$$\omega(0, x) = x,$$
$$\omega(n + m, x) = \omega\big(m, \omega(n, x)\big), \quad \forall n, m \in J, \quad \text{and} \quad x \in T.$$

Definition 2.7. *Let ω be a semi-flow, $J \geq 0 \in \mathbb{Z}$, and $\gamma : T \longrightarrow \mathbb{R}$. Then*

*(i) $\omega : J \times T \longrightarrow T$ is called **weakly γ-persistent**, if*

$$\limsup_{n\to\infty} \gamma\big(\omega(n, x)\big) > 0, \quad \forall x \in T, \quad \gamma(x) > 0.$$

*(ii) ω is called **weakly uniformly γ-persistent**, if there exist some positive number ε such that*

$$\limsup_{n\to\infty} \gamma\big(\omega(n, x)\big) > \varepsilon, \quad \forall x \in T, \quad \gamma(x) > 0.$$

(iii) ω *is called* ***strongly uniformly*** γ***-persistent****, if there exist some positive number* ε *such that*

$$\liminf_{n\to\infty} \gamma\big(\omega(n,x)\big) > \varepsilon, \quad \forall x \in T, \quad \gamma(x) > 0.$$

Definition 2.8. *Let* ω *be a semi-flow such that* $\omega : J \times T \longrightarrow T$ *is called* ***point dissipative****, if there exist bounded subset* B *of* T *which attracts all points in* X*.*

Definition 2.9. *Let* A *be nonempty subset of* T*, then we say* A *is an* ***attractor*** *if there exist a neighborhood* U *of* A *that is attracted to* A*.* U *is called an attractor neighborhood of* A*.*

Definition 2.10. *Let* R *be nonempty subset of* T*, then we say* R *is an* ***reppellor*** *if there exist a neighborhood* U *of* R *such that for all* $x \notin R$*, there is* $0 < n_x \in J$*, and* $\omega(n,x) \notin U$*, where* $n \geq n_x$*.* U *is called an repellor neighborhood of* R*.*

2.7 Bifurcation

In this section, we will explore the fundamental aspects of bifurcation theory, exploring its various types and how they influence the theory. Bifurcation, in essence, refers to the occurrence of topologically distinct behaviors in discrete dynamic systems as a parameter changes. In simple terms, system dynamics change with alterations in specific parameters. We are primarily interested in elucidating how bifurcation points are identified within parameter spaces. In addition, we intend to gain a better understanding of the associated stability implications. To achieve this, we introduce the required conditions and definitions necessary for the thorough examination of our models in this study.

2.7.1 Properties of Bifurcation

Consider a parametric discrete-time dynamical system

$$\mathcal{X} \mapsto F(\mathcal{X}, t), \quad \mathcal{X} \in \mathbb{R}^m, t \in \mathbb{R}$$

where the map F is smooth with respect to both $\mathcal{X}$ and t. For $t = t^*$, and $X, X^* \in \mathcal{X}$, suppose $X = X^*$ represents the hyperbolic steady state. As the parameter t varies, we can determine the stability of the steady state by analyzing the eigenvalues of jacobian matrix $J = DF(X^*, t^*)$.

A steady state X^* is called non-hyperbolic if at least one of the eigenvalues of the jacobian matrix $J = DF(X^*, t^*)$ satisfies one of the conditions below:

- $\lambda = 1$ as positive eigenvalue.
- $\lambda = -1$ as negative eigenvalues.
- $\lambda_1 = e^{i\theta_0}$ and $\lambda_2 = e^{-i\theta_0}$ as a pair of complex eigenvalues where $0 < \theta_0 < \pi$ for some value of the parameter t.

The following Figure 2.5 illustrates the three cases:

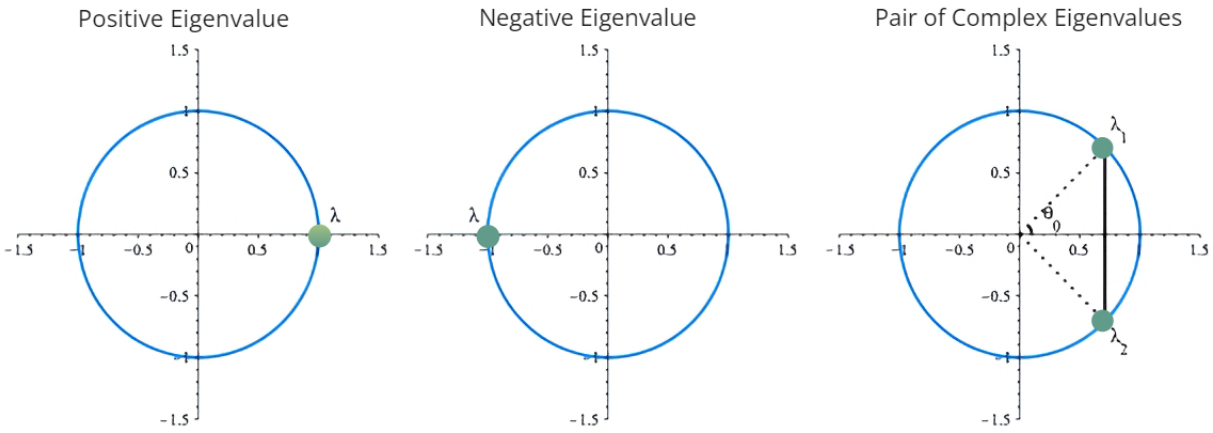

Figure 2.5: *A positive eigenvalue approaches the unit circle ($\lambda = 1$), a negative eigenvalue approaches the unit circle ($\lambda = -1$), or a pair of simple complex eigenvalues reach the unit circle ($\lambda_1 = e^{+i\theta_0}, \lambda_1 = e^{-i\theta_0}, \quad 0 < \theta_0 < \pi$).*

Following, we explore three fundamental types of local bifurcations of the system $X_{n+1} = F(X_n)$, providing some insight into dynamical systems' qualitative characteristics. Bifurcations occur at parameter values where a steady-state or periodic orbit becomes non-hyperbolic, resulting in topologically distinct behavior. It's important to note that steady states of a map become non-hyperbolic when one or more eigenvalues obtained from the Jacobian matrix lie on the unit circle, indicating a potential bifurcation point in the parameter space. Generally, bifurcations can be classified as follows: Period-Doubling Bifurcation, Saddle-Node Bifurcation and Neimark-Sacker Bifurcation.

2.7.2 Period-Doubling Bifurcation

In dynamic systems theory, the Period-Doubling Bifurcation occurs due to slight parameter variations, causing the emergence of an additional periodic trajectory twice as long as the original. This bifurcation results in the system visiting numerical values that repeat themselves after twice as many iterations in discrete dynamic systems. This occurs at non-hyperbolic steady-states, where one eigenvalue of the linearization equals -1, indicating a critical point in the system's dynamics.

Definition 2.11. *A **flip** or **period-doubling** bifurcation occurs when the eigenvalue $\lambda_1 = -1$ appears in the system.*

Methodology of period-doubling bifurcation

Consider a one-parameter family of $\mathcal{C}^n$ where $n \geq 2$ one-dimensional maps

$$x \mapsto f(x,t), \;\; x \in \mathbb{R}^1, t \in \mathbb{R}^1 \tag{2.14}$$

According to Wiggins[49], the sufficient conditions for the occurrence of the period-doubling bifurcation are given as follows:

$$f(0,0) = 0, \tag{2.15}$$

$$\frac{\partial f}{\partial x}(0,0) = -1, \tag{2.16}$$

$$\frac{\partial (f \circ f)}{\partial t}(0,0) = 0, \tag{2.17}$$

$$\frac{\partial^2 (f \circ f)}{\partial x^2}(0,0) = 0, \tag{2.18}$$

$$\frac{\partial^2 (f \circ f)}{\partial x\, \partial t}(0,0) \neq 0, \tag{2.19}$$

$$\frac{\partial^3 (f \circ f)}{\partial x^3}(0,0) \neq 0. \tag{2.20}$$

The sign of the quotient

$$\Big(\frac{\partial^3 (f \circ f)(0,0)}{\partial x^3} \Big/ \frac{\partial^2 (f \circ f)(0,0)}{\partial x\, \partial t}\Big)$$

indicates which branch of the period-doubling bifurcation occurs. The period-doubling bifurcation branch is **stable** if

$$\Big(\frac{\partial^3 (f \circ f)(0,0)}{\partial x^3} \Big/ \frac{\partial^2 (f \circ f)(0,0)}{\partial x\, \partial t}\Big) < 0,$$

and it is **unstable** if

$$\Big(\frac{\partial^3 (f \circ f)(0,0)}{\partial x^3} \Big/ \frac{\partial^2 (f \circ f)(0,0)}{\partial x\, \partial t}\Big) > 0.$$

2.7.3 Saddle-Node Bifurcation

Definition 2.12. *A **fold**, **tangent**, or **saddle-node** bifurcation is identified by the appearance of the eigenvalue $\lambda_1 = 1$. This type of bifurcation shares similar conditions with the period-doubling bifurcation.*

2.7.4 Neimark-Sacker Bifurcation

Definition 2.13. *A* ***Neimark-Sacker*** *or* ***torus bifurcation*** *is characterized by the presence of the eigenvalues* $\lambda_1 = e^{i\theta_0}$ *and* $\lambda_2 = e^{-i\theta_0}$*, where* $0 < \theta_0 < \pi$*. Visualizing this bifurcation requires a map in two or more dimensions.*

The following Figure 2.6 summarizes and illustrates the thresholds of the three main types of bifurcations in the tr-det plane. The Neimark-Sacker bifurcation occurs when crossing the det $= 1$ curve, the Period-Doubling bifurcation occurs when crossing the det $= -\text{tr} - 1$ curve, and the Saddle-Node bifurcation occurs when crossing the det $= \text{tr} - 1$ curve.

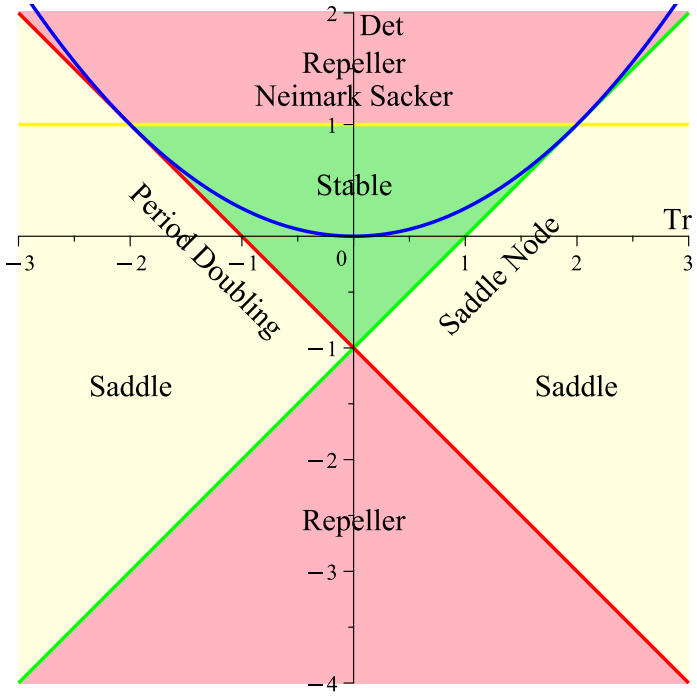

Figure 2.6: *The existence of three primary types of bifurcations in the trace-determinant plane.*

Chapter 3

Exploring Stability in a Modified Nicholson-Bailey Model: Tracing the Path to Period-Doubling Bifurcation

3.1 Introduction

In this chapter, we explore the dynamic behavior of a host-parasite system by a modified Nicholson-Bailey (MNB) model, incorporating three biological parameters within the first quadrant of the phase plane. Using a re-scaling procedure, we then simplify the MNB model to a two-parameter system that retains most of the original model's comprehensive dynamics. The simplified model consistently exhibits three steady states: two boundary steady states and a unique interior steady state, Which can emerge under specific conditions related to one of the parameters.

We proceed by analyzing the local stability of each steady state across different parameter ranges through the linearization of the model around each steady state. For parameter values that result in a non-hyperbolic steady state, we examine the stability and dynamics using bifurcation diagram derived from the center manifold theory. Additionally, we employ the Jacobian matrix to identify thresholds that determine the system's stability or instability.

We then conduct a stability analysis of a period-doubling bifurcation, a specific type of bifurcation leading to chaotic behavior, which may occur as these stability thresholds are crossed, potentially leading to chaotic dynamics. Our findings are corroborated by several simulations.

3.2 Model

Nicholson-Bailey host-parasite model

The original Nicholson-Bailey host-parasite model, incorporating three parameters, was first proposed in 1935. It predicted that the parasite population would eventually reach a stable level of infection, where the rate of infection equals the rate of recovery. This model has been adapted to account for the effects of factors such as seasonality and virulence of the parasite[52].The foundational model is represented by the following two-dimensional map:

$$x_{n+1} = \lambda x_n e^{-ay_n},$$
$$y_{n+1} = cx_n(1 - e^{-ay_n}),$$

where $x_{n+1} = \lambda x_n e^{-ay_n}$ represent the host equation and $y_{n+1} = cx_n(1 - e^{-ay_n})$ represent the parasitoid equation:

i. x_n is the host population with generation n.

ii. y_n is the parasitoid population with generation n.

iii. λ represents the host population's growth rate without parasites.

iv. a is the parameter describes the efficiency of parasitoids in searching for hosts or attack rate of parasitoids.

v. c is the parameter describes average number of viable offspring is produced per parasitized host.

In other word, x_{n+1} describes the host population in the next generation, λx_n describes the possibility of growth of the host population without parasitism and e^{-ay_n} describes percentage of host populations that escape parasitization or survive assuming that parasitism follows a Poisson process. While y_{n+1} describes the parasitoid population in the next generation, and $x_n(1-e^{-ay_n})$ describes the number of hosts that are got parasitized where the transforming factor that transforms parasitized hosts into new parasitoids is given by c.

Modified Nicholson-Bailey host-parasite model (MNB)

The MNB host-parasite model has been further expanded and generalized by different studies to accommodate additional ecological complexities. Among the significant extensions, one introduces density dependence for the host population[53]. In this generalized model, a parameter λ is introduced as a function of the host population x_n with size n. This parameter λ effectively reduces the host population when it reaches a certain threshold density k. The reduction is modeled using the first term of the Poisson distribution[16]. Following is a modified version of the model:

$$\begin{aligned} x_{n+1} &= x_n e^{r\left(1-\frac{x_n}{k}\right)} e^{-ay_n}, \\ y_{n+1} &= cx_n(1-e^{-ay_n}), \end{aligned} \tag{3.1}$$

Generally we can describe the previous model by the following functions:

$$\begin{aligned} f(x) &= e^{r\left(1-\frac{x}{k}\right)}, \\ g(y) &= e^{-ay}, \end{aligned}$$

such that the model (3.1) becomes

$$F(x,y) = xf(x)g(x), \tag{3.2}$$
$$G(x,y) = cx(1-g(y)).$$

In this dissertation, we study another version of Nicholson-Bailey model (3.2) that we modified in the first closed quadrant with the following functions:

$$f(x) = e^{r\left(1-\frac{x}{k}\right)},$$
$$g(y) = \frac{1}{1+\ln(by+1)},$$

where the function $f(x)$ called the host growth function, describes the density dependent growth rate of the host population, taking into account the effects of the environment's carrying capacity. The parameter r (growth rate) describes the rate at which a host population grows. It shows how quickly the host population can grow under suitable conditions without limiting factors. The parameter k (carrying capacity) describes the maximum population size the environment can handle. As the host population approaches k, the growth rate slows down. Over all the exponential term $e^{r\left(1-\frac{x}{k}\right)}$ adjusts the host growth rate based on population density. When the population size x is much smaller than k i.e $x < k$, the term $\frac{x}{k}$ will be small and the exponential term is close to e^r, representing fast growth. As x approaches k i.e. $x = k$, $\frac{x}{k}$ reaches 1, and the exponential term reaches $e^0 = 1$, indicating that the growth rate slows down and becomes stable as the population approaches carrying capacity. When the host population x exceeds k i.e. $x > k$, then $\frac{x}{k}$ is greater than 1, as a result the term $r\left(1-\frac{x}{k}\right)$ becomes negative and the exponentiation $e^{r\left(1-\frac{x}{k}\right)}$ function decreases resulting in having $f(x) < 1$. This means the host population grows slower as the population size exceeds its carrying capacity. In other words, when the population x decreases because the growth rate is less than 1, eventiually the population will return to its carrying capacity. The function $g(y)$ called parasitoid effectiveness function, describes the effectiveness of parasitoids on parasitizing hosts which is reduced as the parasitoid population grows due to the

real world ecological conditions. The parameter b affects parasitoids' effectiveness in finding and parasitizing hosts. It adjusts how the function responds to changes in the parasitoid population y. While the logarithm function $\ln(by+1)$ shows a decreasing effect, this indicates that as the parasitoid population y increases, the rate at which new parasitoids can successfully parasitize hosts slows down. This illustrates the biological reality that beyond a certain point, having more parasitoids does not proportionally increase the parasitism rate. This is due to limitations such as interference among parasitoids or saturation of available hosts. Overall, the term $\frac{1}{1+\ln(by+1)}$ guarantees that the function $g(y)$ decreases as y increases, indicating the decreasing effectiveness of parasitoids in finding new hosts as their population grows.

Given the updated host growth function $f(x)$ and the parasitoid effectiveness function $g(y)$, model (3.2) yields the following form:

$$\begin{aligned} F(x,y) &= xe^{r\left(1-\frac{x}{k}\right)}\left(\frac{1}{1+\ln(by+1)}\right), \\ G(x,y) &= x\left(1-\frac{1}{1+\ln(by+1)}\right). \end{aligned} \tag{3.3}$$

From the two-dimensional map defined by equation (3.3), we define the following system of differential equations:

$$\begin{aligned} x_{n+1} &= x_n e^{r\left(1-\frac{x_n}{k}\right)}\left(\frac{1}{1+\ln(by_n+1)}\right), \\ y_{n+1} &= x_n\left(1-\frac{1}{1+\ln(by_n+1)}\right). \end{aligned} \tag{3.4}$$

By the re-scaling $X_n = \frac{x_n}{k}$, $Y_n = \frac{y_n}{k}$ and $B = bk$, system (3.4) of differential equations become:

$$
\begin{aligned}
X_{n+1} &= X_n e^{r\left(1-X_n\right)}\left(\frac{1}{1+\ln(BY_n+1)}\right),\\
Y_{n+1} &= X_n\left(1-\frac{1}{1+\ln(BY_n+1)}\right).
\end{aligned}
\tag{3.5}
$$

Therefore the functions $f(x)$ and $g(y)$ turn into the form

$$
\begin{aligned}
\tilde{f}(X) &= e^{r(1-X)},\\
\tilde{g}(Y) &= \frac{1}{1+\ln(BY+1)}.
\end{aligned}
$$

For simplicity denote $X_n, Y_n, B, \tilde{f}, \tilde{g}$ by x_n, y_n, b, f, g respectively and replace them in (3.4). As a result, we arrive at model that we will study in the next part in the following final form:

$$
\begin{aligned}
x_{n+1} =& \frac{x_n e^{r(1-x_n)}}{1+\ln(by_n+1)},\\
y_{n+1} =& x_n\left(1-\frac{1}{1+\ln(by_n+1)}\right).
\end{aligned}
\tag{3.6}
$$

In comparison to the Original Nicholson-Bailey Model, the MNB Model has the following characteristics:

- Mathematically: According to Nicholson-Bailey's model, their basic model is rather limited, yielding easy predictions of population fluctuations. However, at the same time, the model is unstable and undergoes oscillations due to the absence of control mechanisms inside the population. While MNB model provides more mathematical complexity than the previous model, where more parameter values can be used to produce dynamic variations such as instability of equilibrium, complex oscillations of the state, or chaos-like motions. As a result, it makes sense since in natural ecosystems,

the size of populations is affected by a number of factors.

- Biologically: The basic Nicholson-Bailey model employs the constant growth rate of the host population λ and represents parasitoids' impact as a simple exponential decay. The efficacy of parasitoids is entirely quantified by the parameter a, the searching efficiency. The model suggests oscillation or sometimes chaotic behavior but there are no processes therein, through which the host population is regulated apart from parasitism. On the other hand, the MNB model includes more realistic biological interactions. The MNB model encompasses biological interactions. Thus, the growth of the host population is dependent both on parasitism and density, adding a logistic aspect to growth. it also adds more complexity to the interaction between host and parasitoid populations by incorporating parameters through denoting by n the interaction between host and parasitoid populations. This interaction includes a logarithmic term $\ln(by_n + 1)$ as an estimate of the impact of parasitoid density on parasitism rates. It is possible that this could mimic real life ecological situations like density-dependent parasitism in which there is always assumed efficiency at a certain level of parasitoid intensity when it comes to parasite density.

The forthcoming study will focus on the described MNB model (3.3), where $x_n \geq 0$, $y_n \geq 0$ and $x_n > y_n$ denote the densities of a host population and a parasitoid population, respectively, at time point n. The model aligns with the Nicholson-Bailey definition outlined in the original paper. The parameters b and r represent key factors: b influences the host-parasitoid interaction, while r denotes the host population growth rate. Additionally, it is assumed that the biological process of reproduction may occur between generation n and $n + 1$ as Wang in her work on difference and differential equations provided valuable insights[54]. This assumption allows us to model host population dynamics, and to study parasite effects on population growth. The parameters b and r are the key determinants of the host-parasitoid interaction, and can be used to model and predict how the host population will change over time.

3.3 Steady States

A steady state of a two-dimensional dynamical system is a point $p = (p_1, p_2) \in \mathbb{R}^2$ such that there is $n_0 \in \mathbb{N}$ with $(x_{n_0+k}, y_{n_0+k}) = (p_1, p_2)$ for every $k \in \mathbb{N}$. To find the steady state(s) of a discrete dynamical system, we should solve $(x_{n+1}, y_{n+1}) = (x_n, y_n) = (p_1, p_2)$ for (p_1, p_2).

For $b > 1$, the steady states of the system (3.6) in the first quadrant are $S_0 = (0, 0)$, $S_1 = (1, 0)$, and $S_i = (x^*, y^*)$. The interior equilibrium point $S_i = (x^*, y^*)$ of system (3.6) is the unique intersection point of the following two maps:

$$f_1(y, b) = \frac{r - \ln\big(1 + \ln(by + 1)\big)}{r},$$
$$f_2(y, b) = \frac{y\big(1 + \ln(by + 1)\big)}{\ln(by + 1)},$$

where $x^* = 1 - \frac{1}{r}\ln\big(1 + \ln(by^* + 1)\big)$ and $y^* = x^*\big(1 - e^{-r(1-x^*)}\big)$. The intersection will fall in the interior of the first quadrant when $b > 1$.

Proposition 3.3.1. *For any $b > 1$, the following functions*

$$f_1(y, b) = \frac{r - \ln\big(1 + \ln(by + 1)\big)}{r},$$
$$f_2(y, b) = \frac{y\big(1 + \ln(by + 1)\big)}{\ln(by + 1)},$$

have a unique intersection falls in the interior of the first quadrant.

Proof. To prove that $f_1(y, b)$ and $f_2(y, b)$ have a unique intersection in the first quadrant where $b > 1$, we will analyze the behavior of these two functions.

Note that f_1 and f_2 are both decreasing functions with respect to b since

$$\frac{\partial f_1}{\partial b}(y, b) = \frac{-y}{r(by + 1)\big(1 + \ln(by + 1)\big)} < 0,$$
$$\frac{\partial f_2}{\partial b}(y, b) = \frac{-y^2}{\ln(by + 1)^2(by + 1)} < 0.$$

Moreover,

$$\frac{\partial f_1}{\partial y} = \frac{-b}{r(by+1)\big(1+\ln(by+1)\big)} < 0,$$
$$\frac{\partial f_2}{\partial y} = \frac{y\big(\ln(by+1)^2 b + \ln(by+1)b - b\big) + \ln(by+1)^2 + \ln(by+1)}{\ln(by+1)^2(by+1)} > 0.$$

Since $b > 0$ and $y > 0$ therefore $\ln(by+1) > 0$ and $by + 1 > 0$, thus $\frac{\partial f_1}{\partial y} < 0$. Now we want to show that $\frac{\partial f_2}{\partial y} > 0$. By analysing numerator $\frac{\partial f_2}{\partial y} > 0$, clearly $\ln(by+1)^2 > 0$, so all what we need is to check the sign of the following function

$$f_{22}(y,b) = y\big(\ln(by+1)b - b\big) + \ln(by+1) = \ln(by+1)(by+1) - by.$$

Note that $\frac{\partial f_{22}}{\partial y} = \ln(by+1)b > 0$, therefore f_{22} is an increasing function with respect to y and $f_{22}(0,b) = 0$, hence f_{22} is a positive function for $y > 0$. That implies $\frac{\partial f_2}{\partial y} > 0$ for $y > 0$. Moreover, $\lim_{y\to 0} f_1(y,b) = 1$, $\lim_{y\to\infty} f_1(y,b) = -\infty$ and $\lim_{y\to 0} f_2(y,b) = \frac{1}{b} < 1$, $\lim_{y\to 0} f_2(y,b) = \infty$. Therefore, f_1 and f_2 have a unique intersection in the interior of the first quadrant for every $b > 1$. □

If $b < 1$ then $\frac{1}{b} > 1$, hence $y^* < 0$ which is outside of our study scope. The following diagram in Figure 3.1 illustrates three cases for different b values. It shows where the unique intersection falls when $b > 1$, $b < 1$ and $b = 1$

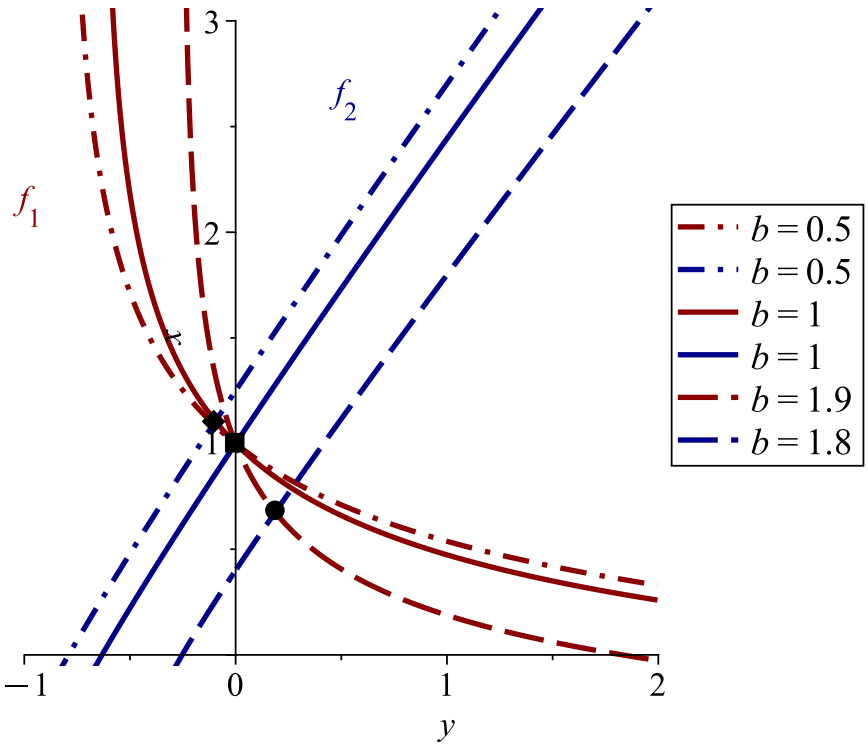

Figure 3.1: *Graph of the unique intersections of the functions f_1 and f_2, for three different values of parameter b, $b < 1$, $b = 1$ and $b > 1$.*

3.4 Analysis of Local Stability of Steady States

In this section, we delve into the local stability analysis of the model described by system (3.6). Local stability, in dynamical systems, involves examining the behavior of a system within small neighborhoods surrounding each of its steady states. The system's stability is evaluated by linearizing it about each steady state, a process facilitated by the computation of the corresponding Jacobian matrix. Subsequently, we proceed to investigate the stability of the steady states of system (3.6) by employing linearization techniques. Prior to this analysis, we establish the relationship between the variables x and y by considering the mappings described in equation (3.2).

The Jacobian matrix of system (3.6) is given by:

$$J\big(F(x,y),G(x,y)\big) = \begin{bmatrix} \partial_x F(x,y) & \partial_y F(x,y) \\ \partial_x G(x,y) & \partial_y G(x,y) \end{bmatrix}$$
$$= \begin{bmatrix} \frac{e^{r(1-x)}}{1+\ln(by+1)} - \frac{xre^{r(1-x)}}{1+\ln(by+1)} & -\frac{xe^{r(1-x)}b}{\big(1+\ln(by+1)\big)^2(by+1)} \\ 1-\frac{1}{1+\ln(by+1)} & \frac{xb}{\big(1+\ln(by+1)\big)^2(by+1)} \end{bmatrix}. \tag{3.7}$$

For $x \neq 0$ the Jacobian matrix (3.7) reduces into the following form

$$J\big(F(x,y),G(x,y)\big) = \begin{bmatrix} 1-rx & \frac{-xb}{\big(1+\ln(by+1)\big)(by+1)} \\ \frac{y}{x} & \frac{xb}{\big(1+\ln(by+1)\big)^2(by+1)} \end{bmatrix}. \tag{3.8}$$

Note that reduced Jacobian matrix (3.8) can be used to study the stability of all steady states except for the steady state $S_0 = (0,0)$.

At the steady state $S_0 = (0,0)$ by equation (3.7), the Jacobin matrix equals to

$$J\big(F(0,0),G(0,0)\big) = \begin{bmatrix} e^r & 0 \\ 0 & 0 \end{bmatrix}.$$

The eigenvalues of $J(0,0)$ are $\lambda_1 = e^r$ and $\lambda_2 = 0$ with the corresponding eigenvectors $v_1 = \langle 1,0\rangle$ and $v_2 = \langle 0,1\rangle$ respectively. Since $|\lambda_1| > 1$ and $|\lambda_2| < 1$, the system repelles in direction of v_1 and is neutrally stable (attracts) in direction of v_2. Therefore, $S_0 = (0,0)$ is a saddle point.

At the second steady state $S_1 = (1,0)$, the Jacobian matrix, as defined by equation (3.7), is as follows:

$$J\big(F(1,0),G(1,0)\big) = \begin{bmatrix} 1-r & -b \\ 0 & b \end{bmatrix}. \tag{3.9}$$

The eigenvalues of $J(1,0)$ are $\lambda_1 = 1-r$ and $\lambda_2 = b$ with the corresponding eigenvectors $v_1 = \langle 1,0\rangle$ and $v_2 = \langle -\frac{b}{-1+r+b}, 1\rangle$ respectively.

Proposition 3.4.1. *For different values of parameters b and r, the location of the eigenvalues λ_1 and λ_2 varies with respect to the unit circle. Therefore, for stability of the steady state $S_1 = (1, 0)$ of MNB given by (3.6), we have the following cases:*

First, we consider the cases when $S_1 = (1, 0)$ is a hyperbolic equilibrium,

i. If $b < 1$ and $0 < r < 2$, then $|\lambda_1| < 1$ or $-1 < \lambda_1 < 1$ and $|\lambda_2| < 1$ or $0 < \lambda_2 < 1$. So the steady state $S_1 = (1, 0)$ is an attracting node (stable node).

ii. If $b < 1$ and $r > 2$, then $\lambda_1 < -1$ and $0 < \lambda_2 < 1$. So the steady state $S_1 = (1, 0)$ is a saddle point (half stable).

iii. If $b > 1$ and $r > 2$, then $\lambda_1 < -1$, and $\lambda_2 > 1$. So the point $S_1 = (1, 0)$ is a repelling node (unstable node).

iv. If $b > 1$ and $0 < r < 2$, then $-1 < \lambda_1 < 1$,and $\lambda_2 > 1$. So the steady state $S_1 = (1, 0)$ is a saddle point (half stable).

Next, in the specific scenario where either $b = 1$ or $r = 2$, the steady state $S_1 = (1, 0)$ becomes non-hyperbolic. The stability analysis of such a non-hyperbolic steady state can be conducted using bifurcation formulas derived from center manifold theory. The proposition provided below delves into the stability of the steady state $S_1 = (1, 0)$ for non-hyperbolic cases in system (3.6).

Proposition 3.4.2. *According to system (3.6), the following statements can be made:*

i. If $b = 1$ and $0 < r < 2$, then the steady state $S_1 = (1, 0)$ is non-hyperbolic semi-stable (unstable).

ii. If $r = 2$ and $b < 1$, then the steady state $S_1 = (1, 0)$ is asymptotically stable.

iii. If $b > 1$, and $r = 2$, or if $b = 1$, and $r > 2$, then the steady state $S_1 = (1, 0)$ in these two cases is unstable.

iv. If $r = 2$ and $b = 1$, then the steady state $S_1 = (1, 0)$ is non-hyperbolic and it is hard to determine wither the steady state $S_1 = (1, 0)$ is stable or not.

Proof. i. By applying center manifold theory and analyzing the dynamic behavior restricted to the center manifold in the first closed quadrant, we will show that $S_1 = (1, 0)$ is an unstable steady state. For simplicity, by the translation $T : (x, y) \to (x + 1, 0)$, the point $S_1 = (1, 0)$ is translated to the origin. Let $\tilde{H}(x, y) = (\tilde{F}(x, y), \tilde{G}(x, y))$, where

$$\begin{aligned}\tilde{F}(x, y) &= \frac{(x+1)e^{-rx}}{1+\ln(by+1)} - 1,\\ \tilde{G}(x, y) &= (x+1)\left(1 - \frac{1}{1+\ln(by+1)}\right).\end{aligned}$$

Therefore, the discrete dynamical system (3.6) after applying the translation T becomes

$$\begin{aligned}x_{n+1} &= \frac{(x_n+1)e^{-rx_n}}{1+\ln(by_n+1)} - 1,\\ y_{n+1} &= (x_n+1)\left(1 - \frac{1}{1+\ln(by_n+1)}\right).\end{aligned} \tag{3.10}$$

First, we calculate the Taylor expansion of $\tilde{F}$ and $\tilde{G}$:

$$\begin{aligned}P_{\tilde{F}}(x, y) = &-(r-1)x - by + \frac{r(r-2)}{2}x^2 + (r-1)bxy + \frac{3b^2}{2}y^2\\ &- \frac{r^2(r-3)}{6}x^3 - \frac{r(r-2)b}{2}x^2y - \frac{3(r-1)b^2}{2}xy^2 - \frac{7b^3}{3}y^3 + O(4),\\ P_{\tilde{G}}(x, y) = &\, by - \frac{3}{2}b^2y^2 + bxy + \frac{7}{3}b^3y^3 - \frac{3}{2}b^2xy^2 + O(4).\end{aligned} \tag{3.11}$$

The Jordan normal form of the linear part of (3.11) is as follows:

$$\begin{bmatrix} x \\ y \end{bmatrix} = \begin{bmatrix} 1 & \frac{-b}{b+r-1} \\ 0 & 1 \end{bmatrix} \begin{bmatrix} u \\ v \end{bmatrix} = \begin{bmatrix} u - \frac{b}{b+r-1}v \\ v \end{bmatrix}. \tag{3.12}$$

Let $J = QDQ^{-1}$ be the diagonalization of J, where Q is a 2×2 matrix with its first

and second column consisting of the eigenvectors of $1-r$ and b respectively, and D is a diagonal matrix with $1-r$ and b on its diagonal. In terms of matrices D and Q, equation (3.10) can be written as:

$$\begin{aligned}\begin{bmatrix} x_{n+1} \\ y_{n+1} \end{bmatrix} &= J \begin{bmatrix} x_n \\ y_n \end{bmatrix} + \begin{bmatrix} P_{\tilde{F},3}(x_n, y_n) \\ P_{\tilde{G},3}(x_n, y_n) \end{bmatrix} \\ &= QDQ^{-1} \begin{bmatrix} x_n \\ y_n \end{bmatrix} + \begin{bmatrix} P_{\tilde{F},3}(x_n, y_n) \\ P_{\tilde{G},3}(x_n, y_n) \end{bmatrix},\end{aligned} \tag{3.13}$$

where $P_{\tilde{F},3}$ and $P_{\tilde{G},3}$ are the non-linear parts of $P_{\tilde{F}}$ and $P_{\tilde{G}}$, respectively.

By the change of variables given as

$$\begin{bmatrix} u_n \\ v_n \end{bmatrix} = Q^{-1} \begin{bmatrix} x_n \\ y_n \end{bmatrix}, \tag{3.14}$$

the system (3.13) reduces to:

$$\begin{bmatrix} u_{n+1} \\ v_{n+1} \end{bmatrix} \mapsto \begin{bmatrix} 1-r & 0 \\ 0 & 1 \end{bmatrix} \begin{bmatrix} u_n \\ v_n \end{bmatrix} + Q^{-1} \begin{bmatrix} P_{\tilde{F},3}(u_n, v_n) \\ P_{\tilde{G},3}(u_n, v_n) \end{bmatrix}, \tag{3.15}$$

where

$$\begin{aligned} Q^{-1}P_{\tilde{F},3}(u_n, v_n) &= \frac{r(r-2)}{2}u^2 + \frac{b(br+1)}{b+r-1}uv + \frac{b^2(br+2r^2-3b-4r+1)}{2(b+r-1)^2}v^2 \\ &\quad - \frac{b^3(5b^2r+13br^2+7r^3-14b^2-35br-21r^2+19b+21r-5)}{6(b+r-1)}v^3 + O(4), \\ Q^{-1}P_{\tilde{G},3}(u_n, v_n) &= buv + \left(-\frac{3b^2}{2} - \frac{b^2}{b+r-1}\right)v^2 + \left(\frac{7b^3}{3} + \frac{3b^3}{2(b+r-1)}\right)v^3 + O(4). \end{aligned}$$

Therefore, the center manifold of system (3.15) is given by:

$$
\begin{aligned}
u = h(v) &= \alpha v^2 + \beta v^3 + O(v^4) \\
&= \frac{2r^2 - 3r - 2}{2r^3} v^2 + \frac{-7r^4 + 32r^3 - 9r^2 - 51r - 18}{6r^5} v^3 + O(v^4),
\end{aligned} \tag{3.16}
$$

where v represents the dynamics of the center manifold and is defined by the map:

$$
V : v \mapsto v + \left(-\frac{3b^2}{2} - \frac{b^2}{b + r - 1} \right) v^2 + O(v^3). \tag{3.17}
$$

Figure 3.2 and Figure 3.3 show the iteration of map (3.17). The green dot represents the starting point of the iteration, and the red dot represents the ending point of the iteration, so any orbit starting at a sufficiently small positive v is attracted to 0 as it shows in Figure 3.2 , and any orbit starting at a sufficiently small negative v is repelled from 0 as it shows in Figure 3.3. Hence, $v = 0$ is a semi-stable (unstable) steady state. By equation (3.12), we have $x = u - \frac{b}{b+r-1} v$ and $y = v$, therefore the center manifold at the point $S_1 = (1, 0)$ in the original coordinates has the following form:

$$
\begin{aligned}
x + 1 &= u - \frac{b}{b + r - 1} v \\
x &= -1 - \frac{b}{b + r - 1} y + \frac{2r^2 - 3r - 2}{2r^3} y^2 + \frac{-7r^4 + 32r^3 - 9r^2 - 51r - 18}{6r^5} y^3.
\end{aligned} \tag{3.18}
$$

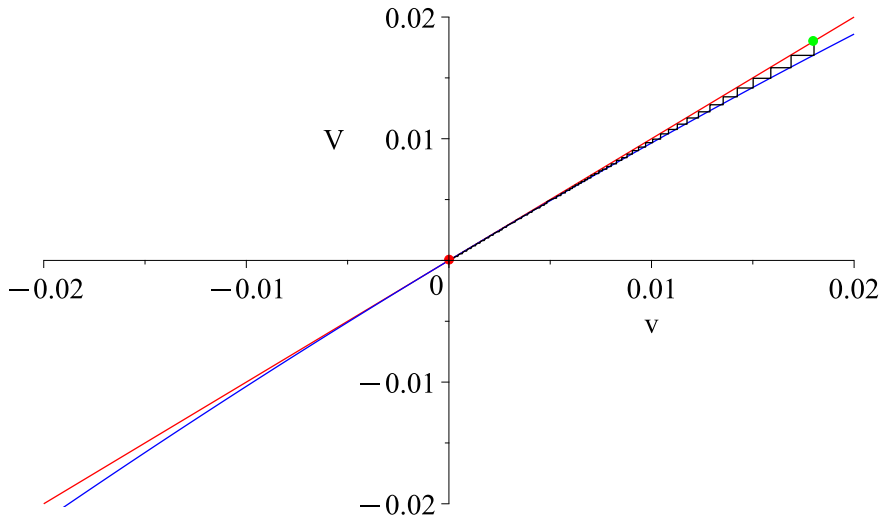

Figure 3.2: *Iteration diagram of non-hyperbolic steady state* $S_1 = (1, 0)$ *for* $b = 1$ *and* $0 < r < 2$. *Any orbit starting at a sufficiently small positive* v *is attracted to origin.*

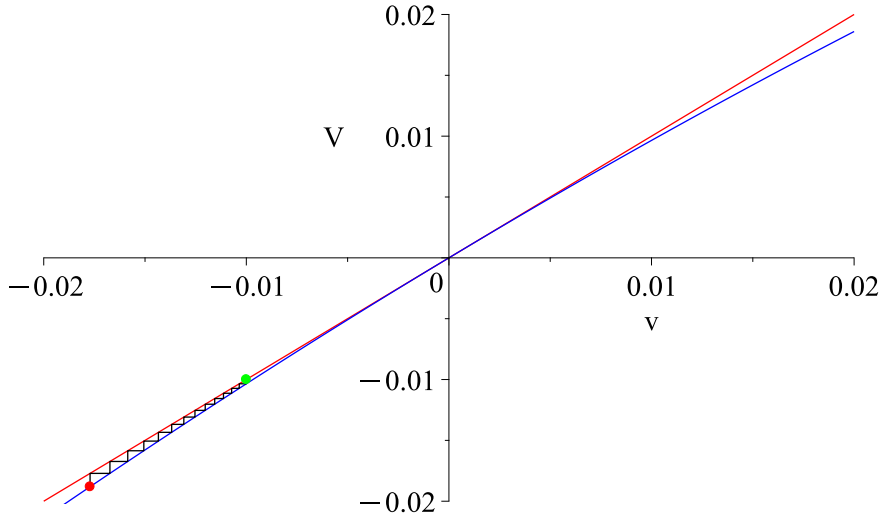

Figure 3.3: *Iteration diagram of non-hyperbolic steady state* $S_1 = (1, 0)$ *for* $b = 1$ *and* $0 < r < 2$. *Any orbit starting at a sufficiently small negative* v *is repelled from origin.*

ii. If $r = 2$ and $b < 1$, then the eigenvalues of $J(1, 0)$ are $\lambda_1 = 1 - r = -1$ and $\lambda_2 = b < 1$. Thus, the steady state $S_1 = (1, 0)$ is asymptotically stable. This is shown by applying center manifold theory since one of eigenvalues modulus is one.

By repeating the same center manifold calculation that we had in (i), we arrive at the following result: The center manifold of system (3.15) is given by:

$$\begin{aligned} v = h(u) &= \alpha u^2 + \beta u^3 + O(u^4) \\ &= 0u^2 - \frac{1}{16}u^3 + O(u^4), \end{aligned} \tag{3.19}$$

where u represents the dynamics of the center manifold and is defined by the map:

$$U : u \mapsto (1-r)u + \frac{2}{3}u^3 + O(u^4). \tag{3.20}$$

Figure 3.4 and Figure 3.5 show the iteration of map (3.20). The green dot represents the starting point of the iteration, and the red dot represents the ending point of the iteration, so any orbit starting at a sufficiently small positive u is attracted to 0 as it shows in Figure 3.4 , and any orbit starting at a sufficiently small negative u is is also attracted to 0 as it shows in Figure 3.5. Hence, $u = 0$ is a stable steady state. By equation (3.12), we have $x = u - \frac{b}{b+1}v$ and $y = v$, therefore the center manifold at the point $S_1 = (1, 0)$ in the original coordinates has the following form:

$$\begin{aligned} x + 1 &= u - \frac{b}{b+1}v \\ x &= -1 + u - \frac{b}{b+1}y \\ &= -1 - (16y)^{\frac{1}{3}} - \frac{b}{b+1}y. \end{aligned} \tag{3.21}$$

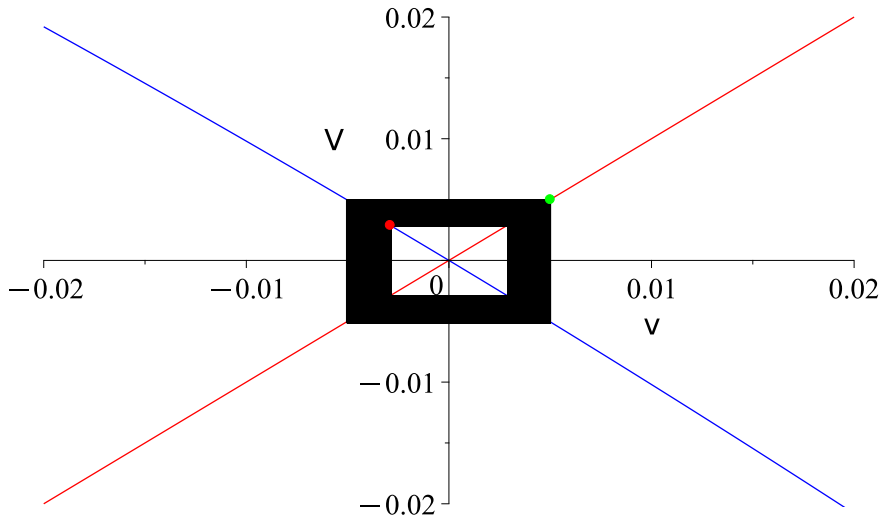

Figure 3.4: *Iteration diagram of non-hyperbolic steady state* $S_1 = (1, 0)$ *for* $r = 2$ *and* $b < 1$. *Any orbit starting at a sufficiently small positive* u *is attracted to origin.*

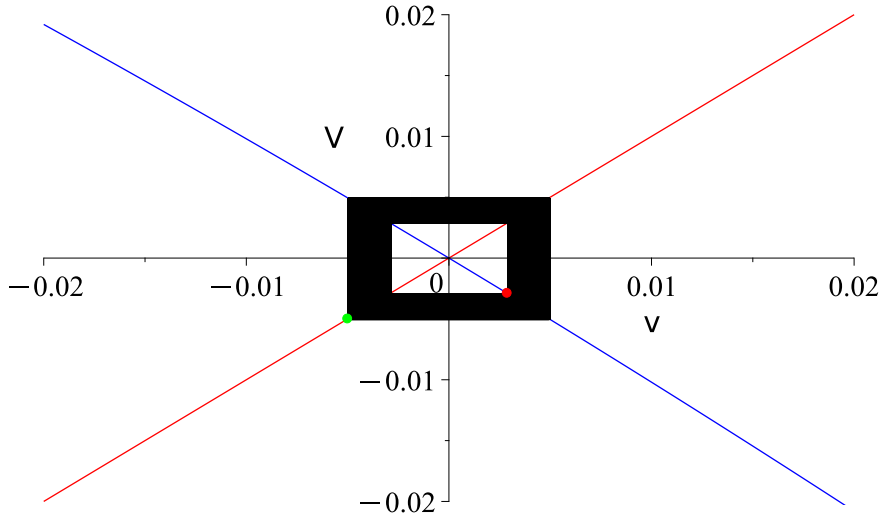

Figure 3.5: *Iteration diagram of non-hyperbolic steady state* $S_1 = (1, 0)$ *for* $r = 2$ *and* $b < 1$. *Any orbit starting at a sufficiently small negative* u *is attracted to origin.*

iii. If $b > 1$, $r = 2$, then we have $|\lambda_1| = 1$, $|\lambda_2| > 1$, and if $b = 1$, $r > 2$, then $|\lambda_1| > 1$, $|\lambda_2| = 1$. Therefore, to determine stability of steady state $S_1 = (1, 0)$ in these two cases we apply center manifold theory which implies that $S_1 = (1, 0)$ is unstable due to the presence of a one-dimensional unstable direction and one-dimensional center direction at the point $S_1 = (1, 0)$.

iv. If $r = 2$ and $b = 1$, then the system (3.6) will reduce to the following system

$$\begin{aligned} x_{n+1} =& \frac{x_n e^{2-2x_n}}{1 + \ln(y_n + 1)}, \\ y_{n+1} =& x_n\Big(1 - \frac{1}{1 + \ln(y_n + 1)}\Big). \end{aligned} \tag{3.22}$$

note that the system (3.22) has no steady state in the interior of the first quadrant $\mathcal{Q}_1$. The steady state $S_0 = (0, 0)$ has eigenvalues $|\lambda_1| = e^2 > 1, |\lambda_2| = 0 < 1$ with corresponding eigenvectors $\langle 1, 0\rangle$ and $\langle 0, 1\rangle$, respectively. Thus at this steady state the x-axis is unstable while the y-axis is stable, hence $S_0 = (0, 0)$ is a hyperbolic saddle point.

On the other hand, the steady state $S_1 = (1, 0)$ is a non-hyperbolic steady state since it has eigenvalues $\lambda_1 = 1,\ \lambda_2 = -1$ with corresponding eigenvectors $\langle 1, 0\rangle$ and $\langle -1, 1\rangle$, respectively. Since both eigenvalues have a modulus of one, we can not apply center manifold theory to analyze the stability at this point. Although a mathematical proof of instability is challenging, numerical simulations indicate that the steady state $S_1 = (1, 0)$ is unstable. This is evident from the trajectories plotted with various initial conditions for x and y, where even after $20,000$ iterations, the trajectories do not converge to $S_1 = (1, 0)$, as shown in Figure 3.6. The plot clearly demonstrates the divergence of the trajectories from the steady state.

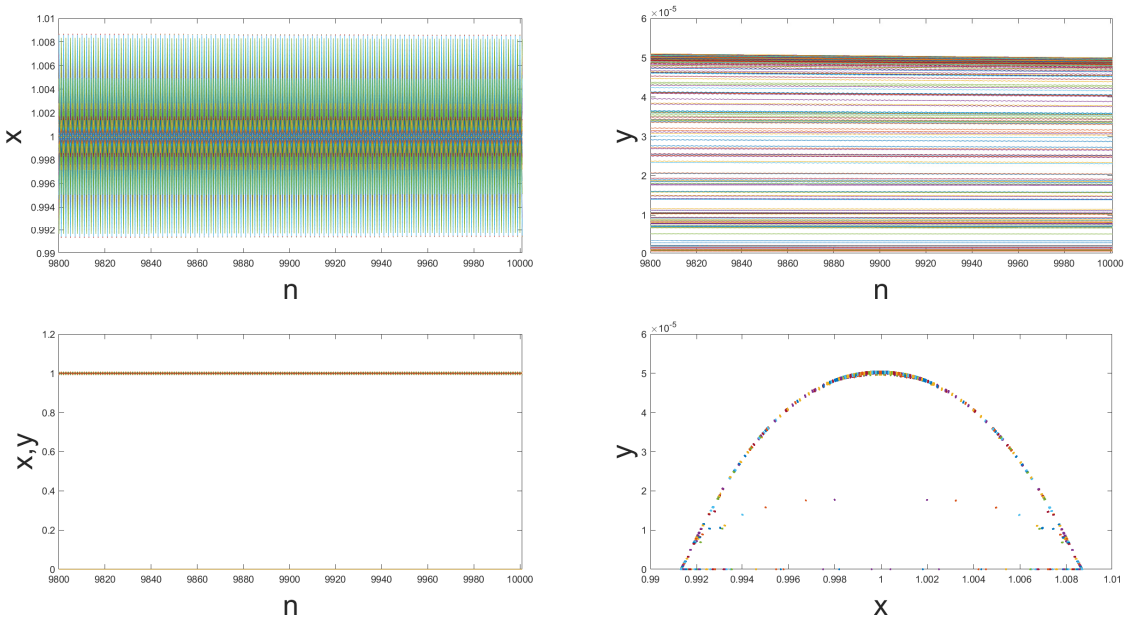

Figure 3.6: *Illustration of the instability of* $S_1 = (1, 0)$ *through numerical simulation, with trajectories starting for* 1000 *different initial points.*

□

Next, We will discuss the stability at the interior positive steady state $S_i = (x^*, y^*)$ in different planes, YR-plane, by-plane, and rb-plane, which we convert to the xy-plane.

3.5 Stability of the Interior Steady State in Different Planes

Now we will steady stability of the interior steady state $S_i = (x^*, y^*)$ in different planes after applying transformations from (tr,det)-plane to YR-plane, by-plane, and rb-plane, which we convert to the xy-plane. We can do that by using the following reduced Jacobian matrix. For the interior steady state $S_i = (x^*, y^*)$ of the map (3.2), the Jacobian matrix (3.7) reduces into the following form

$$J\big(F(x^*,y^*),G(x^*,y^*)\big)=\begin{bmatrix}\partial_{x^*}F(x^*,y^*) & \partial_{y^*}F(x^*,y^*)\\ \partial_{x^*}G(x^*,y^*) & \partial_{y^*}G(x^*,y^*)\end{bmatrix}$$
$$J(x^*,y^*)=\begin{bmatrix}1-rx^* & \frac{-x^*b}{\big(1+\ln(by^*+1)\big)(by^*+1)}\\ \frac{y^*}{x^*} & \frac{x^*b}{\big(1+\ln(by^*+1)\big)^2(by^*+1)}\end{bmatrix},\quad x\neq 0. \tag{3.23}$$

Stability in the YR-plane

Evaluating the Jacobian matrix $J(x^*,y^*)$ at $x^*=\frac{y^*(1+\ln(by^*+1))}{\ln(by^*+1)}$, we get the matrix

$$J\big(y^*\big)=\begin{bmatrix}-\frac{ry^*(1+\ln(by^*+1))}{\ln(by^*+1)}+1 & -\frac{by^*}{\ln(by^*+1)(by^*+1)}\\ \frac{\ln(by^*+1)}{1+\ln(by^*+1)} & \frac{by^*}{\ln(by^*+1)(1+\ln(by^*+1))(by^*+1)}\end{bmatrix}. \tag{3.24}$$

Let $Y=by+1$ and $R=\frac{r}{b}$, where

$$b=\frac{\ln(Y)RY+\ln(1+\ln(Y))\ln(Y)-\ln(Y)R+RY-R}{\ln(Y)R}$$

then $Y\geq 1$. The trace and determinant of $J(y^*)$ in terms of $Y^*=by^*+1$ are given by

$$\mathrm{tr}\big(J(Y^*)\big)=-\frac{R(Y^*-1)(1+\ln(Y^*))}{\ln(Y^*)}+1+\frac{Y^*-1}{\ln(Y^*)(1+\ln(Y^*))Y^*},$$
$$\det\big(J(Y^*)\big)=\frac{\Big(-R(Y^*-1)+\ln(Y^*)\Big)(Y^*-1)}{Y^*\ln^2(Y^*)}.$$

By the Jury test, the positive steady state $S_i=(x^*,y^*)$ is locally asymptotically stable if

$$2>1+\det(J)>|\mathrm{tr}(J)|.$$

In other word, the stable region is the region associated with the constraints $\det(J)<1$, $\det(J)>\mathrm{tr}(J)-1$, and $\det(J)>-\mathrm{tr}(J)-1$. First, we locate the region associated with

$\det(J) < 1$ in the YR-plane. Set $\det(J) - 1 = 0$ and solve it for R, then

$$R = g_1(Y) = -\frac{\ln(Y)\Big(Y\ln(Y) - Y + 1\Big)}{(Y-1)^2}.$$

We call the curve corresponding to the equation $\det(J) - 1 = 0$ the yellow curve. It is clear that the terms $\ln(Y)$ and $(Y-1)^2$ are positive for $Y \geq 1$. In order to determine the sign of g_1, it is sufficient to know the sign of the term $Y\ln(Y) - Y + 1$. Let

$$g_{11}(Y) = Y\ln(Y) - Y + 1,$$

then, $g'_{11}(Y) = \ln(Y) \geq 0$ and $g_{11}(1) = 0$, hence $g_{11}(Y) > 0$ for $Y \geq 1$. Thus for $Y > 1$, $g_1(Y) < 0$, and therefore g_1 has no trajectory in the first quadrant. Moreover, the inequality $\det - 1 < 0$ is equal to

$$-\frac{R(Y-1)^2}{Y\ln(Y)^2} + \frac{-Y\ln(Y)^2 + (Y-1)\ln(Y)}{Y\ln(Y)^2} < 0,$$

thus, the inequality $\det - 1 < 0$ is equivalent to $R > g_1(Y)$ which consequently includes all points of the first quadrant.

Next, we locate the region associated with $\det(J) > \mathrm{tr}(J) - 1$ in the YR-plane. Set $\det(J) - \mathrm{tr}(J) + 1 = 0$ and solve it for R, then

$$R = g_2(Y) = -\frac{\ln(Y)^2}{(\ln(Y)+1)(Y\ln(Y)^2 + Y\ln(Y) - Y + 1)}.$$

We call the curve corresponding to the equation $\det(J) - \mathrm{tr}(J) + 1 = 0$ the green curve. For $Y \geq 1$ the terms $\ln(Y)^2$ and $\ln(Y) + 1$ are positive. To determine the sign of g_2, it is sufficient to know the sign of the term $Y\ln(Y)^2 + Y\ln(Y) - Y + 1$. Let

$$g_{22}(Y) = Y\ln(Y)^2 + Y\ln(Y) - Y + 1,$$

then, for $Y \geq 1$, $g'_{22}(Y) = \ln(Y)(\ln(Y)+3) \geq 0$ and $g_{22}(1) = 0$. Hence, for $Y > 1$, $g_{22}(Y) > 0$. Thus, $g_2(Y) < 0$ and the green curve has no trajectory in the first quadrant. Moreover, the inequality $\det - \mathrm{tr} + 1 > 0$ is equal to

$$\frac{(Y-1)(Y\ln(Y)^3 + 2Y\ln(Y)^2 + \ln(Y) - Y + 1)R}{Y\ln(Y)^2(1+\ln(Y))} + \frac{Y-1}{Y(1+\ln(Y))} > 0,$$

Let $g_{222}(Y) = 2Y\ln(Y)^2 + \ln(Y) - Y + 1$, so

$$g'_{222}(Y) = \frac{(Y\ln(Y)^3 + 5Y\ln(Y)^2 + 4\ln(Y)Y - Y + 1)}{Y}.$$

Note that $g'_{222}(Y)$ is increasing for $Y \geq 1$, also $g'_{222}(1) = 0$, hence, $g_{222}(Y) \geq 0$. Therefore, $g_{222}(Y)$ is increasing for $Y \geq 1$, and $g_{222}(1) = 0$. Thus $g_{222}(Y) \geq 0$ for $Y \geq 1$.
Since $g_{222}(Y) \geq 0$, then

$$R > -\frac{\ln(Y)^2}{Y\ln(Y)^3 + 2Y\ln(Y)^2 + \ln(Y) - Y + 1}.$$

Thus, the inequality $\det - \mathrm{tr} + 1 > 0$ is equivalent to $R > g_2(Y)$ which includes all points of the first quadrant.

Finally, we locate the region associated with $\det(J) > -\mathrm{tr}(J) - 1$ in the YR-plane. Set $\det(J) + \mathrm{tr}(J) + 1 = 0$ and solve it for R, then

$$R = g_3(Y) = \frac{\ln(Y)\Big(2Y\ln(Y)^2 + 3Y\ln(Y) - \ln(Y) + 2Y - 2\Big)}{(Y-1)(\ln(Y)+1)(Y\ln(Y)^2 + Y\ln(Y) + Y - 1)}.$$

We call the curve corresponding to the equation $\det(J)+\mathrm{tr}(J)+1 = 0$ the red curve. For $Y \geq 1$ the terms $\ln(Y)$ and $(Y-1)(\ln(Y)+1)(Y\ln(Y)^2+Y\ln(Y)+Y-1)$ are positive. To determine the sign of g_3, it is sufficient to know the sign of the term $2Y\ln(Y)^2+3Y\ln(Y)-\ln(Y)+2Y-2$. Let

$$g_{33}(Y) = 2Y\ln(Y)^2 + 3Y\ln(Y) - \ln(Y) + 2Y - 2,$$

then, for $Y \geq 1$, $g'_{33}(Y) = \frac{(4\ln(Y)Y+7Y+1)}{Y^2} \geq 0$, and $g_{33}(1) = 0$. Hence, for $Y > 1$, $g_{33}(Y) > 0$.

Thus, for $Y > 1$, $g_3(Y) > 0$. Hence, for $Y > 1$ its trajectory falls in the first quadrant. Moreover the inequality $\det(J) > -\text{tr}(J) - 1$ is equal to

$$\frac{\Big(- Y(Y-1)\ln(Y)^3 + (-2Y^2+2Y)\ln(Y)^2 - 2(Y-1)(Y-\frac{1}{2})\ln(Y) - (Y-1)^2\Big)R}{Y\ln(Y)^2(1+\ln(Y))}$$
$$+ \frac{2Y\ln(Y)^3 + (3Y-1)\ln(Y)^2 - 2(-Y+1)\ln(Y)}{Y\ln(Y)^2(1+\ln(Y))} > 0.$$

Since, $2Y\ln(Y)^3 + (3Y-1)\ln(Y)^2 - 2(-Y+1)\ln(Y) > 0$ and $-Y(Y-1)\ln(Y)^3 + (-2Y^2 + 2Y)\ln(Y)^2 - 2(Y-1)(Y-\frac{1}{2})\ln(Y) - (Y-1)^2 < 0$, then

$$R < \frac{\ln(Y)\Big(2Y\ln(Y)^2 + 3Y\ln(Y) - \ln(Y) + 2Y - 2\Big)}{(Y-1)(\ln(Y)+1)(Y\ln(Y)^2 + Y\ln(Y) + Y - 1)}.$$

Thus, the inequality $\det(J) > -\text{tr}(J) - 1$ is equivalent to $R < g_3(Y)$ which includes all points in the first quadrant which fall under the curve $R = g_3(Y)$.
In conclusion, the stable region is the region located under the red curve $R = g_3(Y)$ in the first quadrant as it shows in Figure 3.7.

Next, we will determine the repeller regions. The first repeller region is located where:

$$\det(J) < \text{tr}(J) - 1, \quad \det(J) < -\text{tr}(J) - 1.$$

While the second repeller region is located where:

$$\det(J) > \text{tr}(J) - 1, \quad \det(J) > -\text{tr}(J) - 1, \quad \text{and} \quad \det(J) > 1.$$

The inequality $\det(J) < \text{tr}(J) - 1$ leads to:

$$R < -\frac{\ln^2(Y)}{Y\ln^3(Y) + 2Y\ln^2(Y) + \ln(Y) - Y + 1} = g_2(Y),$$

and the inequality $\det(J) < -\text{tr}(J) - 1$ implies:

$$R > \frac{\ln(Y)\Big(2Y\ln(Y)^2 + 3Y\ln(Y) - \ln(Y) + 2Y - 2\Big)}{(Y-1)(\ln(Y)+1)(Y\ln(Y)^2 + Y\ln(Y) + Y - 1)} = g_3(Y).$$

Finally, the inequality $\det(J) > 1$ is equivalent to:

$$R < -\frac{\ln(Y)\Big(Y\ln(Y) - Y + 1\Big)}{(Y-1)^2} = g_1(Y).$$

Therefore, the first repeller region corresponds to the inequality $g_3(Y) < R < g_2(Y)$, which has no acceptable solution in the YR-plane since it lies outside of the first quadrant. The second repeller region corresponds to $g_2(Y) < R < g_3(Y)$ and $R < g_1(Y)$ which is an empty set.

The last region that we will determine is the saddle regions. The first saddle region is associated with the solution of $\det(T) < \text{tr}(T) - 1$ and $\det(T) > -\text{tr}(T) - 1$. The second saddle region is associated with the solution of $\det(T) > \text{tr}(T) - 1$ and $\det(T) < -\text{tr}(T) - 1$. Therefore, the first saddle region corresponds to the feasible region of the system of inequalities $R < g_2(Y)$ and $R < g_3(Y)$, which has no accessible solution in the first quadrant. The second saddle region corresponds to the feasible region of the system of inequalities $R > g_2(Y)$ and $R > g_3(Y)$ which is a non-empty region in the first quadrant and it is illustrated in Figure 3.7.

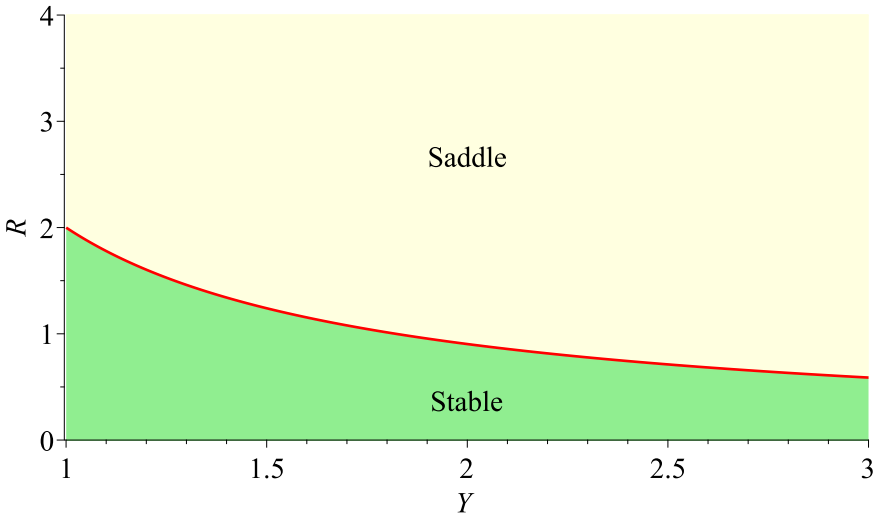

Figure 3.7: *Stability diagram in YR-Plane*

Stability at by-plane

By substituting $x^* = \frac{y^*(1+\ln(by^*+1))}{\ln(by^*+1)}$, and $r = -\frac{\ln(1+\ln(by+1))\ln(by+1)}{y\ln(by+1)-\ln(by+1)+y}$ in equation (3.23), the trace and determinant of the Jacobian matrix $J(b,y)$ in terms of b and y are given by:

$$\begin{aligned}\operatorname{tr}(J(b,y)) &= \frac{y\ln(by+1)\big(1+\ln(by+1)\big)^2(by+1)\ln(1+\ln(by+1))}{(by+1)\ln(by+1)\big((y-1)\ln(by+1)+y\big)(1+\ln(by+1))} \\ &\quad + \frac{\big((y-1)\ln(by+1)+y\big)\big((by+1)\ln(by+1)^2+(by+1)\ln(by+1)+by\big)}{(by+1)\ln(by+1)\big((y-1)\ln(by+1)+y\big)(1+\ln(by+1))}, \\ \det(J(b,y)) &= \frac{by\big(y\ln(1+\ln(by+1))+(y-1)\ln(by+1)+y\big)}{(by+1)\ln(by+1)\big((y-1)\ln(by+1)+y\big)}.\end{aligned}$$

The stable region is the region associated with the constraints $\det(J) < 1$, $\det(J) > \operatorname{tr}(J) - 1$, and $\det(J) > -\operatorname{tr}(J) - 1$. First, we locate the region associated with $\det(J) < 1$ in the by-plane. We call the curve corresponding to the equation $\det(J) = 1$ the yellow curve.

We have:

$$\det(J) - 1 = \frac{by^2\ln(1+\ln(by+1)) - \big((by+1)\ln(by+1)-by\big)\big((y-1)\ln(by+1)+y\big)}{(by+1)\big((y-1)\ln(by+1)+y\big)\ln(by+1)}.$$

Now we analysis the graph of implicit equation $\det(J) = 1$. The term $(by+1)\ln(by+1)$ is monotone increasing on $(0,\infty)$ for $b, y > 0$ since:

$$\frac{\partial}{\partial y}\Big((by+1)\ln(by+1)\Big) = b\ln(by+1) + b > 0 \quad \text{for} \quad (0,\infty).$$

Also, $(by+1)\ln(by+1)\big|_{y=0} = 0$. Hence, in the first quadrant of the by-plane, the sign of $\det(J) - 1$ and the following expression agree:

$$Q(b,y) = \frac{by^2\ln(1+\ln(by+1)) - \big((by+1)\ln(by+1) - by\big)\big((y-1)\ln(by+1) + y\big)}{(y-1)\ln(by+1) + y}.$$

In order to determine sign of $\det(J) - 1$, it is enough to determine sign of $Q(b,y)$. For simplicity, let's denote the numerator and denominator of the expression in $Q(b,y)$ by $N(b,y)$ and $D(b,y)$ respectively. We have:

$$\begin{aligned} N(b,y) &= by^2\ln(1+\ln(by+1)) - \big((by+1)\ln(by+1) - by\big)\big((y-1)\ln(by+1) + y\big), \\ D(b,y) &= (y-1)\ln(by+1) + y, \\ \frac{\partial D}{\partial y}(b,y) &= \ln(by+1) + \frac{(y-1)b}{by+1} + 1. \end{aligned}$$

For $b > 1$ fixed, denote $N(b,y)$, $D(b,y)$, and $Q(b,y)$ by $N_b(y)$, $D_b(y)$, and $Q_b(y)$ respectively. Observe that $D_b(0) = 0$, $D_b'(0) = 1 - b < 0$, and $D_b'(y)$ has a unique root $y_{D_b'} = -\frac{-b-1+\text{LambertW}\left((b+1)e^2\right)}{\text{LambertW}\left((b+1)e^2\right)b}$ on $(0,\infty)$. Also, $\lim_{y\to\infty} D_b(y) = \infty$. Thus, $D_b(y)$ has a single root y_{D_b} on $(0,\infty)$, and its curve resembles an upward parabola on $(0,\infty)$ passing through the origin, see Figure 3.8 curve colored in cyan.

Let $N_b(y) = N_1(y) - N_2(y)D_b(y)$, where $N_1(y) = by^2\ln(1+\ln(by+1))$ and $N_2(y) = (by+1)\ln(by+1) - by$. Note that $N_2(0) = 0$, $N_2'(y) = b\ln(by+1) > 0$ on $(0,\infty)$, and $\lim_{y\to\infty} N_2(y) = \infty$. Hence, $N_2(y)$ is monotone increasing on $(0,\infty)$ and has no root on $(0,\infty)$.

Therefore, by a similar argument applied to $D_b(y)$, $-N_2(y)D_b(y)$ resembles a downward parabola. Both $-N_2(y)D_b(y)$ and $D_b(y)$ have a unique root on $(0,\infty)$, and their root

is identical. Also, $N_1(0) = 0$ and $N_1(y)$ is a monotone increasing function on $(0, \infty)$ as $N_1'(y) = \frac{b^2y^2}{(by+1)(1+\ln(by+1))} + 2\ln(1+\ln(by+1))by > 0$ on $(0, \infty)$.

Therefore, the graph of $N_b(y)$ will move upward from the graph of $-N_2(y)D_b(y)$ by the amount of $N_1(y)$ for each y. Hence, $N_b(y)$ has exactly one root y_{N_b} on $(0, \infty)$ and its root is larger than the root of $-N_2(y)D_b(y)$. Consequently, $y_{D_b} < y_{N_b}$, thus $N_b(y)$ is positive on $(0, y_{N_b})$ and negative on (y_{N_b}, ∞).

Therefore, $\det(J) - 1 < 0$ on $(0, y_{D_b}) \cup (y_{N_b}, \infty)$ and $\det(J) - 1 > 0$ on (y_{D_b}, y_{N_b}). The following diagram in Figure 3.8 demonstrates the behavior of $Q_b(y)$, $N_b(y)$, and $D_b(y)$ for a certain value of $b > 1$.

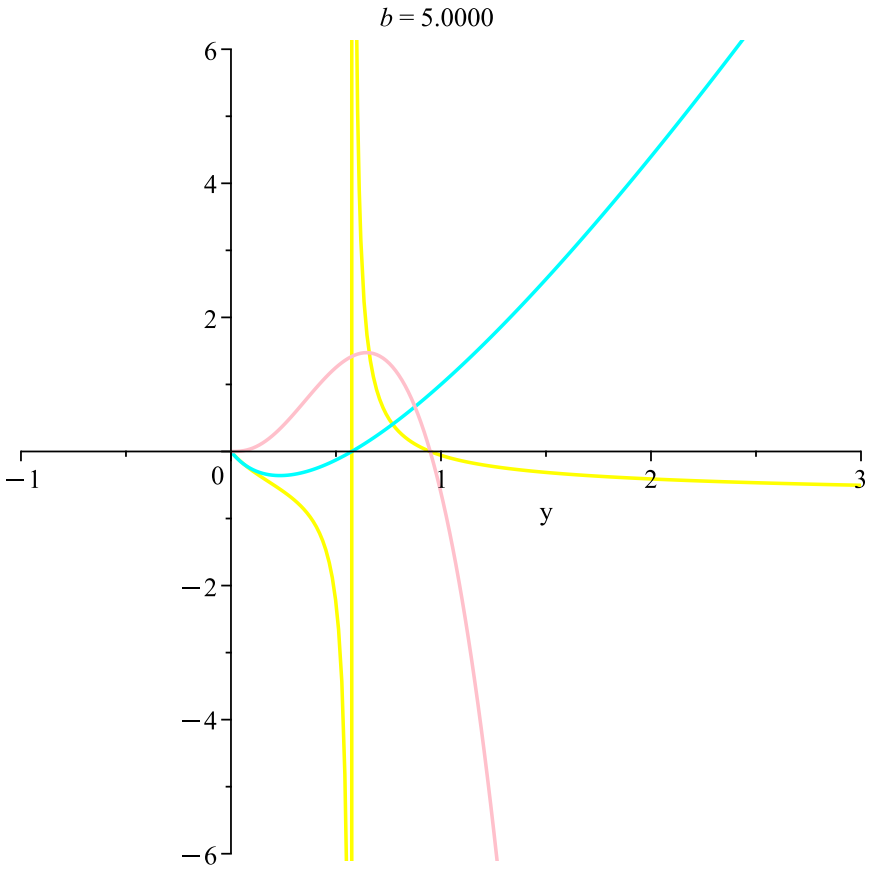

Figure 3.8: *The pink, cyan, and yellow curves represent $N_b(y)$, $D_b(y)$, and $Q_b(y)$ respectively for parameter value $b = 5$.*

In conclusion of $\det(J) - 1$ analysis, $\det(J) < 1$ for $y \in (0, y_{D_b}) \cup (y_{N_b}, \infty)$ and $\det(J) > 1$ for $y \in (y_{D_b}, y_{N_b})$, which is summarized in Figure 3.9.

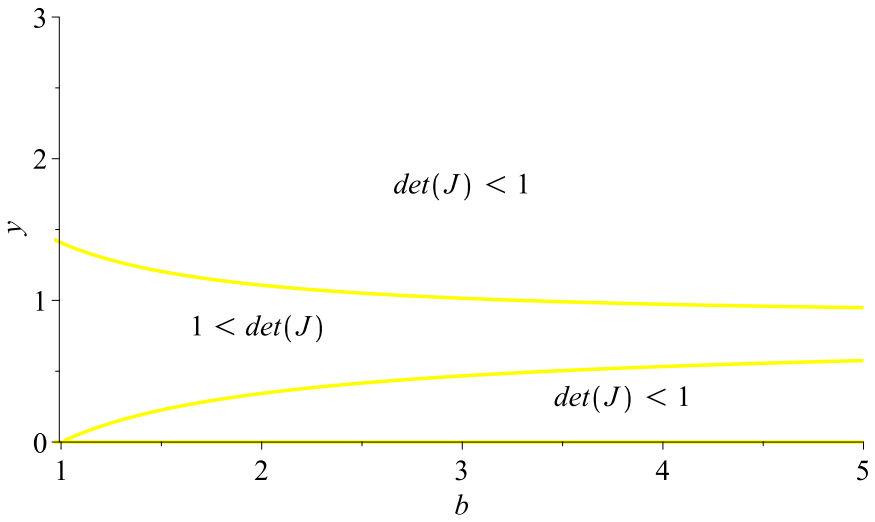

Figure 3.9: *Graph of yellow curve in the by-plane and the regions associated with inequality* $det(J) < 1$.

Next, we will locate the region associated with the constraint $\det(J) > \operatorname{tr}(J) - 1$. We call the curve corresponding to the equation $\det(J) = \operatorname{tr}(J) - 1$ the green curve. We have

$$\det(J) - \operatorname{tr}(J) + 1 = \frac{-y\Big(\big((y-1)\ln(by+1)+y\big)\ln(by+1)b\Big)}{\big((y-1)\ln(by+1)+y\big)(by+1)\big(1+\ln(by+1)\big)\ln(by+1)}$$
$$- \frac{y\Big(\big((by+1)\ln(by+1)^3+(2by+2)\ln(by+1)^2+\ln(by+1)-by\big)\ln\big(1+\ln(by+1)\big)\Big)}{\big((y-1)\ln(by+1)+y\big)(by+1)\big(1+\ln(by+1)\big)\ln(by+1)}.$$

Next, we analysis the graph of implicit equation $\det(J) = \operatorname{tr}(J) - 1$. The terms $by + 1$, $\ln(by + 1)$, and $1 + \ln(by + 1)$ are positive for $b, y > 0$. Hence, in the first quadrant of the by-plane, the sign of $\det(J) - \operatorname{tr}(J) + 1$ and the following expression agree:

$$Q(b,y) = \frac{-y\Big(\big((y-1)\ln(by+1)+y\big)\ln(by+1)b\Big)}{(y-1)\ln(by+1)+y}$$
$$- \frac{y\Big(\big((by+1)\ln(by+1)^3+(2by+2)\ln(by+1)^2+\ln(by+1)-by\big)\ln\big(1+\ln(by+1)\big)\Big)}{(y-1)\ln(by+1)+y}.$$

In order to determine sign of $\det(J) - \operatorname{tr}(J) + 1$, it is enough to determine sign of $Q(b, y)$. For simplicity in our discussion, indicate the numerator and denominator of the expression

in $Q(b,y)$ again by $N(b,y)$ and $D(b,y)$ respectively. We have

$$N(b,y) = -y\Big((y-1)\ln(by+1)+y\Big)\ln(by+1)b\Big) \tag{3.25}$$
$$-\,y\Big(\big((by+1)\ln(by+1)^3+(2by+2)\ln(by+1)^2+\ln(by+1)-by\big)\ln\big(1+\ln(by+1)\big)\Big),$$
$$D(b,y) = (y-1)\ln(by+1)+y,$$
$$\frac{\partial D}{\partial y}(b,y) = \ln(by+1)+\frac{(y-1)b}{by+1}+1.$$

Suppose $b>1$ is fixed. Denote $N(b,y)$, $D(b,y)$, and $Q(b,y)$ by $N_b(y)$, $D_b(y)$, and $Q_b(y)$ respectively. Similar arguments that we applied for $D_b(y)$ in the yellow curve section can be applied for $D_b(y)$ of the green curve resulting that $D_b(y)$ has a unique root y_{D_b} on $(0,\infty)$ and its curve shape is roughly like an upward parabola. On the other hand, $N_b(y)$ is always negative on $(0,\infty)$.

By substitution $Y = by+1$ in (3.25) and dropping negative sign yields

$$N(Y) = \ln(1+\ln(Y)) - Y\ln(Y)^2+\ln(Y)^2+\ln(Y)^2b-\ln(Y)Y+\ln(Y) \tag{3.26}$$
$$+\ln(1+\ln(Y))Y\ln(Y)^3+2\ln(1+\ln(Y))Y\ln(Y)^2+\ln(1+\ln(Y))\ln(Y)-\ln(1+\ln(Y))Y,$$

where $N(Y) = -N_b(y)$. As a means of simplifying our analysis, substitution of $Y = e^z$ in (3.26) gives us

$$N(z) = \big((z^3+2z^2-1)e^z+1+z\big)\ln(1+z)+z\big((-z-1)e^z+1+(b+1)z\big),$$

where

$$N'(z) = (1+(z^3+5z^2+4z-1)e^z)\ln(1+z)+(-2z-2)e^z+2+(2b+2)z,$$
$$N''(z) = \frac{e^z\big(z^3+11z^2+30z+17\big)(1+z)^2\ln(1+z)}{(1+z)^2}$$
$$+\frac{(2z^4+15z^3+29z^2+16z+1)e^z-1}{(1+z)^2}\geq 0,$$

and $N(0) = N'(0) = N''(0) = 0$, $N''(z) \geq 0$ for $z \geq 0$, hence $N'(z) > 0$, consequently $N(z) \geq 0$ on $[0, \infty)$. Thus $N(Y) \geq 0$ on $[0, \infty)$. Hence, $N_b(y) < 0$ on $[0, \infty)$. Therefore, $Q_b(y) > 0$ on $y \in (0, y_{D_b})$ and $Q_b(y) < 0$ on $y \in (y_{D_b}, \infty)$. The following diagram in Figure 3.5 demonstrates the behavior of $Q_b(y)$, $N_b(y)$, and $D_b(y)$ for a certain value of $b > 1$.

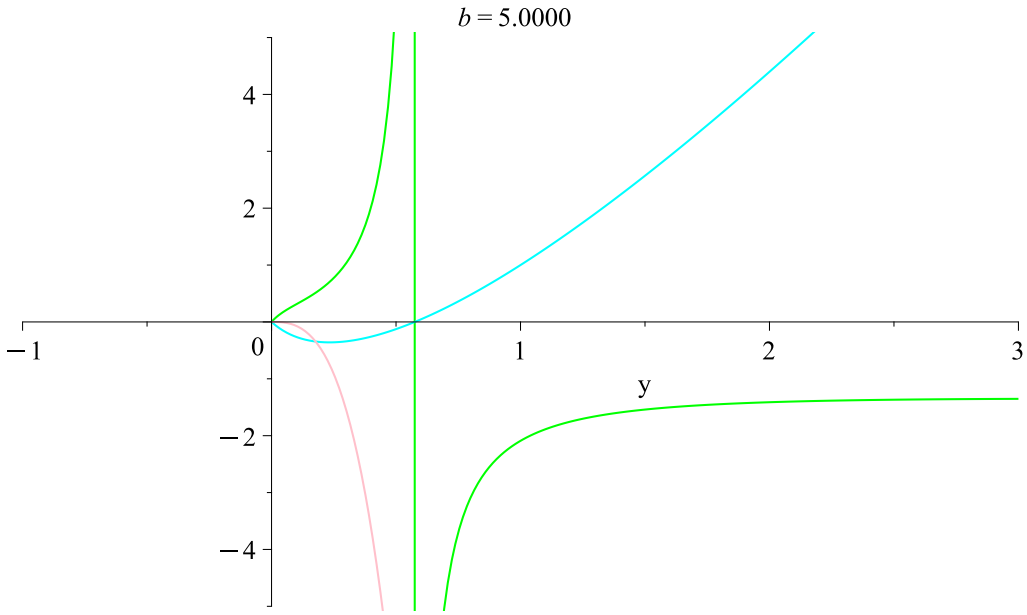

Figure 3.10: *The pink, cyan and yellow curves represent $N_b(y)$, $D_b(y)$ and $Q_b(y)$ respectively for parameter value $b = 5$.*

Thus, $\det(J) > \text{tr}(J) - 1$ on $y \in (0, y_{D_b})$ and $\det(J) < \text{tr}(J) - 1$ on $y \in (y_{D_b}, \infty)$, which is summarized in the following diagram in Figure 3.5.

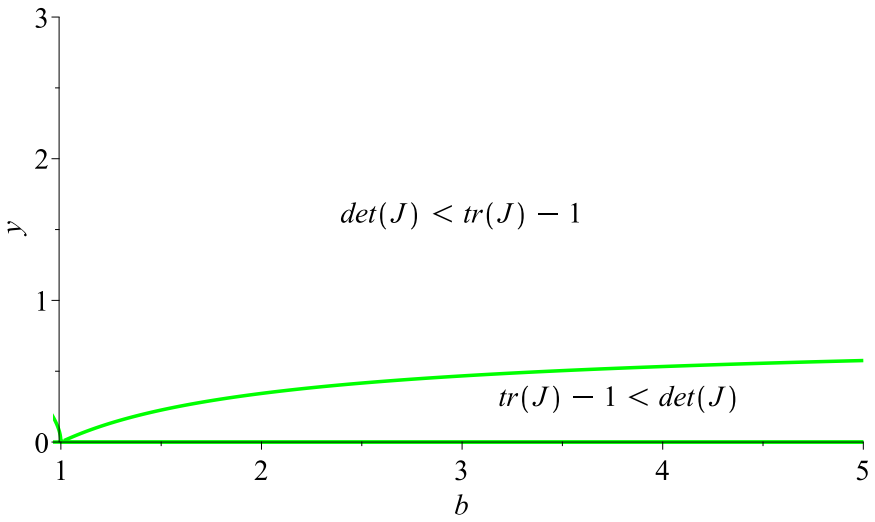

Figure 3.11: *Graph of green curve in by-plane and the regions associated with inequality* $det(J) > tr(J) - 1$.

Finally, we will locate the region associated with the constraints $\det(J) > -\mathrm{tr}(J) - 1$. We call the curve corresponding to the equation $\det(J) = -\mathrm{tr}(J) - 1$ the red curve. We have

$$\det(J) + \mathrm{tr}(J) + 1 = \frac{2\Big((by+1)\ln(by+1)^2 + \big(\frac{3by}{2}+1\big)\ln(by+1) + by\Big)}{(by+1)\ln(by+1)\big((y-1)\ln(by+1)+y\big)\big(1+\ln(by+1)\big)}$$
$$+ \frac{y\big(1+\ln(by+1)\big)\Big((by+1)\ln(by+1)^2 + (by+1)\ln(by+1) + by\Big)\ln\big(1+\ln(by+1)\big)}{(by+1)\ln(by+1)\big((y-1)\ln(by+1)+y\big)\big(1+\ln(by+1)\big)}.$$

The terms $by+1$, $\ln(by+1)$, and $1+\ln(by+1)$ are positive for $b, y > 0$, hence in the first quadrant of the by-plane the sign of $\det(J) + \mathrm{tr}(J) + 1$ and the following expression agree

$$Q(b,y) = \quad + \frac{2\Big((by+1)\ln(by+1)^2 + \big(\frac{3by}{2}+1\big)\ln(by+1) + by\Big)}{(y-1)\ln(by+1)+y}$$
$$+ \frac{y\big(1+\ln(by+1)\big)\Big((by+1)\ln(by+1)^2 + (by+1)\ln(by+1) + by\Big)\ln\big(1+\ln(by+1)\big)}{(y-1)\ln(by+1)+y}.$$

In order to determine sign of $\det(J) + \mathrm{tr}(J) + 1$, it is enough to determine sign of $Q(b,y)$. For simplicity in our discussion, indicate the numerator and denominator of the expression

in $Q(b,y)$ by $N(b,y)$ and $D(b,y)$ respectively. We have

$$N(b,y) = y\big(1+\ln(by+1)\big)\Big((by+1)\ln(by+1)^2 + (by+1)\ln(by+1) + by\Big)\ln\big(1+\ln(by+1)\big)$$
$$+ 2\Big((by+1)\ln(by+1)^2 + (\frac{3by}{2}+1)\ln(by+1) + by\Big)\big((y-1)\ln(by+1)+y\big),$$
$$D(b,y) = (y-1)\ln(by+1) + y.$$

Suppose $b > 1$ is fixed. Denote $N(b,y)$, $D(b,y)$ and $Q(b,y)$ by $N_b(y)$, $D_b(y)$ and $Q_b(y)$ respectively. We couldn't prove mathematically that this is true, but through computer simulations, we can observe that, the function $N_b(y)$ has a unique root y_{N_b} and a unique absolute min $N_b(0) = 0$ and $\lim_{y\to\infty} N_b(y) = \infty$. Also, $D_b(y)$ has a unique root with a unique a absolute min $D_b(0) = 0$ and $\lim_{y\to\infty} D_b(y) = \infty$. Moreover, $0 < y_{N_b} < y_{D_b}$ for every b. Therefore, based on the analysis of the graphs of $N_b(y)$ and $D_b(y)$, we conclude that: On $(0, y_{N_b}) \cup (y_{D_b}, \infty)$, we have $Q_b(y) > 0$. While on (y_{N_b}, y_{D_b}), we have $Q_b(y) < 0$ which is depicted in the Figure 3.12.

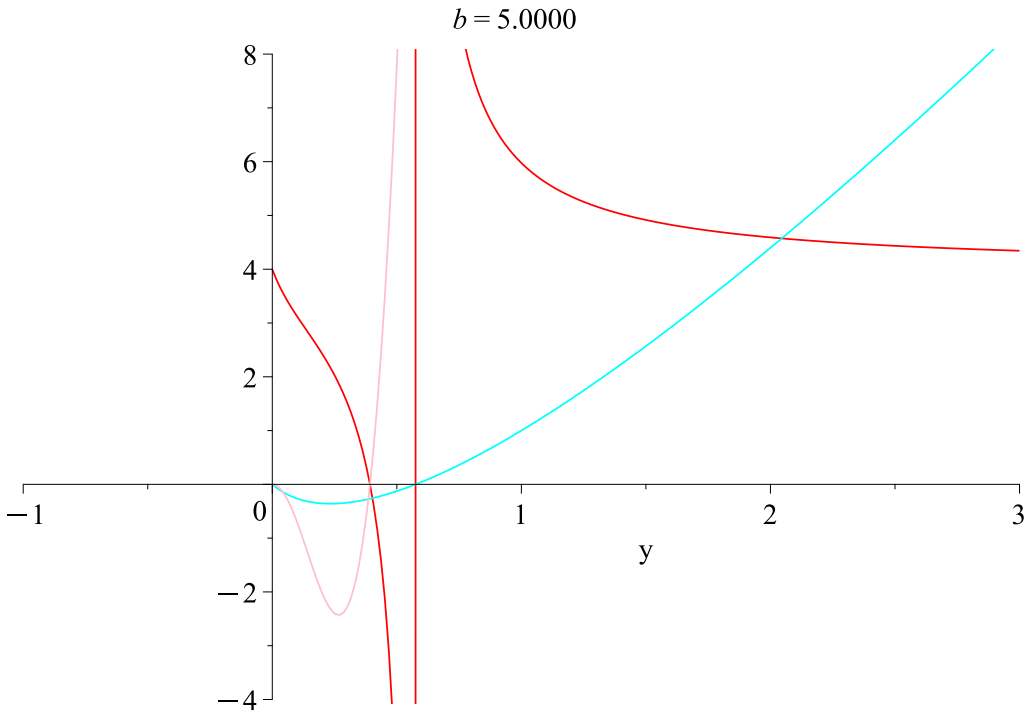

Figure 3.12: *The pink, cyan and red curves represent $N_b(y)$, $D_b(y)$ and $Q_b(y)$ respectively for parameter value $b = 5$.*

Consequently, $\det(J) > -\text{tr}(J) - 1$ on $(0, y_1) \cup (y_2, \infty)$ and $\det(J) < -\text{tr}(J) - 1$ on (y_1, y_2), which is illustrated in Figure 3.13.

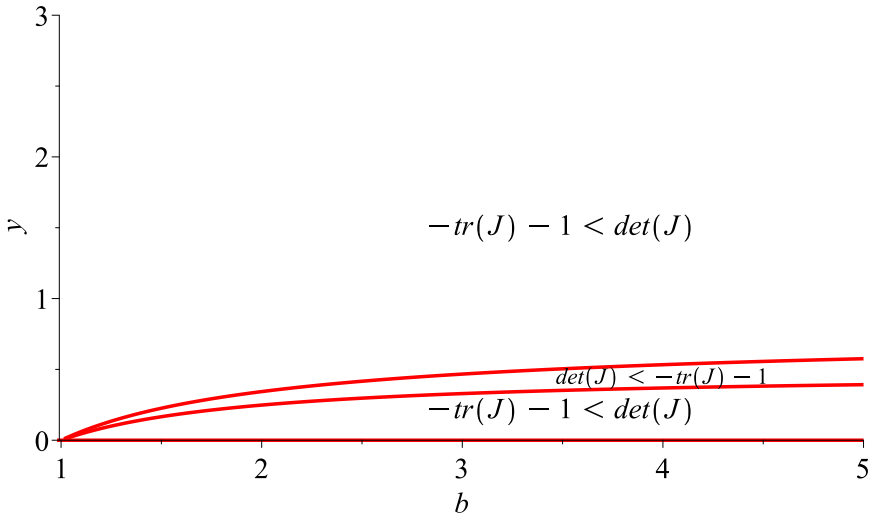

Figure 3.13: *Graph of red curve in by-plane and regions associated with inequality* $det(J) > -tr(J) - 1$.

The stability regions in the first quadrant of the *by*-plane are summarized in the following diagram in Figure 3.14.

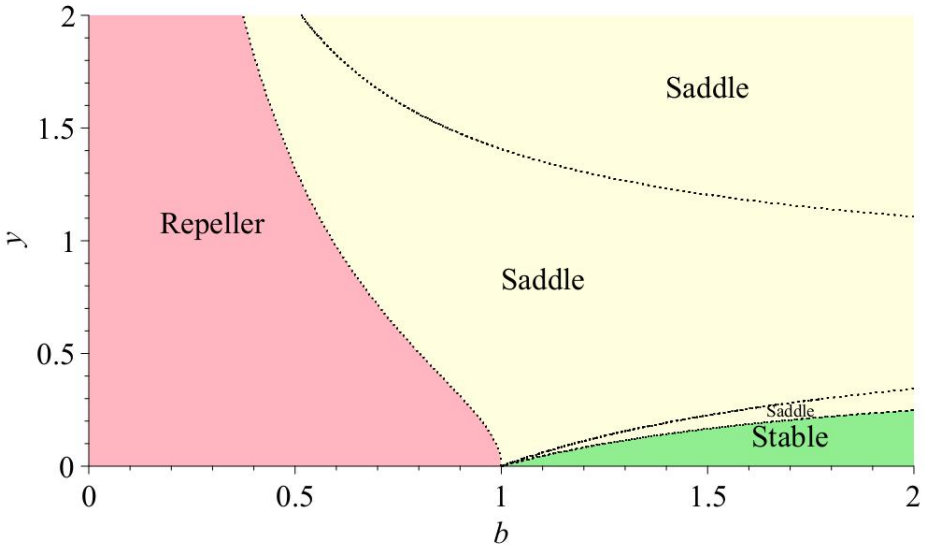

Figure 3.14: *Stability diagram in by-plane*

Stability at xy-plane

Finally, we will determine stability in the first quadrant of xy-plane. Equation (3.7) yields:

$$\begin{aligned}\mathrm{tr}(J) &= 1 - rx + \frac{b(x-y)^2}{x(by+1)},\\ \det(J) &= \frac{-b(x-y)(rx-ry-1)}{by+1}\end{aligned}$$

where

$$r = -\frac{\ln\left(\frac{x}{x-y}\right)}{x-1}, \text{ and } b = \frac{e^{\left(\frac{y}{x-y}\right)}-1}{y}. \tag{3.27}$$

The stable region is the region associated with the constraints $\det(J) < 1$, $\det(J) > \mathrm{tr}(J) - 1$, and $\det(J) > -\mathrm{tr}(J) - 1$.

First we locate the region associated with $\det(J) < 1$ on xy-plane. We call the curve corresponded to equation $\det(J) = 1$ the yellow curve. We have

$$\begin{aligned}\det(J) - 1 = &\frac{-(x-y)\big((-x+y)\ln(x-y) + (x-y)\ln(x) - 1 + x)e^{-\frac{y}{x-y}}\big)}{y(-1+x)}\\ &- \frac{(x-y)^2\ln(x-y) + (x-y)^2\ln(x) + (-1+x)(x-2y)}{y(-1+x)}.\end{aligned}$$

For simplicity in our discussion, let $Q(x,y) = \det(J) - 1$ and indicate the numerator and the denominator of $Q(x,y)$ by $N(x,y)$ and $D(x,y)$ respectively. In order for r and b to be defined in equation (3.27), we require that $0 < y < x < 1$. For every fixed x, denote $N(x,y)$, $D(x,y)$ and $Q(x,y)$ by $N_x(y)$, $D_x(y)$ and $Q_x(y)$ respectively. One can verify that $N_x(y)$

satisfies the following inequality

$$
\begin{aligned}
N_x(y) &= -(x-y)\big((-x+y)\ln(x-y)+(x-y)\ln(x)-1+x)e^{-\frac{y}{x-y}}\big)\\
&\quad -(x-y)^2\ln(x-y)+(x-y)^2\ln(x)+(-1+x)(x-2y)\\
&= (x-y)\bigg(\Big((x-y)\big(\ln(x)-\ln(x-y)\big)+x-1\Big)(1-e^{-\frac{y}{x-y}})+x-1\bigg)+(1-x)x,\\
&\geq \Big(1-e^{-\frac{y}{x-y}}\Big)(x-y)(-(1-x))+(1-x)y,\\
&= (x-y)\Big(1-e^{-\frac{y}{x-y}}\Big)-x+2y,\\
&= (1-x)\bigg((x-y)\Big(y-(1-e^{-\frac{y}{x-y}})\Big)\bigg) = M_x(y).
\end{aligned}
$$

We want to show that $N_x(y) > 0$, that is enough to show that $M_x(y) > 0$. We have $M_x(0) = 0$, and $M_x''(y) = \frac{e^{-\frac{y}{x-y}}x^2}{(x-y)^3}$. Hence for $0 < y < x < 1$, $M_x''(y) > 0$, and $M_x''(0) = 0$ which shows that $M_x(y)$ concave up on $(0,\infty)$, thus, $M_x(y)$ is positive on $(0,\infty)$, consequently so is $N_x(y)$. On the other hand, $D_x(y)$ is negative on $(0,\infty)$. Therefore, $Q(x,y) \neq 0$ for $0 < y < x < 1$, i.e $\det(J) \neq 1$ for $0 < y < x < 1$ which proves that the yellow curve does not have trajectory in xy-plane for $0 < y < x < 1$. Here is Figure 3.15 summarizing this

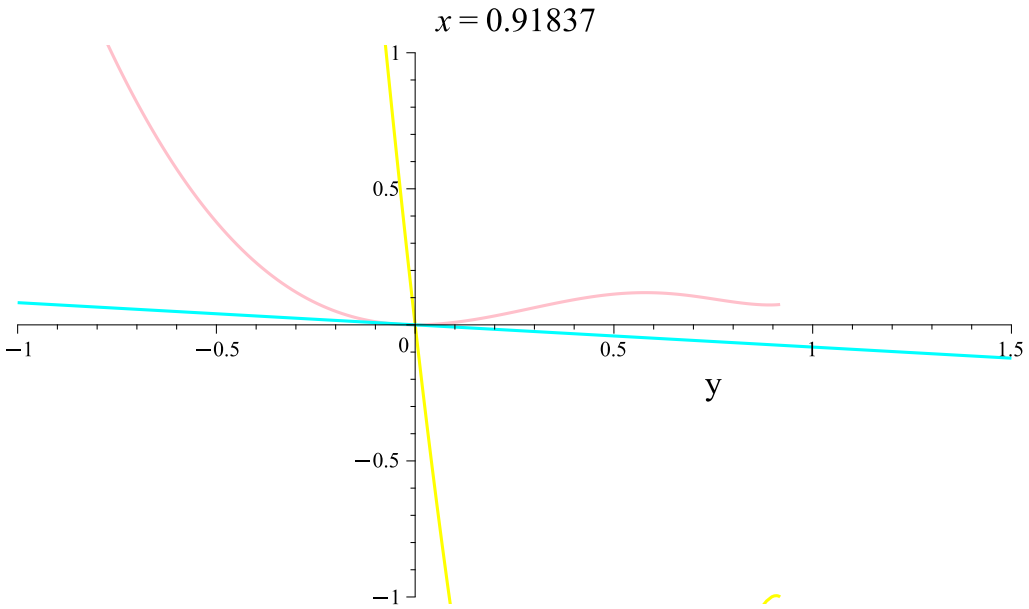

Figure 3.15: *The pink, cyan and yellow curves represent $N_x(y)$, $D_x(y)$ and $Q_x(y)$ respectively for parameter value $x = 0.9$.*

Next we will locate the region associate with the constraint $\det(J) > \mathrm{tr}(J) - 1$. We call the curve corresponded to the equation $\det(J) = \mathrm{tr}(J) - 1$ the green curve. In term of x and y we have

$$\det(J) - \mathrm{tr}(J) + 1 = \frac{-(x-y)\big(-(x-y)x\ln(x-y) + (x-y)x\ln(x) + (-1+x)y\big)e^{-\frac{y}{x-y}}}{y(-1+x)x}$$
$$+ \frac{(-x^3+3x^2y-xy^2)\ln(x-y) + x(x^2-3xy+y^2)\ln(x) + y(-1+x)(x-y)}{y(-1+x)x}.$$

For the sake of simplicity, let $Q(x,y) = \det(J) - \mathrm{tr}(J) + 1$, and indicate the numerator and the denominator of the expression in $Q(x,y)$ by $N(x,y)$ and $D(x,y)$ respectively. For every fixed x, where $0 < y < x < 1$, denote $N(x,y)$, $D(x,y)$ and $Q(x,y)$ by $N_x(y)$, $D_x(y)$ and $Q_x(y)$ respectively. As can be seen from the inequality, $N_x(y)$ satisfies

$$
\begin{aligned}
N_x(y) &= -(x-y)(-(x-y)x\ln(x-y)+(x-y)x\ln(x)+(x-1)y)e^{\frac{-y}{x-y}} \\
&\quad + (-x^3+3x^2y-xy^2)\ln(x-y)+x(x^2-3xy+y^2)\ln(x)+y(x-1)(x-y), \\
&= x\big(\ln(x)-\ln(x-y)\big)\Big(x^2-3xy+y^2-(x-y)^2e^{-\frac{y}{x-y}}\Big) \\
&\quad + y(-1+e^{\frac{-y}{x-y}})(x-1)(x-y), \\
&\leq x\big(\ln(x)-\ln(x-y)\big)\Big(x^2-3xy+y^2-(x-y)^2e^{-\frac{y}{x-y}}\Big), \\
&= x\big(\ln(x)-\ln(x-y)\big)\Big((x-y)^2(1-e^{-\frac{y}{x-y}})-xy\Big).
\end{aligned}
$$

Since $\frac{x}{x-y} \geq 1$, and $\ln\left(\frac{x}{x-y}\right) > 0$, it is sufficient to verify the sign of $(x-y)^2(1-e^{-\frac{y}{x-y}})-xy$ in order to determine sign of $N_x(y)$. But

$$
\begin{aligned}
(x-y)^2\big(1-e^{-\frac{y}{x-y}}\big)-xy &\leq (x-y)^2\big(1-e^{-\frac{y}{x-y}}\big)-xy+y^2, \\
&= (x-y)^2\big(1-e^{-\frac{y}{x-y}}\big)-y(x-y), \\
&= (x-y)\Big((x-y)\big(1-e^{-\frac{y}{x-y}}\big)-y\Big)
\end{aligned}
$$

Let $M_x(y) = (x-y)\big(1-e^{-\frac{y}{x-y}}\big)-y$. We Show that $M_x(y) < 0$ on $(0,x)$ which implies that $N_x(y) < 0$ on $(0,x)$. To prove this, note that $M_x(0) = 0$, $M_x'(0) = 0$ and $M_x''(y) = -\frac{x^2e^{-\frac{y}{x-y}}}{(x-y)^3}$. Hence for $0 < y < x < 1$, $M_x''(y) < 0$, which shows $M_x(y)$ concave down on $(0,\infty)$, thus $M_x(y)$ is negative on $(0,x)$. On the other hand, $D_x(y)$ is clearly negative on $(0,x)$. Therefore, $Q(x,y) > 0$ for $0 < y < x < 1$, i.e $\det(J) > \mathrm{tr}(J) - 1$ for $0 < y < x < 1$ which proves that the green curve on xy-plane does exist for $0 < y < x < 1$. The following diagram in Figure 3.16 summarizes these for green curve

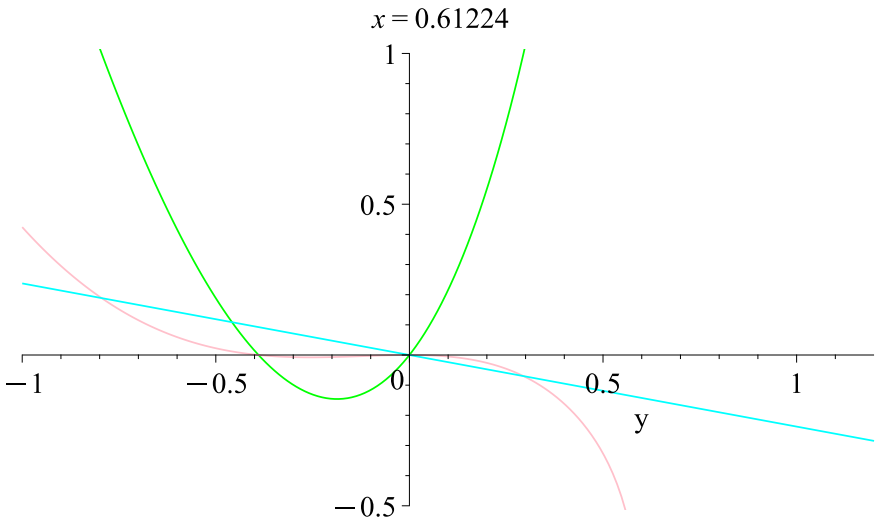

Figure 3.16: *The pink, cyan and green curves represent $N_x(y)$, $D_x(y)$ and $Q_x(y)$ respectively for parameter value $x = 0.6$.*

We conclude our discussion for the xy-plane regions by locating the region that is associated with the constraint $\det(J) > -\mathrm{tr}(J) - 1$. We call the curve corresponded to equation $\det(J) = -\mathrm{tr}(J) - 1$ the red curve. We have

$$\det(J) + \mathrm{tr}(J) + 1 = \frac{-(x-y)\big((x-y)x\ln(\frac{x}{x-y}) + 2(-1+x)(x-\frac{y}{2})\big)\ e^{-\frac{y}{x-y}}}{y(-1+x)x} + \frac{x(x^2-xy+y^2)\ln(\frac{x}{x-y}) + 2(-1+x)(x^2-\frac{1}{2}xy+\frac{1}{2}y^2)}{y(-1+x)x}.$$

For Simplicity, let us define $Q(x,y) = \det(J) + \mathrm{tr}(J) + 1$, and indicate the numerator and the denominator of the expression in $Q(x,y)$ by $N(x,y)$ and $D(x,y)$ respectively. For every fixed x, where $0 < y < x < 1$, denote $N(x,y)$, $D(x,y)$ and $Q(x,y)$ by $N_x(y)$, $D_x(y)$ and $Q_x(y)$ respectively. As the first step, we demonstrate that $N_x(y)$ has a unique root y_{N_x} on $(0,x)$. In order to establish the existence of the root y_{N_x}, it should be noted that $N_x(0) = 0$, and $N_x'(0) = 4x(x-1)$ is negative for $0 < x < 1$. Furthermore, $\lim\limits_{y\to x^-} N_x(y) = \infty$ is positive for $0 < x < 1$, owing to the following calculation:

$$N_x'(y) = \frac{x(x-y)(x-2y)\ln(x-y) - x(x-y)(x-2y)\ln(x) + (2y+1)x^2}{x-y}$$
$$+ \frac{(-y^2-3y)x+2y^2}{x-y} + \frac{\Big(-3(x-y)x(x-\frac{2y}{3})\ln(x-y) + 3(x-y)x(x-\frac{2y}{3})\ln(x)\Big)e^{-\frac{y}{x-y}}}{x-y}$$
$$+ \frac{\Big(+4x^3+(-4y-5)x^2+(y^2+6y)x-2y^2\Big)e^{-\frac{y}{x-y}}}{x-y}.$$

It follows that, for every $0 < y < x < 1$, $N_x(y)$ has at least a root on $(0, x)$. Next step, we demonstrate the uniqueness of the root of $N_x(y)$ on $(0, \infty)$. In order to simplify the study of $N_x(y)$, we rewrite $N_x(y)$ as follows:

$$N_x(y) = N_1(y) + N_2(y) + N_3(y)$$

where,

$$N_1(y) = \ln\Big(\frac{x}{x-y}\Big)\Big((x-y)^2\ e^{-\frac{y}{x-y}} - x^2 + xy - y^2\Big)x,$$
$$N_2(y) = \Big((y-2x)(x-y)\Big)\ e^{-\frac{y}{x-y}}(-1+x),$$
$$N_3(y) = (2x^2 - xy + y^2)(-1+x).$$

Let

$$N_4(y) = \begin{cases} -N_2(y) - N_3(y), & 0 \le y \le \frac{x}{2} \\ -N_2(y) - \frac{7x^2(x-1)}{4}, & \frac{x}{2} \le y \le x \end{cases}$$

then, $-N_4(y)$ is a continuous, increasing and concave down function on $[0, x]$. Moreover, $N_1(y)$ is an increasing and concave up function on $[0, x]$. Also, $N_1(0) = N_4(0) = 0$, $N_1'(y) = 0 < N_4'(0)$ and

$$N_4(\frac{x}{2}) = \frac{(x-1)x^2(-7+3e^{-1})}{4} > -\frac{\ln(2)x^3(e^{-1}-3)}{4} = N_1(\frac{x}{2}).$$

In addition, $N_4(y) < -N_2(y) - N_3(y)$ on $[0, x]$, $\lim\limits_{y \to x^-} N_1(y) = \infty$, $\lim\limits_{y \to x^-} N_4(y) = -\frac{7x^2(x-1)}{4} \geq 0$, and $\lim\limits_{y \to x^-} -N_2(y) - N_3(y) = -2x^3 + 2x^2 > 0$, hence $N_1(y)$ and $N_4(y)$ have a unique root on $[0, x]$. Consequently, $N_1(y)$ and $-N_2(y) - N_3(y)$ have a unique root on $[0, x]$ as illustrated in the following Figure 3.17.

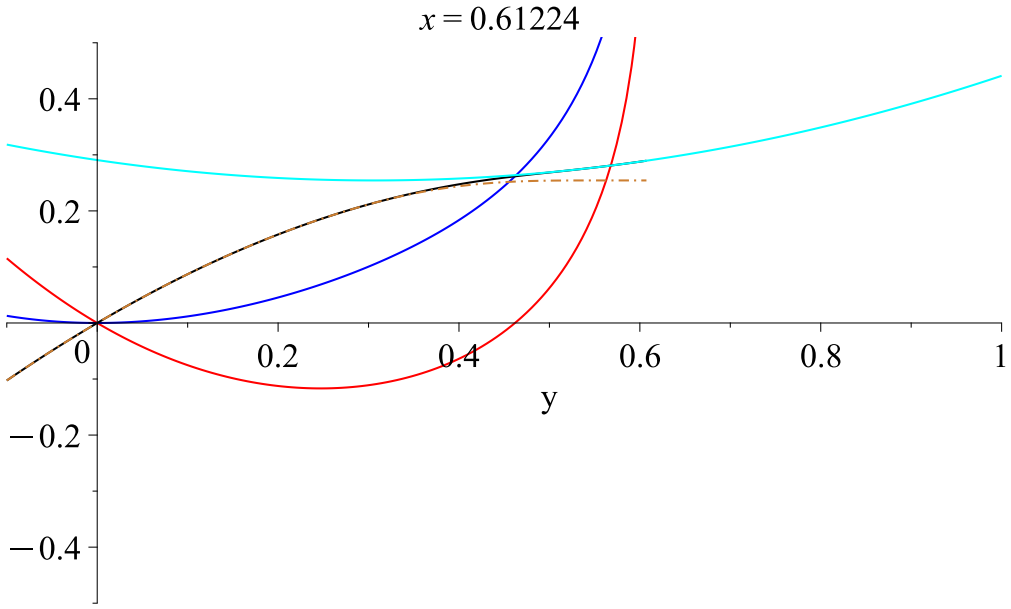

Figure 3.17: *The red, blue, black and gold curves represent the functions $N_x(y)$, $N_1(y)$, $N_2(y)$, $N_4(y)$, respectively for $x = 0.7$.*

In conclusion, on $(0, y_{N_x})$, $Q(x, y) > 0$ and $Q(x, y) < 0$ on (y_{N_x}, ∞). The following diagram in Figure 3.18 illustrates it.

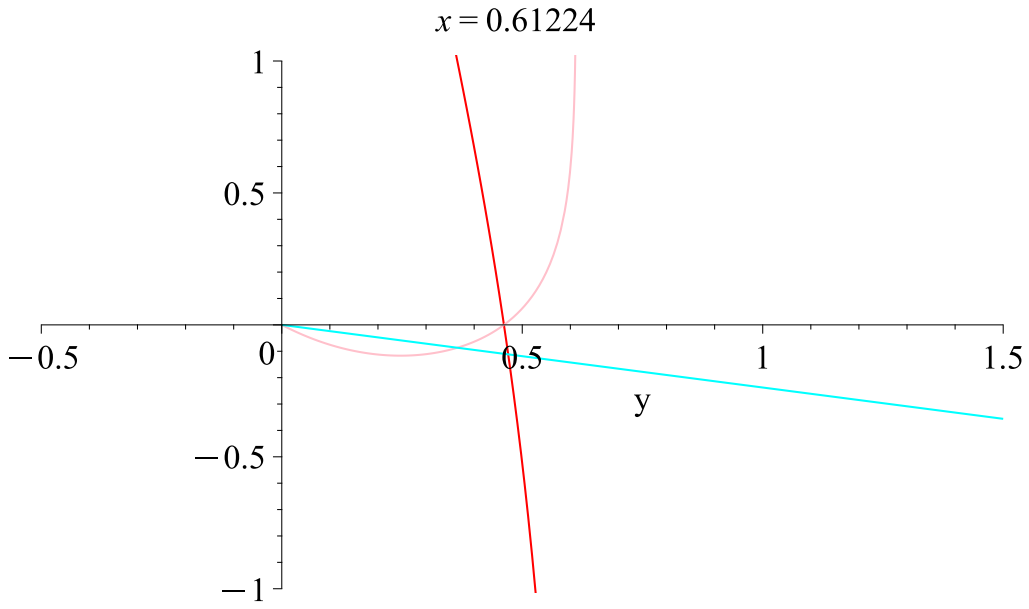

Figure 3.18: *The pink, cyan and red curves represent* $N_x(y)$, $D_x(y)$ *and* $Q_x(y)$ *respectively for parameter value* $x = 0.6$.

Therefore, the stability regions in the first quadrant of the xy-plane are summarized in the following diagram in Figure 3.5,

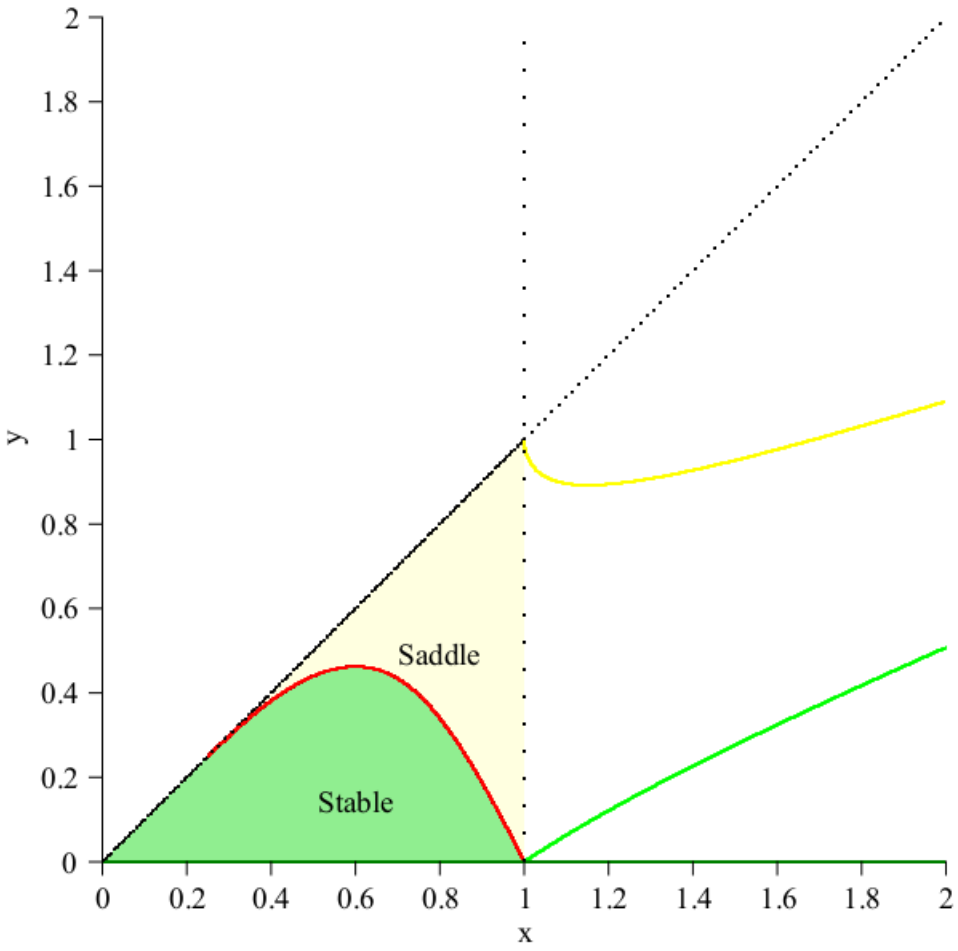

Figure 3.19: *Stability diagram in xy-Plane*

3.6 Global Stability of The Boundary Steady State

In this section we will study the global Stability of the boundary steady state $S_1 = (0, 1)$ of the following two dimensional model:

$$\begin{aligned} x_{n+1} =& \frac{x_n e^{r(1-x_n)}}{1 + \ln(by_n + 1)}, \\ y_{n+1} =& x_n \left(1 - \frac{1}{1 + \ln(by_n + 1)}\right). \end{aligned} \tag{3.28}$$

where $0 < b < 1$ and $0 < r < 2$.

For any initial values $x_0 > 0$ and $y_0 \geq 0$, as follows

$$\begin{aligned} x_n =& \frac{x_{n-1}e^{r(1-x_{n-1})}}{1+\ln(by_{n-1}+1)}, \\ y_n =& x_{n-1}\left(1-\frac{1}{1+\ln(by_{n-1}+1)}\right). \end{aligned} \tag{3.29}$$

The maximum value of $f(x) = xe^{r(1-x)}$ for $x > 0$ occurs at $x = \frac{1}{r}$ with the value $\frac{e^{r-1}}{r}$. Therefore, $x_n = \frac{x_{n-1}e^{r(1-x_{n-1})}}{1+\ln(by_{n-1}+1)} \leq \frac{e^{(r-1)}}{r}$. Since $y_n \leq x_n$, then $y_n \leq \frac{e^{(r-1)}}{r}$. Consequently,

$$\begin{aligned} x_n + y_n =& \frac{x_{n-1}\left(e^{r(1-x_{n-1})}+\ln(by_{n-1}+1)\right)}{1+\ln(by_{n-1}+1)}, \\ \leq& 2\frac{e^{(r-1)}}{r}. \end{aligned} \tag{3.30}$$

Next we will introduce the persistence of the host theory in order to establish the global stability of the boundary steady state $S_1 = (1, 0)$.

3.6.1 Persistence of the Host

We will study the persistence of the host theory in order to establish the global stability of the MNB system that we introduced earlier (3.28). The following section will discuss the host's persistence, so I would like to introduce a few terms that will be used. The host's persistence will be measured by the host population's carrying capacity and the mortality rate of the host population. The carrying capacity is the maximum population size that the host population can sustain, while the mortality rate is the rate at which the host population dies[55].

Lemma 3.6.1. *Let*

$$\mathcal{Q}_1 = \big\{(x,y)|\ x \geq 0,\ y \geq 0\big\},$$
$$A_{(1,0)} = \big\{(x,y)|\ x > 0,\ y \geq 0\big\},$$
$$\partial A_{(1,0)} = \big\{(x,y)|\ x = 0,\ y \geq 0\big\},$$

then the system of equations (3.28) *is uniformly persistent with respect to* $\big(A_{(1,0)}, \partial A_{(1,0)}\big)$.

Proof. Note that $\mathcal{Q}_1$ and $A_{(1,0)}$ are positively invariant. For $x_{n+1} \geq 0$, if $x_n \geq 0$ then

$$x_{n+1} = \frac{x_n e^{r(1-x_n)}}{1+\ln(by_n+1)} \geq 0,$$

since $e^{r(1-x_n)} \geq 0$ and $\frac{1}{1+\ln(by_n+1)} > 0$ as long as $y_n \geq 0$. Thus, $x_{n+1} \geq 0$ if $x_n \geq 0$. Similar to that, for $y_{n+1} \geq 0$, it is obvious from the equation

$$y_{n+1} = x_n\left(1 - \frac{1}{1+\ln(by_n+1)}\right),$$

if $x_n \geq 0$ and $y_n \geq 0$, then $y_{n+1} \geq 0$. Therefor, $\mathcal{Q}_1$ is positively invariant.
Similarly, if $x_n > 0,\ y_n \geq 0$ with same argument we have $x_{n+1} > 0$ and $y_{n+1} \geq 0$ so $A_{(1,0)}$ is positively invariant. Moreover, $\partial A_{(1,0)}$ is relatively closed in $\mathcal{Q}_1$.
Next, we will show the system is point dissipative. Let (x_n, y_n) be any positive solution of the system (3.28), then for n large enough

$$x_{n+1} < x_n e^{r(1-x_n)} < \frac{e^{r-1}}{r} = M.$$

Also, $y_n < \frac{e^{r-1}}{r} = M$ since $y_n < x_n$. Note that, $e^{r(1-x_n)}$ is maximized when $x_n = 1$ and decreases as x_n goes to infinity, so x_n will not grow unbounded. Moreover, for large x_n, the term $e^{r(1-x_n)}$ decays exponentially. On the other hand the term $\frac{1}{1+\ln(by_n+1)}$ is bounded above by 1. Therefore x_n bounded. For y_n, since $y_n < x_n$ and x_n is bounded and the term $1 - \frac{1}{1+\ln(by_n+1)}$ is bounded by 1. Hence, both x_n and y_n are bounded, and therefore, the

system is point dissipative.

Finally, we will show that with positive x_n, $\partial A_{(1,0)}$ repels uniformly the solutions of the system (3.28). In other word, the soluation will not converge to the boundary $\partial A_{(1,0)}$. We will prove this by contradiction. Suppose that there exist a solution (x_n, y_n) where x_n goes to zero as n goes to infinity and y_n goes to zero as x_n goes to zero. In

$$x_{n+1} = \frac{x_n e^{r(1-x_n)}}{1 + \ln(by_n + 1)},$$

we see that for x_n going to zero, $e^{r(1-x_n)}$ approaches e^r and $\frac{1}{1+\ln(by+1)}$ approaches one. Hence

$$x_{n+1} \approx x_n e^r.$$

We know that $e^r > 1$, so this implies that x_{n+1} is increasing for small x_n which contradicts the assumption that x_n approaches zero. Therefore, the boundary $\partial A_{(1,0)}$ repels solutions proving that the system is uniformly persistent in $A_{(1,0)}$. □

Lemma 3.6.2. *For any positive x_0, there exist a positive constant c such that*

$$c < x_n < \frac{e^{r-1}}{r}.$$

Proof. According to the above lemma (3.6.1), the proof of this theorem is evident. □

Theorem 3.6.1. *The system (3.28) exhibits global stability if $0 < r < 2$ and $0 < b < 1$.*

To demonstrate the global stability of the system (3.28), we begin by establishing the following conditions for system (3.28) when $0 < r < 2$ and $0 < b < 1$. For $n \geq 1$ and for any initial conditions $x_0 > 0$ and $y_0 \geq 0$, we have the following calculations:

$$\begin{aligned}\frac{y_{n+1}}{x_{n+1}} &= \frac{x_n\left(1-\frac{1}{1+\ln(by_n+1)}\right)}{\frac{x_n e^{r(1-x_n)}}{1+\ln(by_n+1)}} \\ &= \frac{\left(1-\frac{1}{1+\ln(by_n+1)}\right)(1+\ln(by_n+1))}{e^{r(1-x_n)}} \\ &= \frac{\ln(by_n+1)}{e^{r(1-x_n)}} \\ &= e^{r(x_n-1)}\ln(by_n+1).\end{aligned}$$

So,

$$\frac{y_{n+1}}{x_{n+1}} = \mathrm{e}^{r(-1+x_n)}\ln\left(by_n+1\right). \tag{3.31}$$

While,

$$\begin{aligned}\frac{y_{n+1}}{y_n} &= \frac{x_n\left(1-\frac{1}{1+\ln(by_n+1)}\right)}{y_n} \\ &= \frac{x_n\frac{\ln(by_n+1)}{1+\ln(by_n+1)}}{y_n} \\ &= \frac{x_n\ln(by_n+1)}{\big(1+\ln(by_n+1)\big)y_n}.\end{aligned}$$

By substituting:

$$y_n = x_{n-1}\frac{\ln(by_{n-1}+1)}{1+\ln(by_{n-1}+1)}$$

we have:

$$\frac{y_{n+1}}{y_n} = \frac{x_n\ln(by_n+1)}{\big(1+\ln(by_n+1)\big)\left(x_{n-1}\frac{\ln(by_{n-1}+1)}{1+\ln(by_{n-1}+1)}\right)}$$

Given that $0<b<1$ and $y_n \geq 0$ we have

$$\frac{x_n\ln(by_n+1)}{(1+\ln(by_n+1))\left(x_{n-1}\frac{\ln(by_{n-1}+1)}{1+\ln(by_{n-1}+1)}\right)} \leq \frac{bx_n}{1+\ln(by_n+1)}$$

Thus,

$$\frac{y_{n+1}}{y_n} = \frac{x_n \ln(by_n + 1)}{(1 + \ln(by_n + 1))\, y_n} \leq \frac{bx_n}{1 + \ln(by_n + 1)} \tag{3.32}$$

In addition,

$$\begin{aligned}
\ln\left(\frac{x_{n+1}}{x_n}\right) &= \ln\left(\frac{\frac{x_n e^{r(1-x_n)}}{1+\ln(by_n+1)}}{x_n}\right) \\
&= \ln\left(\frac{e^{r(1-x_n)}}{1 + \ln(by_n + 1)}\right) \\
&= r(1 - x_n) - \ln(1 + \ln(by_n + 1)) \\
&= r\Big((1 - x_n) - \frac{\ln(1 + \ln(by_n + 1)}{r}\Big).
\end{aligned}$$

Thus,

$$\ln\left(\frac{x_{n+1}}{x_n}\right) = r\left((1 - x_n) - \frac{\ln(1 + \ln(by_n + 1))}{r}.\right) \tag{3.33}$$

To prove inequality (3.32), let

$$h(y) = \frac{\ln(by + 1)}{y}$$

then $h(y) \leq b$, i.e $h(y)$ is bounded above by b. Since the function $h(y)$ is decreasing on $(0, \infty)$ since

$$h'(y) = \frac{-\ln(by + 1)by + by - \ln(by + 1)}{(by + 1)y^2} < 0.$$

Note that $-\ln(by + 1)by + by - \ln(by + 1) < 0$, is equivalent to $\ln(by + 1)by + \ln(by + 1) > by$. Moreover, $by|_{y=0} = 0$ and $\ln(by + 1)by + \ln(by + 1)|_{y=0} = 0$. Also, $(by)' = b$ and $\Big(\ln(by + 1)by + \ln(by + 1)\Big)' = (\ln(by + 1) + 1)b$, so $\ln(by + 1)by + \ln(by + 1) > by$. Hence, $h(y)$ is decreasing on $[0, \infty)$. Also, $\lim_{y\to 0^+} h(y) = b$, so $h(y) \leq b$ on $(0, \infty)$.

From equation (3.33), we have:

$$\begin{aligned}
\ln\left(\frac{x_{n+m}}{x_n}\right) &= \ln\left(\frac{x_{n+1}}{x_n}\cdot\frac{x_{n+2}}{x_{n+1}}\cdots\frac{x_{n+m}}{x_{n+m-1}}\right) \\
&= \ln\left(\frac{x_{n+1}}{x_n}\right) + \ln\left(\frac{x_{n+2}}{x_{n+1}}\right) + \cdots + \ln\left(\frac{x_{n+m}}{x_{n+m-1}}\right) \\
&= \sum_{i=n}^{n+m-1} \ln\left(\frac{x_{i+1}}{x_i}\right) \\
&= \sum_{i=n}^{n+m-1} \Big[r(1-x_i) - \ln\Big(1+\ln(by_i+1)\Big)\Big]
\end{aligned}$$

Thus:

$$\ln\left(\frac{x_{n+m}}{x_n}\right) = \sum_{i=n}^{n+m-1} r(1-x_i) - \sum_{i=n}^{n+m-1} \ln\Big(1+\ln(by_i+1)\Big)$$

$$\sum_{i=n}^{n+m-1} r\left(x_i + \frac{\ln(1+\ln(by_i+1))}{r}\right) = rm - \ln\left(\frac{x_{n+m}}{x_n}\right)$$

Averaging over m terms:

$$\frac{1}{m}\sum_{i=n}^{n+m-1}\left(x_i + \frac{\ln(1+\ln(by_i+1))}{r}\right) = 1 - \frac{\ln\left(\frac{x_{n+m}}{x_n}\right)}{rm} \tag{3.34}$$

Define the operator F_n:

$$F_n := \frac{y_{n+1}}{y_n}.$$

From (3.32), we know

$$F_n \le \frac{bx_n}{1+\ln(by_n+1)},$$

Thus,

$$\frac{y_{n+m}}{y_n} = \prod_{i=n+1}^{n+m}\frac{y_i}{y_{i-1}} = \prod_{i=n}^{n+m-1} F_i \le \prod_{i=n}^{n+m-1}\frac{bx_i}{1+\ln(by_n+1)}. \tag{3.35}$$

Hence,

$$\begin{aligned}
\frac{y_{n+m}}{y_n} &< \prod_{i=n}^{n+m-1} b\left(x_i + \frac{\ln\left(1+\ln(by_i+1)\right)}{r}\right) \cdot \prod_{i=n}^{n+m-1} \frac{1}{1+\ln(by_n+1)} \\
&\leq \left(\frac{1}{m}\sum_{i=n}^{n+m-1} b\left(x_i + \frac{\ln\left(1+\ln(by_i+1)\right)}{r}\right)\right)^m \cdot \prod_{i=n}^{n+m-1} \frac{1}{1+\ln(by_n+1)} \\
&= \left(b^m\left(1 - \frac{\ln\left(\frac{x_{m+n}}{x_n}\right)}{mr}\right)\right) \cdot \prod_{i=n}^{n+m-1} \frac{1}{1+\ln(by_n+1)} \\
&< b^m \max\left\{\left|\left(1-\frac{\frac{1}{c}}{mr}\right)^m\right|, \left|\left(1-\frac{C}{mr}\right)^m\right|\right\} \cdot \prod_{i=n}^{n+m-1} \frac{1}{1+\ln(by_n+1)}.
\end{aligned}$$

Last inequality is true because by lemma (3.6.2), we have

$$0 < c < x_n < M \quad \text{and} \quad 0 < c < x_{n+m} < M,$$

where $M = \frac{e^{r-1}}{r}$. In addition,

$$\frac{1}{M} < \frac{1}{x_n} < \frac{1}{c},$$

then

$$\frac{c}{M} < \frac{x_{n+m}}{x_n} < \frac{M}{c},$$

also,

$$\ln\frac{c}{M} < \ln\frac{x_{n+m}}{x_n} < \ln\frac{M}{c},$$

then

$$-\ln\frac{M}{c} < -\ln\frac{x_{n+m}}{x_n} < -\ln\frac{c}{M},$$

it follows that

$$1 - \frac{\ln\frac{M}{c}}{mr} < 1 - \frac{\ln\frac{x_{n+m}}{x_n}}{mr} < 1 - \frac{\ln\frac{c}{M}}{mr}.$$

As a result, we have

$$\left(1 - \frac{\ln\frac{x_{n+m}}{x_n}}{mr}\right)^m < \max\left\{\left(1+\frac{C}{mr}\right)^m, \left(1-\frac{C}{mr}\right)^m\right\},$$

where $\ln\left(\frac{c}{M}\right) = C$. We also know that

$$\lim_{m\to\infty}\left(1+\frac{x}{m}\right)^m = e^x,$$

thus

$$\lim_{m\to\infty}\left(1-\frac{C}{mr}\right)^m = e^{\left(-\frac{C}{r}\right)} \quad \text{and} \quad \lim_{m\to\infty}\left(1+\frac{C}{mr}\right)^m = e^{\left(\frac{C}{r}\right)}.$$

So we have

$$\left(1-\frac{\ln\frac{x_{n+m}}{x_n}}{mr}\right)^m < \max\left\{\left|e^{\left(\frac{C}{r}\right)}\right|, \left|e^{-\frac{C}{r}}\right|\right\} := K.$$

We know that the sequence $\{y_n\}$ is bounded from above. Now we need to show that the sequence $\{y_n\}$ approaches zero. To the contrary, suppose that $\lim_{n\to\infty} y_n \neq 0$, so $\lim_{n\to\infty}\ln(1+by_n) \neq 0$. Hence $\{\ln(1+by_0)\}_{n\geq 1}$ has a sub-sequence $\{\ln(1+by_{n_k}\}_{k\geq 1}$ bounded away from zero. That is, there exists $\varepsilon > 0$ such that $\forall k \in \mathbb{N}, \ln(1+by_{n_k}) > \varepsilon$. It then follows that

$$\begin{aligned}
\prod_{i=1}^{n+m-1}\frac{1}{1+\ln(1+by_i)} &= \prod_{\substack{i=1\\ \ln(1+by_i)\geq\varepsilon}}^{n+m-1}\frac{1}{1+\ln(1+by_i)} \cdot \prod_{\substack{i=1\\ \ln(1+by_i)\geq\varepsilon}}^{n+m-1}\frac{1}{1+\ln(1+by_i)} \\
&\leq 1 \cdot \prod_{\substack{i=1\\ \ln(1+by_i)\geq\varepsilon}}^{n+m-1}\frac{1}{1+\ln(1+by_i)} \\
&= 1 \cdot \prod_{1\leq n_k\leq n+m-1}\frac{1}{1+\ln(1+y_{n_k})},
\end{aligned}$$

hence

$$\prod_{i=1}^{n+m-1}\frac{1}{1+\ln(1+by_i)} \leq \prod_{1\leq n_k\leq n+m-1}\frac{1}{1+\varepsilon}.$$

Thus,

$$\frac{y_{n+m}}{y_n} < b^m K \prod_{i=1}^{n+m-1} \frac{1}{1+\ln(1+by_i)} \longrightarrow y_{n+m} < b^m K \left(\prod_{i=1}^{n+m-1} \frac{1}{1+\ln(1+by_i)} \right) y_n,$$

meaning that

$$y_{n+m} \leq b^m K \left(\prod_{1 \leq n_k \leq n+m-1} \frac{1}{1+\varepsilon} \right) y_n.$$

Thus,

$$0 \leq \lim_{m\to\infty} y_m \leq \lim_{m\to\infty} b^m K \left(\prod_{1 \leq n_k \leq m-1} \frac{1}{1+\varepsilon} \right) y_n.$$

But

$$\lim_{m\to\infty} b^m = 1 \quad \text{as} \quad 0 < b < 1,$$

also,

$$\lim_{m\to\infty} \left(\prod_{1 \leq n_k \leq m-1} \frac{1}{1+\varepsilon} \right) = 0,$$

hence,

$$\lim_{m\to\infty} y_m = 0,$$

which is a contradiction. Hence, $\lim_{m\to\infty} y_m \neq 0$ is false, thus

$$\lim_{m\to\infty} y_m = 0.$$

The sequence $y_{m\geq 1}$ converges to 0 as m tends to infinity. This behavior suggests that the system (3.28) reaches a stable steady state at $y = 0$ for all initial conditions within the specified range of parameters that we extrapolated ($0 < r < 2$ and $0 < b < 1$). Therefore, the sequence $x_{n\geq 0}$ will asymptotically act like the Ricker's model[46] which has previously been proved by others that it is globally stable for $r < 2$. In-conclusion, we have shown that y_m converges to 0 as m tends to infinity, which demonstrates the uniform persistence of the system of equations (3.28) with respect to the given sets $A_{(1,0)}$ and $\partial A_{(1,0)}$.

3.7 Bifurcation Analysis

The aim of this section is to examine the local bifurcation of the steady states of the system (3.6), including period-doubling bifurcation for interior steady state $S_i = (x^*, y^*)$, in more details.

3.7.1 Period-Doubling Bifurcation of the Interior Steady State

Period-doubling bifurcation is the bifurcation that is associated with the appearance of $\lambda = -1$. According to Wiggins[49], the sufficient conditions for the occurrence of a period-doubling bifurcation for a one-parameter family of C^r $(r \geq 3)$ one-dimensional maps

$$x \mapsto f(x, \mu), \quad x \in \mathbb{R},\ \mu \in \mathbb{R}$$

are:

$$\begin{aligned} f(0,0) &= 0, \\ \frac{\partial f}{\partial x}(0,0) &= -1, \\ \frac{\partial (f \circ f)}{\partial \mu}(0,0) &= 0, \\ \frac{\partial^2 (f \circ f)}{\partial x^2}(0,0) &= 0, \\ \frac{\partial^2 (f \circ f)}{\partial x \partial \mu}(0,0) &\neq 0, \\ \frac{\partial^3 (f \circ f)}{\partial x^3}(0,0) &\neq 0. \end{aligned} \tag{3.36}$$

In our system, the case of $b > 1$, period doubling bifurcation occurs when $J_{r=g_3(Y)}(x^*, y^*)$ satisfies the Jacobian matrix (3.23) of the system (3.6). Essentially, the period doubling bifurcation occurs shortly after crossing the line $\det + \mathrm{tr} + 1 = 0$. In order to examine whether the period doubling bifurcation is stable or unstable, we will first have to take into account the normal form of the equilibrium (x^*, y^*).There will be a demonstration of the dynamic behaviour of the system under the condition $r = r^*$ with $\lambda_1 = -1$ and $\lambda_2 < 1$.

First, we apply the change of variable

$$x = x^* + \bar{x},\ y = y^* + \bar{y} \text{ and } r = r^* + \bar{r}.$$

Through this change of variables, the system (3.6), transforms into the following two-dimensional map

$$\begin{aligned} f(\bar{x},\bar{y}) &= \frac{(x^*+\bar{x})\ e^{(r^*+\bar{r})(1-x^*-\bar{x})}}{1+\ln(b(y^*+\bar{y})+1)} - x^*, \\ g(\bar{x},\bar{y}) &= (x^*+\bar{x})\left(1 - \frac{1}{1+\ln\left(b(y^*+\bar{y})+1\right)}\right) - y^*. \end{aligned}$$

By applying the second order of the Taylor series to f and g, we approximate the previous system as follows:

$$\begin{aligned} f(\bar{x},\bar{y}) &= \frac{-(by^*+1)(r^*x^*-1)\ln(by^*+1) + (-br^*y^*-r^*)x^* + by^* + 1}{(1+\ln(by^*+1))(by^*+1)}\ \bar{x} \\ &\quad - \frac{x^*b}{(1+\ln(by^*+1))(by^*+1)}\ \bar{y} + O(2), \qquad (3.37) \\ g(\bar{x},\bar{y}) &= \frac{(by^*+1)\ln(by^*+1)^2 + (by^*+1)\ln(by^*+1)}{(1+\ln(by^*+1))^2(by^*+1)}\ \bar{x} + \frac{x^*b}{(1+\ln(by^*+1))^2(by^*+1)}\ \bar{y} + O(2), \\ &\qquad (3.38) \end{aligned}$$

where $x^* = \frac{y^*(1+\ln(by^*+1))}{\ln(by^*+1)}$. Now to simplify the computation for the system, we will apply a transformation that makes the system easier to calculate by changing variables as follows

$$X = X^* + \bar{X},\ Y = Y^* + \bar{Y} \text{ and } R = R^* + \bar{R}$$

where $Y = by + 1$, $X = x$, $R = \frac{r}{b}$,

$$b = \frac{\ln(Y)RY + \ln(1+\ln(Y))\ln(Y) - \ln(Y)R + RY - R}{\ln(Y)R},$$

and

$$r = g_3(Y) = \frac{\ln(Y)(2\ln(Y)^2Y + 3\ln(Y)Y - \ln(Y) + 2Y - 2)b}{(Y-1)(\ln(Y)+1)(\ln(Y)^2Y + \ln(Y)Y + Y - 1)}.$$

When $\bar{R} = 0$, we will have the eigenvalues of the Jacobin matrix $J_{r=g_3(Y)}(X^*, Y^*)$ are

$$\lambda_1 = -1,$$
$$\lambda_2 = -\frac{(Y-1)(\ln(Y)^3 Y - \ln(Y)Y - Y + 1)}{\big(Y(\ln(Y)+1)\ln(Y)\big(\ln(Y)^2 Y + \ln(Y)Y + Y - 1\big)},$$

We show that $|\lambda_2| < 1$ for $Y \geq 1$. Let

$$N_{\lambda_2}(Y) = (Y-1)(\ln(Y)^3 Y - \ln(Y)Y - Y + 1),$$
$$D_{\lambda_2}(Y) = \big(Y(\ln(Y)+1)\ln(Y)\big(\ln(Y)^2 Y + \ln(Y)Y + Y - 1\big),$$

then $\lim_{Y\to 1^+} N_{\lambda_2}(Y) = 0$ and $N(Y) > 0$ on $Y \geq 1$. Also, $\lim_{Y\to 1^+} D_{\lambda_2}(Y) = 0$ on $Y \geq 1$. Furthermore, for all $Y \geq 1$,

$$\begin{aligned} D'_{\lambda_2}(Y) - N'_{\lambda_2}(Y) &= 2Y\ln(Y)^4 + 6Y\ln(Y)^3 + 7Y\ln(Y)^2 + 2\ln(Y)^2 \\ &\quad + 8Y\ln(Y) - 4\ln(Y) + 4Y - 4 + \ln(Y)^3 \\ &= 2Y\ln(Y)^4 + 6Y\ln(Y)^3 + 7Y\ln(Y)^2 + 2\ln(Y)^2 \\ &\quad + 4Y\ln(Y) + 4\ln(Y)(Y-1) + 4(Y-1) + \ln(Y)^3 > 0. \end{aligned}$$

Hence, for all $Y \geq 1$, $D'_{\lambda_2}(Y) - N'_{\lambda_2}(Y) > 0$ and $D'_{\lambda_2}(Y) - N'_{\lambda_2}(Y)$ is a continuous function on $(1,\infty)$. Thus $D_{\lambda_2}(Y) - N_{\lambda_2}(Y) > 0$ on $(1,\infty)$. So, $D_{\lambda_2}(Y) > N_{\lambda_2}(Y)$ on $(1,\infty)$ and $D_{\lambda_2}(Y) \neq 0$ on $(1,\infty)$. Therefore, $0 < \frac{N_{\lambda_2}(Y)}{D_{\lambda_2}(Y)} < 1$, hence $|\lambda_2| = |-\frac{N_{\lambda_2}(Y)}{D_{\lambda_2}(Y)}| < 1$.
The eigenvectors that associate with λ_1 and λ_2 are

$$v_1 = \Big\langle -\frac{\ln(Y)^2 Y + \ln(Y) Y + Y - 1}{\ln(Y)^2 Y}, 1 \Big\rangle$$
$$v_2 = \Big\langle -\frac{(Y-1)(\ln(Y)+1)}{\ln(Y)^2 Y + \ln(Y) Y + Y - 1}, 1 \Big\rangle$$

respectively. We can represent v_1, and v_2 in matrix form as follows:

$$p = \begin{bmatrix} -\frac{\ln(Y)^2 Y + \ln(Y) Y + Y - 1}{\ln(Y)^2 Y} & -\frac{(Y-1)(\ln(Y)+1)}{\ln(Y)^2 Y + \ln(Y) Y + Y - 1} \\ 1 & 1 \end{bmatrix}.$$

Next, we change variables X and Y in terms of u and v by matrix diagonalizable:

$$\begin{bmatrix} X \\ Y \end{bmatrix} = \begin{bmatrix} -\frac{\ln(Y)^2 Y + \ln(Y) Y + Y - 1}{\ln(Y)^2 Y} & -\frac{(Y-1)(\ln(Y)+1)}{\ln(Y)^2 Y + \ln(Y) Y + Y - 1} \\ 1 & 1 \end{bmatrix} \begin{bmatrix} u \\ v \end{bmatrix}. \tag{3.39}$$

By applying this change of coordinates to maps (3.37), and (3.38), we can obtain the following two maps, which have linear terms as their first part, while non-linear terms as their second part,

$$\begin{bmatrix} u \\ v \end{bmatrix} \mapsto \begin{bmatrix} -1 & 0 \\ 0 & \lambda_2 \end{bmatrix} \begin{bmatrix} u \\ v \end{bmatrix} + \begin{bmatrix} \tilde{F}(u, v, R) \\ \tilde{G}(u, v, R) \end{bmatrix}, \tag{3.40}$$

Where

$$\tilde{F}(u, v, R) = \tilde{F}_{201} u^2 R + \tilde{F}_{300} u^3 + \tilde{F}_{101} u R + \tilde{F}_{200} u^2 + \cdots, \tag{3.41}$$
$$\tilde{G}(u, v, R) = \tilde{G}_{400} u^4 + \tilde{G}_{300} u^3 + \tilde{G}_{200} u^2 + \cdots. \tag{3.42}$$

Our goal now is to find the center manifold on u and R, which is

$$v = h^c(u, R) = a u^2 + O(|(u, R)|^3).$$

Substituting v into the equations (3.41) and (3.42) results in

$$\tilde{F}(u,v,R) = a\tilde{F}_{201}u^2R + a\tilde{F}_{300}u^3 + \tilde{F}_{101}uR + \tilde{F}_{200}u^2 + \cdots,$$
$$\tilde{G}(u,v,R) = a^2\tilde{G}_{400}u^4 + a\tilde{G}_{300}u^3 + \tilde{G}_{200}u^2 + \cdots$$

where some of the functions we needed were as follows. Note that the following equations are provided in terms of R and Y. However, they can be similarly converted to the (u,v) plane using the appropriate transformation equations (3.39).

$$\begin{aligned}
\tilde{F}_{101} = &-\Big(\left(-1+R^2Y^3+(-2R^2-3R)Y^2+(R^2+3R+2)Y\right)Y^2\ln(Y)^6 \\
&+4\left(R^2Y^3+\left(-2R^2-\frac{5}{2}R\right)Y^2+\left(R^2+\frac{11}{4}R+\frac{7}{4}\right)Y-\frac{R}{4}-\frac{5}{4}\right)Y^2\ln(Y)^5 \\
&+\left(8R^2Y^5+(-18R^2-18R)Y^4+(12R^2+27R+8)Y^3+(-2R^2-9R-8)Y^2+Y\right)\ln(Y)^4 \\
&+10(Y-1)Y\left(R^2Y^3+\left(-\frac{8}{5}R^2-\frac{19}{10}R\right)Y^2+\left(\frac{3}{5}R^2+\frac{17}{10}R+\frac{1}{2}\right)Y-\frac{R}{10}-\frac{3}{10}\right)\ln(Y)^3 \\
&+8(Y-1)^2Y\left(R^2Y^2+\left(-R^2-\frac{13}{8}R\right)Y+\frac{R^2}{8}+\frac{3R}{4}+\frac{1}{8}\right)\ln(Y)^2 \\
&+4R(Y-1)^3\left(RY-\frac{1}{2}R-\frac{5}{4}\right)Y\ln(Y) \\
&+R(Y-1)^4(RY-1)\Big)\left(\ln(1+\ln(Y))\ln(Y)+R(1+\ln(Y))(Y-1)\right) \\
&\Big/\Big(R\left(Y^2\ln(Y)^4+(Y^2+Y)\ln(Y)^3+(2Y^2-Y)\ln(Y)^2+(2Y^2-2Y)\ln(Y)+(Y-1)^2\right) \\
&\times Y\ln(Y)^2\left(\ln(Y)^2Y+\ln(Y)Y+Y-1\right)\Big),
\end{aligned}$$

$$\tilde{F}_{110} = -\Bigg(Y(RY - R - 1)\ln(Y)^2 + (Y-1)(RY-1)\ln(Y) + R(Y-1)^2 \Bigg) \ln(1+\ln(Y))$$
$$+ R(Y-1)\Big(\ln(Y)^2 Y + \ln(Y)Y + Y - 1 \Big)\Big(1+\ln(Y)\Big)\Big(\ln(Y)^2 Y + \ln(Y)Y + Y - 1 \Big)$$
$$\Bigg/ \Bigg(\ln(1+\ln(Y))\ln(Y) + R(1+\ln(Y))(Y-1) \Bigg)$$
$$\times \Bigg(Y^2\ln(Y)^4 + (Y^2+Y)\ln(Y)^3 + (2Y^2 - Y)\ln(Y)^2 + (2Y^2-2Y)\ln(Y) + (Y-1)^2 \Bigg),$$

$$\tilde{F}_{200} = -\Bigg(RY^3(RY - R - 2)\ln(Y)^6 + \Big(3R^2Y^4 + (-3R^2-6R)Y^3 + (2R+3)Y^2 - Y\Big)\ln(Y)^5$$
$$+ \Big(6R^2Y^4 + (-9R^2-10R)Y^3 + (3R^2+8R+2)Y^2 - 2Y\Big)\ln(Y)^4$$
$$+ 7R\Bigg(\frac{4}{7} + RY^2 + \Big(-\frac{6R}{7} - \frac{10}{7}\Big)Y\Bigg)(Y-1)Y\ln(Y)^3$$
$$+ 6R(Y-1)^2 Y\left(RY - \frac{1}{2}R - 1\right)\ln(Y)^2 + 3R(Y-1)^3\left(RY - \frac{2}{3}\right)\ln(Y)$$
$$+ R^2(Y-1)^4\Bigg) \Bigg/ \Bigg(2R\Big(Y^2\ln(Y)^4 + (Y^2+Y)\ln(Y)^3 + (2Y^2-Y)\ln(Y)^2$$
$$+ (2Y^2-2Y)\ln(Y) + (Y-1)^2\Big)Y\ln(Y)^4 \Bigg),$$

$$
\begin{aligned}
\tilde{F}_{300} = -\Bigg(& R^2Y^4(RY-R-3)\ln(Y)^9 + \Big(5R^3Y^5 + (-5R^3-15R^2)Y^4 + (3R^2+9R)Y^3 \\
& + (-3R-5)Y^2 + 2Y\Big)\ln(Y)^8 \\
& + \Big(14R^3Y^5 + (-18R^3-39R^2)Y^4 + (4R^3+21R^2+24R)Y^3 \\
& + (-12R-17)Y^2 + 8Y\Big)\ln(Y)^7 \\
& + \Big(26R^3Y^5 + (-42R^3-66R^2)Y^4 + (16R^3+63R^2+39R)Y^3 \\
& + (-9R^2-39R-9)Y^2 + (6R+9)Y\Big)\ln(Y)^6 \\
& + 35RY\left(\frac{18}{35} + R^2Y^4 + \left(-\frac{71}{35}R^2 - \frac{78}{35}R\right)Y^3\right. \\
& \left. + \left(\frac{6}{5}R^2 + \frac{111}{35}R + \frac{36}{35}\right)Y^2 - \frac{6(R+3)^2Y}{35}\right)\ln(Y)^5 \\
& + 35R\left(\frac{3}{35} + R^2Y^4 + \left(-\frac{52}{35}R^2 - \frac{66}{35}R\right)Y^3\right. \\
& \left. + \left(\frac{18}{35}R^2 + \frac{9}{5}R + \frac{3}{5}\right)Y^2 + \left(-\frac{9R}{35} - \frac{24}{35}\right)Y\right)(Y-1)\ln(Y)^4 \\
& + 26R(Y-1)^2\left(-\frac{3}{13} + R^2Y^3 + \left(-R^2 - \frac{3}{2}R\right)Y^2\right. \\
& \left. + \left(\frac{2}{13}R^2 + \frac{21}{26}R + \frac{3}{13}\right)Y\right)\ln(Y)^3 \\
& + 14R^2(Y-1)^3\left(\frac{3}{14} + RY^2 + \left(-\frac{4R}{7} - \frac{15}{14}\right)Y\right)\ln(Y)^2 \\
& + 5R^2\left(RY - \frac{1}{5}R - \frac{3}{5}\right)(Y-1)^4\ln(Y) \\
& + R^3(Y-1)^5\Bigg) \\
\Big/ & 6R^2\Big(Y^2\ln(Y)^4 + (Y^2+Y)\ln(Y)^3 + (2Y^2-Y)\ln(Y)^2 \\
& + (2Y^2-2Y)\ln(Y) + (Y-1)^2\Big)Y^2\ln(Y)^7,
\end{aligned}
$$

$$
\begin{aligned}
G_{200} = & \left((\ln(1+\ln(Y))\ln(Y) + R(1+\ln(Y))(Y-1)) \right) \\
& \times \Bigg(RY^3(RY-R-2)\ln(Y)^6 + \left(4R^2Y^4 + (-4R^2-8R)Y^3 + (2R+3)Y^2 - Y\right)\ln(Y)^5 \\
& + \left(8R^2Y^4 + (-10R^2-14R)Y^3 + (2R^2+8R+2)Y^2 - 2Y\right)\ln(Y)^4 \\
& + \left(10R^2Y^4 + (-16R^2-14R)Y^3 + (6R^2+14R-3)Y^2 + (-2R+1)Y\right)\ln(Y)^3 \\
& + 8\left(\frac{1}{8} + R^2Y^3 + (-R^2-R)Y^2 + \left(\frac{1}{8}R^2 + \frac{1}{2}R - \frac{5}{8}\right)Y\right)(Y-1)\ln(Y)^2 \\
& + 4(Y-1)^2\left(-\frac{1}{2} + R^2Y^2 + \left(-\frac{1}{2}R^2 - \frac{1}{2}R\right)Y\right)\ln(Y) \\
& + R^2Y(Y-1)^3\Bigg)\left(\ln(Y)^2Y + \ln(Y)Y + Y - 1\right) \\
\Big/ & \Bigg(2R\Big(Y^2\ln(Y)^4 + (Y^2+Y)\ln(Y)^3 + (2Y^2-Y)\ln(Y)^2 \\
& + (2Y^2-2Y)\ln(Y) + (Y-1)^2\Big)Y^2\ln(Y)^4(1+\ln(Y))\Bigg).
\end{aligned}
$$

As a result of the computing center manifold, we have

$$v = h^c(u,R) = -\tfrac{\tilde{G}_{200}}{\lambda_2 - 1} + O(|(u,R)|^3).$$

The next step is to define the function $K(u,R)$ using the reduced map $u \to K(u,R)$,

$$K(u,R) = -u + \tilde{F}_{110}uR + \tilde{F}_{200}u^2 + \left(\tilde{F}_{210} - \tfrac{\tilde{F}_{011}\tilde{G}_{200}}{\lambda_2-1}\right)Ru^2 + \left(\tilde{F}_{300} - \tfrac{\tilde{F}_{101}\tilde{G}_{200}}{\lambda_2-1}\right)u^3 + O(|(u,R)|^3).$$

Moreover,

$$K(K(u,R),R) = u - 2\tilde{F}_{110}uR - \tilde{F}_{110}\tilde{F}_{200}Ru^2 + \tilde{F}_{110}^2R^2u + \left(-2\tilde{F}_{300} + 2\tfrac{\tilde{F}_{101}\tilde{G}_{200}}{\lambda_2-1} - 2\tilde{F}_{200}^2\right)u^3 + O(4).$$

By the conditions given in (3.36), the period doubling bifurcation can be calculated based on the following function

$$\mathcal{K} = -2\tilde{F}_{300} + 2\frac{\tilde{F}_{101}\tilde{G}_{200}}{\lambda_2 - 1} - 2\tilde{F}_{200}^2 \neq 0.$$

This can be seen using numerical simulations for different values of (R, k) in Figure 3.20. The result in table 3.1 shows that the period doubling bifurcation $\mathcal{K}$ is stable.

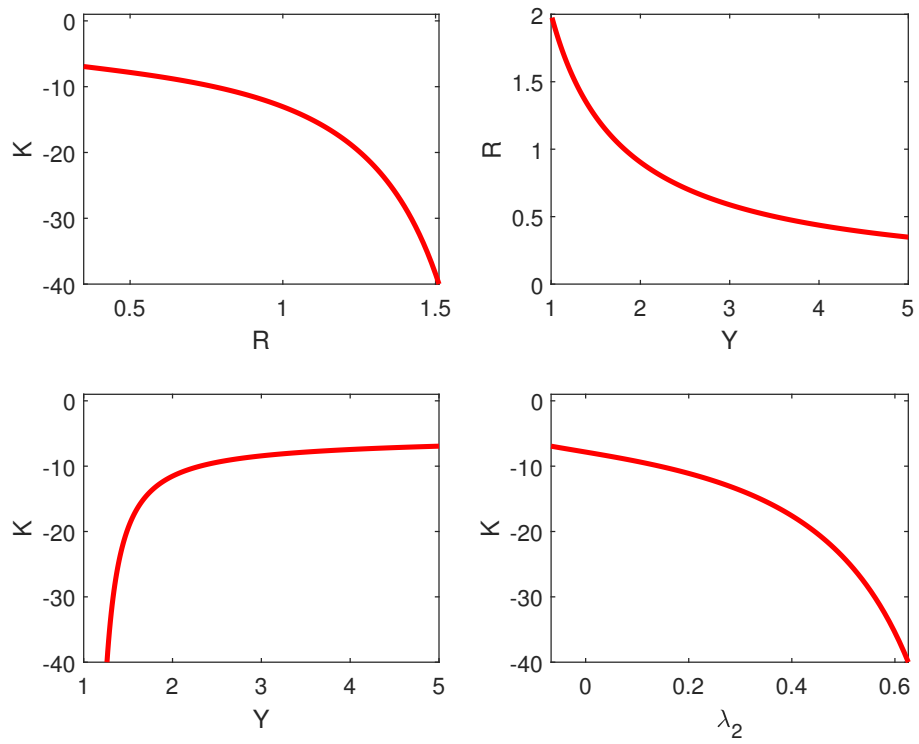

Figure 3.20: *Stability of the period doubling bifurcation of system* (3.6).

Value of second eigenvalue and some of coefficients of $\mathcal{K}$ for certain parameter values of b are given in the following table:

b	R	$x^\star$	Y	λ_2	$\tilde{F}_{200}$	$\tilde{F}_{300}$	$\tilde{F}_{110}$	$\tilde{F}_{101}$	$\mathcal{K}$
1.01	1.9876	0.9975	1.0049	0.9901	0.4981	108158.1698	-1.0012	1.4981	-47600.6168
2.01	1.2392	0.8631	1.5012	0.4345	0.2973	27.9783	-1.1045	1.1955	-19.4214
3.01	0.9073	0.8080	1.9924	0.2212	0.1422	13.0415	-1.1691	0.9107	-11.5792
4.01	0.7179	0.7755	2.4802	0.1116	0.0351	9.2867	-1.2093	0.7004	-9.4595
5.01	0.5951	0.7532	2.9655	0.3923	-0.0397	7.6659	-1.2349	0.5471	-8.4727
6.01	0.5088	0.7366	3.4488	0.0037	-0.0933	6.7818	-1.2516	0.4332	-7.8896
7.01	0.4448	0.7234	3.9304	-0.0259	-0.1327	6.2305	-1.2627	0.3468	-7.4961
8.01	0.3954	0.7127	4.4106	-0.0476	-0.1623	5.8556	-1.2702	0.2796	-7.2074
9.01	0.3560	0.7037	4.8896	-0.0638	-0.1851	5.5845	-1.2751	0.2264	-6.9837

Table 3.1: *Period doubling bifurcation stability for the given numerical values*

As a conclusion, the stability of steady states for this study is presented as follows: Based on this population dynamics model, there are three steady states present in $\mathcal{Q}_1$:

(i) The origin steady state $S_0 = (0, 0)$.

(ii) The boundary steady state is located on the x-axis $S_1 = (1, 0)$.

(iii) One interior steady state $S_i = (x^*, y^*)$ exists if and only if $b > 1$.

Note that, the origin steady state $S_0 = (0, 0)$ is saddle point, while the stability of the boundary steady state $S_1 = (1, 0)$ falls in several cases based on Figure 3.1 and propositions (3.4.1) and (3.4.2):

i. If $b = 1$ and $0 < r < 2$, then the steady state $S_1 = (1, 0)$ is non-hyperbolic semi-stable (unstable).

ii. If $r = 2$ and $b < 1$, then the steady state $S_1 = (1, 0)$ is asymptotically stable.

iii. If $b > 1$, and $r = 2$, or if $b = 1$, and $r > 2$, then the steady state $S_1 = (1, 0)$ in these two cases is unstable.

iv. If $r = 2$ and $b = 1$, then the steady state $S_1 = (1, 0)$ is non-hyperbolic and it is hard to determine wither the steady state $S_1 = (1, 0)$ is stable or not.

3.7.2 Concluding Thoughts and Simulation Results

This chapter studies a generalized discrete-time predator-prey model for the Modified Nicholson-Bailey model. We first study the stability of the three steady states of the system, then we investigated the local stability of three steady states and the global stability of the boundary steady state. Finally, we analysis period doubling bifurcations of a generalized Nicholson-Bailey host–parasitoid model. In this study, we computed the center manifold coefficients of the period doubling bifurcation for the interior steady state(x^*, y^*) and the boundary fix point $(1, 0)$. Due to the long coefficients equations, we provided final results as well as phase diagrams.

Bibliography

[1] VA Bailey and AJ Nicholson. The balance of animal populations. In *Proc. Zool. Soc. Lond*, volume 3, pages 551–598, 1935.

[2] Seyed M Moghadas and Majid Jaberi-Douraki. *Mathematical modelling: a graduate textbook*. John Wiley & Sons, 2018.

[3] Bin Gong and Guangfu Zhang. Interactions between plants and herbivores: a review of plant defense. *Acta Ecologica Sinica*, 34(6):325–336, 2014.

[4] Luigi Boitani and Todd Fuller. *Research techniques in animal ecology: controversies and consequences*. Columbia University Press, 2000.

[5] Zhujun Jing and Jianping Yang. Bifurcation and chaos in discrete-time predator–prey system. *Chaos, Solitons & Fractals*, 27(1):259–277, 2006.

[6] SM Sohel Rana. Bifurcation and complex dynamics of a discrete-time predator-prey system. *Computational Ecology and software*, 5(2):187, 2015.

[7] Tim Loossens, Francis Tuerlinckx, and Stijn Verdonck. A comparison of continuous and discrete time modeling of affective processes in terms of predictive accuracy. *Scientific reports*, 11(1):1–11, 2021.

[8] HCJ Godfray and MP Hassell. Discrete and continuous insect populations in tropical environments. *The Journal of Animal Ecology*, pages 153–174, 1989.

[9] JR Metcalfe. Observations on the ecology of saccharosydne saccharivora (westw.)(hom., delphacidae) in jamaican sugar-cane fields. *Bulletin of entomological research*, 60(4): 565–597, 1971.

[10] Henry Plotkin. *Darwin machines and the nature of knowledge*. Harvard University Press, 1997.

[11] Hsiang-Ke Chao. Three kinds of the lotka–volterra model transfer from biology to economics. *Synthese*, 202(4):124, 2023.

[12] Zhilan Feng and Donald DeAngelis. *Mathematical models of plant-herbivore interactions*. Chapman and Hall/CRC, 2017.

[13] Konrad Dettner, Gerhard Bauer, and Wolfgang Völkl. Evolutionary patterns and driving forces in vertical food web interactions. In *Vertical Food Web Interactions: Evolutionary Patterns and Driving Forces*, pages 337–377. Springer, 1997.

[14] G Caughley. Wildlife management and the dynamics of ungulate populations. applied biology. vol. 1, 1976.

[15] Rex Clark Robinson. *An introduction to dynamical systems: continuous and discrete*, volume 19. American Mathematical Soc., 2012.

[16] Yun Kang, Dieter Armbruster, and Yang Kuang. Dynamics of a plant–herbivore model. *Journal of biological dynamics*, 2(2):89–101, 2008.

[17] AP Gutierrez, DW Williams, and H Kido. A model of grape growth and development: the mathematical structure and biological considerations 1. *Crop science*, 25(5):721–728, 1985.

[18] Leah Edelstein-Keshet. Mathematical theory for plant—herbivore systems. *Journal of Mathematical Biology*, 24:25–58, 1986.

[19] Thomas Flatt and Wolfgang W Weisser. The effects of mutualistic ants on aphid life history traits. *Ecology*, 81(12):3522–3529, 2000.

[20] Ernst-Detlef Schulze and Harold A Mooney. *Biodiversity and ecosystem function*. Springer Science & Business Media, 2012.

[21] Linda JS Allen, Mary K Hannigan, and Monty J Strauss. Mathematical analysis of a model for a plant-herbivore system. *Bulletin of mathematical biology*, 55(4):847–864, 1993.

[22] Robert V O'Neill. *A hierarchical concept of ecosystems*. Number 23. Princeton University Press, 1986.

[23] Michael Begon and Roger G Bowers. Host-host-pathogen models and microbial pest control: the effect of host self regulation. *Journal of Theoretical Biology*, 169(3):275–287, 1994.

[24] Michael Shub. *Global stability of dynamical systems*. Springer Science & Business Media, 2013.

[25] James A Powell, Jesse A Logan, and Barbara J Bentz. Local projections for a global model of mountain pine beetle attacks. *Journal of Theoretical Biology*, 179(3):243–260, 1996.

[26] DR Geiszler, VF Gallucci, and RI Gara. Modeling the dynamics of mountain pine beetle aggregation in a lodgepole pine stand. *Oecologia*, 46:244–253, 1980.

[27] James Powell, Bruce Kennedy, Peter White, Barbara Bentz, Jesse Logan, and David Roberts. Mathematical elements of attack risk analysis for mountain pine beetles. *Journal of Theoretical Biology*, 204(4):601–620, 2000.

[28] James A Powell and Jesse A Logan. Insect seasonality: circle map analysis of temperature-driven life cycles. *Theoretical population biology*, 67(3):161–179, 2005.

[29] John Pastor. *Mathematical ecology of populations and ecosystems*. John Wiley & Sons, 2008.

[30] Fernando Vadillo. Comparing stochastic lotka–volterra predator-prey models. *Applied Mathematics and Computation*, 360:181–189, 2019.

[31] Danny Summers, Justin G Cranford, and Brian P Healey. Chaos in periodically forced discrete-time ecosystem models. *Chaos, Solitons & Fractals*, 11(14):2331–2342, 2000.

[32] HN Agiza, EM Elabbasy, H El-Metwally, and AA Elsadany. Chaotic dynamics of a discrete prey–predator model with holling type ii. *Nonlinear Analysis: Real World Applications*, 10(1):116–129, 2009.

[33] S Kartal. Dynamics of a plant–herbivore model with differential–difference equations. *Cogent Mathematics*, 3(1):1136198, 2016.

[34] Qamar Din, M Sajjad Shabbir, M Asif Khan, and Khalil Ahmad. Bifurcation analysis and chaos control for a plant–herbivore model with weak predator functional response. *Journal of biological dynamics*, 13(1):481–501, 2019.

[35] Alexander John Nicholson. Supplement: the balance of animal populations. *The Journal of Animal Ecology*, pages 131–178, 1933.

[36] JR Beddington, CA Free, and JH Lawton. Dynamic complexity in predator-prey models framed in difference equations. *Nature*, 255(5503):58–60, 1975.

[37] RM May, MP Hassell, RM Anderson, and DW Tonkyn. Density dependence in host-parasitoid models. *The Journal of Animal Ecology*, pages 855–865, 1981.

[38] ANW Hone, MV Irle, and GW Thurura. On the neimark–sacker bifurcation in a discrete predator–prey system. *Journal of biological dynamics*, 4(6):594–606, 2010.

[39] Rasoul Asheghi. Bifurcations and dynamics of a discrete predator–prey system. *Journal of biological dynamics*, 8(1):161–186, 2014.

[40] William Edwin Ricker. Stock and recruitment. *Journal of the Fisheries Board of Canada*, 11(5):559–623, 1954.

[41] Anonymous. Life cycle of the gypsy moth. *Entomology Today*, 2022. Retrieved from: https://entomologytoday.org/life-cycle-of-the-gypsy-moth/.

[42] Andrew M Liebhold, Joel A Halverson, and Gregory A Elmes. Gypsy moth invasion in north america: a quantitative analysis. *Journal of Biogeography*, pages 513–520, 1992.

[43] JS Elkinton and AM Liebhold. Population dynamics of gypsy moth in north america. *Annual review of entomology*, 35(1):571–597, 1990.

[44] Yuri A. Kuznetsov. *Elements of Applied Bifurcation Theory*. Springer Science & Business Media, 2013.

[45] Mustafa RS Kulenovic and Gerasimos Ladas. *Dynamics of Second Order Rational Difference Equations: With Open Problems and Conjectures*. Chapman and Hall/CRC, 2001.

[46] Rafael Luis, Saber Elaydi, and Henrique Oliveira. Stability of a ricker-type competition model and the competitive exclusion principle. *Journal of Biological Dynamics*, 5(6): 636–660, 2011.

[47] Nicholas Karydas and John Schinas. The center manifold theorem for a discrete system. *Applicable Analysis*, 44(3-4):267–284, 1992.

[48] Jerrold E Marsden and Marjorie McCracken. *The Hopf bifurcation and its applications*, volume 19. Springer Science & Business Media, 2012.

[49] Stephen Wiggins. *Introduction to Applied Nonlinear Dynamical Systems and Chaos*. Springer, 2003.

[50] Malgorzata Guzowska, Rafael Luís, and Saber Elaydi. Bifurcation and invariant manifolds of the logistic competition model. *Journal of Difference Equations and Applications*, 17(12):1851–1872, 2011.

[51] Hal L Smith and Horst R Thieme. *Dynamical systems and population persistence*, volume 118. American Mathematical Soc., 2011.

[52] Alexander J. Nicholson and Victor A. Bailey. The balance of animal populations.—part i. *Proceedings of the Zoological Society of London*, 105(3):551–598, 1935.

[53] Sinan Kapçak, Ünal Ufuktepe, and Saber Elaydi. Stability and invariant manifolds of a generalized beddington host-parasitoid model. *Journal of biological dynamics*, 7(1): 233–253, 2013.

[54] Wendi Wang. Difference and differential equations. *American Mathematical Society*, 42:357–361, 2004.

[55] JBR Hernandez and PY Kim. *Epidemiology Morbidity And Mortality*. StatPearls Publishing, Treasure Island (FL), 2024. URL https://www.ncbi.nlm.nih.gov/books/NBK547668/. [Updated 2022 Oct 3].